New Insights into the Pathogenesis of the *Mycoplasma suis* Infection

---

Dissertation

zur

Erlangung der naturwissenschaftlichen Doktorwürde

(Dr. sc. nat.)

vorgelegt der

Mathematisch-naturwissenschaftlichen Fakultät

der

Universität Zürich

von

Katrin Gröbel

aus

Deutschland

Promotionskomitee

Prof. Dr. Leo Eberl (Vorsitz)

PD Dr. Ludwig E. Hölzle (Leitung der Dissertation)

Prof. Dr. Jakob Pernthaler

Prof. Dr. Max M. Wittenbrink

Zürich, 2010

Table of contents

Summary

Mycoplasma (*M.*) *suis* is a member of the haemotrophic mycoplasmas (HM), a group of cell wall-less bacteria known to parasitize on the surface of the red blood cells (RBCs) of a wide variety of vertebrate animals. *M. suis* is strongly adapted to the swine and causes infectious anaemia in pigs (IAP), an infectious disease mainly occurring in weaned and feeder pigs that are immunosuppressed. The acute form of the disease is characterised by a febrile anaemia, icterus and cyanosis at the acrae. Chronic infections are mainly asymptomatic, can however be accompanied by growth retardation, reduced reproduction rate of sows and a higher susceptibility to other diseases.

Basic research on HM is complicated due to the impossibility to cultivate these organisms. In this study high-resolution microscopic techniques were applied on blood and tissue of *M. suis* infected pigs in order to study the host-pathogen interaction in more detail and examine the dissemination of *M. suis* within the host.

In temporal connection with research activities on the *M. suis* infection, an increased incidence of acute IAP in feeder pigs was observed with predominantly fatal outcome despite antibiotic therapy. Contrary to the expected high numbers of *M. suis* cells on and between the erythrocytes in acridine orange-stained blood smears - the established diagnostic feature of acute IAP - only marginal numbers of the bacterial cells were noticed. This microscopic finding completely conflicted with the results of quantitative real-time PCR that detected high numbers of *M. suis* (10^9 to 10^{10} cells per ml blood) in the same blood samples. This striking difference between microscopy and PCR raised the issue of an intracellular localisation of *M. suis* within the erythrocytes. In this thesis verification of this hypothesis was carried out work by means of experimental infection of splenectomised pigs with the highly virulent *M. suis* strain 08/07 and microscopic analysis of infected RBCs using scanning (SEM) - and transmission electron microscopy (TEM) as well as confocal laser scanning microscopy. We concluded that the organism invades the erythrocytes in an endocytosis-like process and is initially surrounded by the host cell membrane. *M. suis* could also be found floating freely in the cytoplasm. In this study it was shown for the first time that a member of the haemoplasma group is able to invade the erythrocytes of its host.

Several authors have reported about haemorrhagic diathesis in pigs with acute IAP as well as about intravascular coagulation and subsequent consumption of platelets indicating vascular damages during the *M. suis* infection. Further observations confirming the assumption of

vascular injury during IAP is the massive change in erythrocyte morphology, RBC aggregation and subsequent development of cyanoses in areas with less blood circulation (ear, tail).

Using SEM and TEM a massive endothelial injury was detected on the luminal side of the vessel walls of acutely diseased *M. suis* infected pigs. Damages were associated with endothelial alterations as well as denudation of endothelial cells, which could be confirmed by histochemical analysis. Erythrocytes were found to be attached to the vascular wall – either alone or together with leucocytes and platelets embedded in a network of fibrin fibres, forming arterial thrombi. In addition, bacterial biofilms were observed on the luminal side of the blood vessels. Infrequently, single *M. suis* cells were found being attached to the endothelium. Applying TEM and histochemical staining intravascular coagulation could be detected in capillaries of parenchymas such as kidney, lung, and liver.

Endothelial cell death is often associated with an increased TNF-α concentration in the blood. However, no elevated serum concentrations of porcine TNF-α could be detected in acutely diseased pigs. Therefore, endothelial apoptosis is probably triggered by other serum factors or by attachment or invasion of *M. suis* to the endothelial cells itself.

In *in vitro* studies with porcine aortic endothelial cells (PAECs) and *M. suis* containing plasma of diseased pigs attachment of *M. suis* to PAECs could be confirmed. At the point of attachment an aggregation of the host cell actin was observed. In addition, PAECs incubated with porcine plasma and sera from acutely diseased *M. suis* infected pigs had a higher apoptosis rate than PAECs incubated with control plasma and sera.

In conclusion, the results of this thesis, specifically the intraerythrocytary localisation of *M. suis* in combination with the formation of biofilms on the vascular endothelium, help to explain the long-life persistence of this bacteria (and other HM). Biofilm formation as well as intracellular localisation generally protects bacteria from the host immune system and from killing by antibiotics. Therefore, this study serves as the basis for novel strategies in the HM research, e.g. treatment or prophylaxis.

Zusammenfassung

Mycoplasma (*M.*) *suis* ist ein Vertreter der hämotrophen Mycoplasmen (HM), einer Gruppe von zellwandlosen Bakterien, die auf der Oberfläche der roten Blutzellen einer Vielzahl von Säugetieren parasitieren. *M. suis* verursacht die infektiöse Anämie des Schweins (IAP), eine Infektionskrankheit welche hauptsächlich bei Absatzferkeln und Mastschweinen vorkommt, wenn diese unter Belastung stehen. Die akute Form der Krankheit äussert sich in einer fieberhaften Anämie, Ikterus und Zyanosen an den Akren. Chronische Infektionen sind grösstenteils asymptomatisch, können aber von Wachstumsstagnationen, einer verminderten Fruchtbarkeit und einer erhöhten Anfälligkeit gegenüber Infektionen gekennzeichnet sein.

Die Erforschung der hämotrophen Mycoplasmen wird durch die Unkultivierbarkeit der Erreger erschwert. In dieser Dissertation wurden Blut- und Gewebeproben von mit *M. suis* infizierten Schweinen hochauflösenden mikroskopischen Techniken unterzogen, um Wirt-Pathogen-Interaktionen und die Verbreitung des Erregers im Wirt zu untersuchen.

In zeitlichem Zusammenhang mit Forschungsarbeiten zu *M. suis*-Infektionen sind wir auf ein vermehrtes Auftreten akuter IAP in Mastschweinen aufmerksam geworden. Trotz antibiotischer Behandlung waren diese Erkrankungen vorwiegend tödlich. Im Gegensatz zu den erwarteten hohen Erregerzahlen in mit Acridine Orange gefärbten Blutausstrichen – einem üblichen diagnostischen Befund bei akuter IAP – konnten wir nur wenige Erreger nachweisen. Dieser mikroskopische Befund stand in starkem Widerspruch zu den Ergebnissen der quantitativen Real-Time PCR, mit der hohe Erregermengen (10^9-10^{10} Zellen pro ml Blut) in denselben Blutproben detektiert werden konnten. Dieser auffällige Unterschied zwischen Mikroskopie und PCR warf die Hypothese auf, dass es sich um ein neues *M. suis* Isolat handelt, welches in die Erythrozyten invadiert. In dieser Arbeit erfolgte die Bestätigung dieser Hypothese nach experimenteller Infektion splenektomierter Schweine mit dem hochvirulenten *M. suis*-Isolat 08/07 und anschließender mikroskopischer Untersuchung infizierter Erythrozyten im Transmissions - und Rasterelektronenmikroskop sowie im konfokalen Laserrastermikroskop. *M. suis* invadiert den Erythrozyten in einem endozytoseähnlichen Prozess und ist anfangs von der Wirtszellmembran umschlossen. Der Erreger wurde auch frei im Zytoplasma des Erythrozyten vorgefunden. Damit konnte zum ersten Mal gezeigt werden, dass ein Vertreter der HM in der Lage ist, in die Erythrozyten zu invadieren.

In verschiedenen Publikationen wird auf eine erhöhte hämorrhagische Diathese,

intravaskuläre Koagulation und Thrombozytopenie in Schweinen mit akuter IAP hingewiesen, was auf vaskuläre Schäden während der *M. suis*-Infektion hinweist. Weitere Beobachtungen, welche diese Vermutung untermauern, sind die massiven Änderungen in der Erythrozytenmorphologie, die verstärkte Aggregation der roten Blutzellen und die Ausprägung von Zyanosen in Körperbereichen mit geringer Blutzirkulation (Ohr, Schwanz).

Mit Hilfe von raster- und transmissionselektronenmikroskopischen Verfahren konnte eine massive Veränderung des Endothels in Blutgefässen akut erkrankter *M. suis*-infizierter Schweine aufgezeigt werden. Die Schädigungen beinhalteten grossflächige Ablösung der Endothelzellen, sowie morphologische Veränderungen, welche in histologischen Untersuchungen bestätigt wurden. Wandhaftende Erythrozyten sowie arterielle Thromben, bestehend aus dichten Fibrinnetzwerken in welche Leukozyten, Thrombozyten und Erythrozyten eingebettet sind, wurden vorgefunden. Weiterhin wurden bakterielle Biofilme auf der Endothelschicht beobachtet. Gelegentlich wurden auch einzelne *M. suis* Zellen auf der Innenseite der Gefässe detektiert. In transmissionselektronenmikroskopischen und histochemischen Untersuchungen wurden intravaskuläre Koagulationen in Kapillaren von grossen Parenchymen, wie der Niere, der Lunge und der Leber bestätigt.

Endothelialer Zelltod ist oft verbunden mit einer erhöhten TNF-α Konzentration im Blut. Es konnte jedoch kein erhöhter TNF-α Spiegel im Blutserum akut erkrankter Schweine nachgewiesen werden. Daher wird die Endothelzellapoptose wahrscheinlich durch andere Serumkomponenten oder auch durch die Adhäsion von *M. suis* an Endothelzellen selbst ausgelöst.

In *in vitro* Versuchen mit porzinen aortischen Endothelzellen (PAECs) und erregerhaltigem Plasma von *M. suis*-infizierten Schweinen konnten wir die Adhäsion von *M. suis* an Endothelzellen bestätigen. Ausserdem konnte eine Aggregation des Wirtzellaktins an den Kontaktstellen zu *M. suis* festgestellt werden. PAECs, welche mit Plasma und Seren akut infizierter Tiere inkubiert wurden, wiesen zudem eine höhere Apoptoserate auf als PAECs, welche mit Kontrollplasma und Seren inkubiert wurden.

Zusammenfassend dienen die Ergebnisse dieser Dissertation, insbesondere die intrazelluläre Lokalisation des Erregers sowie dessen Fähigkeit zur Biofilmbildung auf Endothelzellen, der Aufklärung der Persistenz von *M. suis* (und anderen HM). Bakterien innerhalb von Biofilmen oder Wirtszellen sind generell resistenter gegen die Immunantwort des Wirtes und geschützt vor einer Eliminierung durch Antibiotika. Daher kann diese Studie als Grundlage für neue

Strategien zur Verbesserung der medikamentösen Behandlung und Prophylaxe von Hämoplameninfektionen dienen.

Abbreviations

ATPase	adenosintriphosphatase
BSA	bovine serum albumine
CLSM	confocal laser scanning microscopy
CFU	colony forming unit
DAPI	4'-6-diamidin-2'-phenylindoldihydrochlorid
DNA	deoxyribonuleic acid
dpi	days post infectionem
E. coli	*Escherichia coli*
EC	endothelial cell
EDTA	ethylene diamine tetra-acetic acid
FACS	fluorescence activated cell sorter
FITC	fluorescein isothiocyanate
GA	glutaraldehyde
GAPDH	glyceraldehyde-3-phosphate dehydrogenase
HM	haemotrophic mycoplasmas
hip mutants	high persister mutants
HspA1	heat shock protein A1
IAP	infectious anaemia in pigs
ICAM-1	intercellular adhesion molecule-1
i. e.	id est (lat.: that is)
IgM	immunoglobulin M
IL	interleukin
kbp	kilobasepairs
LFA-1	leukocyte function antigen 1
LPS	lipopolysaccharide
MS	mass spectrometry
M. suis	*Mycoplasma suis*
msg1	*M. suis* GAPDH-like protein 1 gene
n	number
NaCl	sodium chloride
NO	nitric oxide
PAMP	pathogen-associated molecular pattern

PBS	phosphate buffered saline
PCD	programmed cell death
PCR	polymerase chain reaction
PFA	paraformaldehyde
pi	post infectionem
PI	propidium iodide
PS	phosphatidyl serine
RBC	red blood cell
RNA	ribonucleic acid
ROS	reactive oxygen species
SD	standard deviation
SDS	sodium dodecyl sulfate
SEM	scanning electron microscopy
TA	toxin-antitoxin
TEM	transmission electron microscopy
TLR	*toll*-like receptor
TNF-α	tumor necrosis factor alpha
Tris	Tris-(hydroxymethyl)aminomethane
TRITC	tetramethyl rhodamine iso-thiocyanate
U	unit
VCAM-1	vascular cellular adhesion molecule-1
vol	volume

1. Introduction

1.1 Haemotrophic mycoplasmas

1.1.1 General characteristics

Haemotrophic mycoplasmas (HM) belong to a highly specialised and so far uncultivable group of bacteria within the genus Mycoplasma. They represent a distinct new *Mycoplasma* cluster and are described to parasitize on the surface of the red blood cells (RBCs) of a wide variety of vertebrate animals. Like other *Mycoplasma* organisms, HM are not found in nature as free-living organisms as they depend on essential host cell compounds for their propagation (75). The genomic sizes of the organisms range from 1245 kbp [*M. haemofelis*, (7)] to as small as 745 kbp [*M. suis* (76)], thereby approaching the theoretical minimum size of a self-replicating organism. HM cause acute haemolytic to subtle chronic anaemia (49, 75), and the clinical spectrum of the infection ranges from asymptomatic to life-threatening depending on host susceptibility and bacterial virulence. All HM species show morphological similarities. These pleomorphic bacteria can be found in form of cocci, rings, or rods on the surface of RBCs (49, 75, 97, 135) and are enclosed by a single limiting membrane. Small granules and a few filamentous structures can be found in the cytoplasm (49, 75). According to the current state of knowledge HM have a strict host specificity meaning that a given mycoplasmal species infects only a single host species (49, 75). It is noteworthy that organisms that morphologically resemble HM have also been detected in the blood of humans (2, 20, 21, 103, 133).

1.1.2 Taxonomy

Members of the HM, formerly known as *Haemobartonella* and *Eperythrozoon* species, were originally classified as members of the family *Anaplasmataceae* within the order *Rickettsiales* based on biologic and phenotypic properties (79). However, due to some phenotypic characteristics such as RBC parasitism, small size, no cell-wall, no flagella, resistance to penicillin and susceptibility to tetracycline there was a long-held suspicion that *Eperythrozoon* and *Haemobartonella* spp. were rather closely related to the *Mollicutes* than to the *Rickettsiales* (119). The *Mollicutes* are a phylogenetically diverse group compromising more than 150 species (75, 121) in eight genera (*Mycoplasma, Ureaplasma, Spiroplasma, Acholeplasma, Anaeroplasma, Asteroleplasma, Mesoplasma,* and *Entomoplasma*). These

bacteria are distinguished by the absence of a cell wall and the term "Mollicutes" is derived from the Latin (*mollis* meaning "soft", and *cutis* meaning "skin"). A precise phylogenetic classification of *Haemobartonella* and *Eperythrozoon* organisms was made possible by sequence analysis of the 16S ribosomal RNA genes (77, 84, 102). The sequences indicated a close phylogenetic relation to *Mycoplasma* species. Finally, Neimark and co-workers proposed the reclassification of all members of the genera *Haemobartonella* and *Eperythrozoon* to the genus *Mycoplasma* (82, 83). Despite the close phylogenetic relationship between this group of red cell pathogens and the pneumoniae group of mycoplasmas, haemotrophic mycoplasmas represent a distinct new cluster within the genus *Mycoplasma* (75). Recent phylogenetic analysis of *Mycoplasma* species using partial sequences of the RNase P RNA gene (*rnpB*) basically confirmed results of the 16S rRNA gene phylogeny. It was proven that all haemoplasmas were present within a single clade and most closely related to *Mycoplasma fastidiosum*. Furthermore, it was shown that haemoplasmas are subdivided into two groups; the haemominutum group, including *M. suis, M. wenyonii, M. ovis, Candidatus* M. haemolamae, *Candidatus* M. haemominutum, *Candidatus* M. kahanei and *Candidatus* M. haematoparvum and the haemofelis group, including *M. haemofelis, M. haemocanis, M. coccoides* and *M. turicensis* (93).

1.1.3 Infectious anaemia of pigs

Mycoplasma suis is strongly adapted to swine and causes infectious anaemia in pigs (IAP), a disease mainly occurring in weaned and feeder pigs when they are under stress as well as in pregnant sows immediately prepartum (46, 75, 113). During acute clinical IAP pigs suffer from heavy *M. suis* bacteraemia that causes severe and haemolytic anaemia occasionally leading to death (75, 135). Typical clinical signs include skin pallor, icteroanaemia with inappetence, hypoglycaemia, cyanosis at the acrae, general unthriftiness, poor weight gain, enhanced susceptibility to other infections as well as fever reaching up to 42 °C (42, 49). Recent studies addressing the development of autoimmune haemolytic anaemia during clinical IAP identified actin as a target protein for autoreactive antibodies during the acute state of the disease (26). Confirmation of an *M. suis* infection in routine diagnosis is done by direct detection of *M. suis* particles on and between the erythrocytes in acridine orange-stained blood smears (48, 75). In addition, Hoelzle and co-workers established a quantitative LightCycler PCR assay based on the *msg1* gene of *M. suis* (LC MSG1 PCR) representing a powerful tool for the diagnosis and quantification of *M. suis* within infected blood samples as

well as for prevalence and pathogenesis studies (50).

Clinical symptoms of the IAP are successfully cured by tetracycline medication. Nevertheless, pigs once infected with *M. suis* remain lifelong carrier animals and are, therefore of epidemiological importance (15, 42, 49, 113). In fact, the majority of IAP-associated economic losses in swine industry are attributed to the chronic low-grade *M. suis* infections as they are associated with growth retardation, poor reproductive performance, general economic inefficiency, chronic anaemia as well as higher susceptibility to respiratory and enteric infections. In chronic *M. suis* infections no or only a few *M. suis* particles are detected in peripheral blood smears as well as when using quantitative real-time PCR (50) .

1.1.4 Microbial properties of *Mycoplasma suis*

Due to the unculturability of the organism it is difficult to analyse the basic microbiological features and virulence factors of *M. suis* and to perform host–pathogen interaction analyses. To date, we still have to use the splenectomised pig for propagation of the organism (42, 135). High-resolution electron microscopic examinations allowed a morphologic description of *M. suis* (97, 135): A distinct hallmark of the disease is the close association of the bacteria with the host erythrocytes, where the attached pathogen typically forms deep indentations on the surface leading to severely deformed membrane areas (Fig. 1). Fine fibrils, contained in a 30-nm electron lucent zone, connect the organism with the RBC membrane (75). The changes in the erythrocyte morphology induce the production of IgM cold agglutinins during acute IAP which are directed against the RBC surface and lead to an immune-mediated haemolytic anaemia (48, 49, 136).

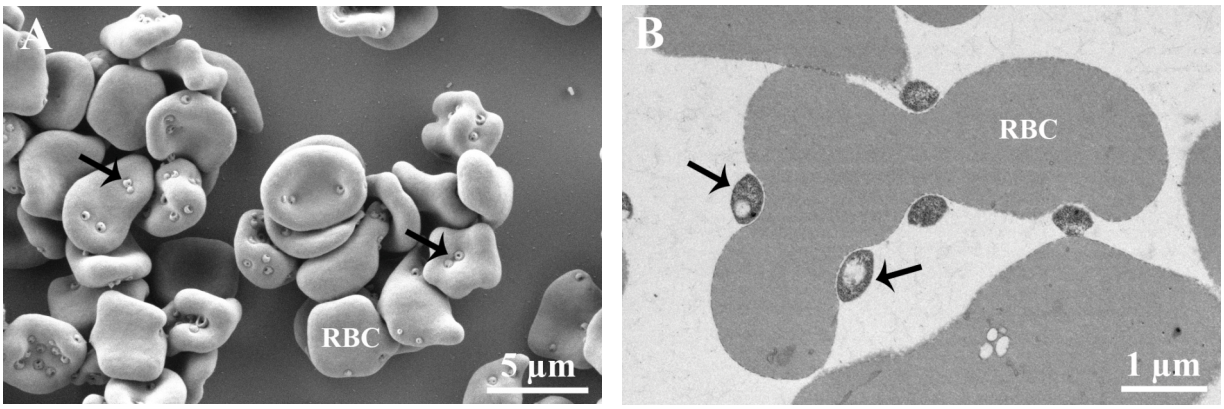

Figure 1: Scanning **(A)** and transmission **(B)** electron micrographs of porcine red blood cells (RBC) infected with *M. suis* (black arrows). An agglutination of the RBCs and deformations of RBC membranes can be observed.

To date, little is known about the mechanisms of adhesion and replication of *M. suis* on RBCs. Hoelzle and co-workers identified one protein which is presumably involved in adhesion of *M. suis* to the RBC membrane (52). MSG1 is a surface-localised protein of *M. suis* with glycolytic activity. The encoding gene *msg1* has an overall identity of the deduced amino acid sequence to GAPDHs of other pathogenic mycoplasmas ranging from 52.6 % to 54.5%. *Escherichia* (*E.*) *coli* transformants expressing MSG1 on their surface acquire the ability to adhere to porcine RBCs. Therefore, MSG1 was identified as an adhesion protein and a putative virulence factor of *M. suis*. During acute IAP a drastic reduction of blood glucose levels can be observed in infected pigs. This phenomenon is clearly associated with the *M. suis* metabolism (42, 87, 114). With MSG1, the first glycolytically active *M. suis* protein probably involved in glucose consumption was identified.

Six additional *M. suis* antigens expressed during clinical IAP and targeted by the porcine immune system were identified in our group by proteome analysis. These potential pathogenicity factors were identified as two heat shock proteins (DnaK, GroEL), two carbohydrate metabolism enzymes (enolase, pyruvate dehydrogenase), an RNA helicase involved in RNA rearrangement, and an actin-analogous protein (49, 53). In further studies the encoding gene of the DnaK-like protein (HspA1) could be identified by screening genomic *M. suis* DNA libraries. The protein was characterised upon recombinant expression in *E. coli*. HspA1 is located in the cytoplasm of *M. suis* as well as in the membrane and exhibits ATPase activity and antigenicity in experimentally infected pigs (51).

1.2 Bacterial persistence

1.2.1 Definition

The term ‘bacterial persistence’ is defined as ‘the capacity of bacteria to tolerate exposure to lethal concentrations of bactericidal antibiotics’ which is restricted to a small slow-growing subpopulation of cells and has a mechanistic basis of origin which is not fully understood (55, 61). However, it was Bigger (11) who first noticed the existence of a tiny fraction of bacterial survivors, of the order 10^{-6} or less, in cultures of *Staphylococcus aureus* treated with high concentrations of penicillin. These cells regrew after removal of the antibiotic and turned out to be as sensitive to penicillin as the original culture, again leaving a small fraction of survivors or ‘persisters’.

1.2.2 Genetic analysis of persister cells

As the frequency of persisters in a given population of cells is rather low it is difficult to obtain persister cells in sufficient quantity for experimentation. The isolation of *E. coli* high persister (*hip*) mutants by Moyed and co-workers in the early 1980s [*hip BA* operon (12, 80, 81)] and by Wolfson and co-workers [(*hip Q*) (131)] was therefore a breakthrough allowing isolation of persister cells in sufficient numbers for analysis. Based on experimental data of these mutants Balaban and co-workers (3) divided wild-type *E. coli* cells in three subpopulations, namely, normal (non-persister) cells, type I persisters, a subpopulation of non-growing cells generated at the stationary phase of the previous growth cycle having a very long lag phase (~14 h) and type II persisters, generated during growth. The slow-growing persister cells turned out to be ampicillin-tolerant while the fast-growing normal cells were ampicillin-sensitive. Based on these observations Kussel and co-workers (61) described persistence as an 'insurance' strategy of bacteria optimized to face very rare antibiotic challenges.

Many studies have been focused on the identification of genes responsible for the generation of persisters and on the molecular mechanism of persistence. Gene expression profiles of isolated persister cells showed an overexpression of genes belonging to the SOS family (*recA, umuDC, uvrAB, sulA,* etc.), genes grouped into the heat and cold shock response family (htrA, htpX, cspH, etc.), many genes that are toxin-antitoxin (TA) modules (*dinJ/yafQ, relBE, mazEF,* etc.), and a gene encoding for a translational inhibitor (*rmf*) (58). In contrast, genes involved in energy production and non-essential functions such as flagellar synthesis are generally downregulated, supporting the hypothesis that persisters are in a state of dormancy, a period in the life-cycle when growth is temporarily stopped (11, 55, 66). TA modules are operons consisting of two genes, one of them encoding a stable toxin and the other one an unstable antitoxin which neutralises its cognate toxin. Transcription of the genes can be repressed upon binding of the TA complex or the antitoxin to the DNA in the promoter region. The toxin inhibits important cellular functions such as translation, cell wall synthesis and DNA replication, thereby inactivating the targets of action of antibiotics. If persisters are dormant and non-proliferative, then the antibiotics can bind to, but will be unable to corrupt the function of their target molecules (66). The toxin gene component of the *relBE* operon, for instance, codes for a translation inhibitor (16) that, when overexpressed by plasmid-borne *relE,* increases the resistance of the cell to ofloxacin (a fluoroquinolone), cefotaxime (a

cephalosporin), and tobramycin (an amyloglycoside) by 10-10'000-fold, leading to the production of dormant persister cells. Despite of the identification of genes involved in persister formation many aspects of the mechanisms of persistence are still unclear. However, it is assumed that there are many different mechanisms that might be involved.

1.2.3 Persister cells in latent infections

Persisters pose tremendous difficulties in the treatment of many infectious diseases (55, 63, 64, 66). In most chronic (persistent) infections it seems that pathogens circumvent their clearance by antibiotic treatment and are also shielded from the host's immune defence system. Those bacteria apparently hide in biological niches, such as biofilms (*Pseudomonas aeruginosa*) (64, 66) or macrophages and granulomas (*Mycobacterium tuberculosis*), displaying a potential source for the emergence of heritable antibiotic resistance (63). It is assumed that dormant persister cells are responsible for the latent and asymptomatic stages of disease (66). HM show a tendency to establish chronic and often clinically inapparent infections (8, 75, 113) Although clinical symptoms of acute IAP can usually be treated successfully by means of tetracyclines, glucose, and iron dextran it is impossible to eliminate *M. suis* from infected pigs (35). Even though the chronic nature of mycoplasma infections has already been observed for other mycoplasmal species no biological niche containing dormant persister cells has been found, so far.

1.2.4 Persisters in bacterial biofilms

Bacteria are discussed to persist within their host by the formation of biofilms (74). Bacterial biofilms are highly organised, surface-adherent structures, consisting of bacterial communities embedded in an exopolysacharide matrix (55). In comparison to the free-floating (planctonic) cells they are recalcitrant to host defences and stress, such as elimination by antibiotics (30, 64, 65, 67). Brooun and co-workers (14) showed that even at high doses of ciprofloxacin, an antibiotic that could kill growing as well as non-growing cells, a fraction of cells survives in biofilms suggesting that they are persisters. According to a model of Lewis (64) treatment with ciprofloxacin eliminates the planctonic cells as well as the majority of biofilm-associated cells except the persisters. Upon withdraw of the antibiotic, the persisters inside the biofilm grow and repopulate the niche leading to secondary infection which, in turn, produces antibiotic-sensitive as well as antibiotic-resistant persisters.

Biofilms can cause severe host damage as attracted phagocytes that fail in phagocytosis release phagocytic enzymes which damage the surrounding tissue and aggravate the infection (74). In addition to the establishment of chronic infection biofilms may cause attacks of acute infection when planctonic cells are periodically released from the biofilm.

1.2.5 Mycoplasma biofilms

Little is known about the virulence mechanisms of mycoplasmas and the methods of persistence in the host, such as the formation of biofilms. In their study McAuliffe and co-workers examined a wide range of *Mycoplasma* species for their ability to form a biofilm *in vitro* (74). Most of the studied *Mycoplasma* species (e.g. *Mycoplasma putrefaciens, M. cottewii, M. yeatsii, M. agalactiae* and *M. bovis*) produced prolific biofilms that were considerably more resistant to stress, including heat and desiccation, than planktonic cells. It was shown by several research groups that *in vitro* formed mycoplasmal biofilms contain all of the highly differentiated structural features, such as honeycombed regions and areas of outgrowths referred to as mushrooms or towers, found in biofilms that are formed by other bacteria (74, 109). In comparison to the honeycombed regions mycoplasmal cells in the tower structures are more densely packed together. *In vitro* studies of Simons and Dybvig (110) demonstrated that cells within the honeycomb region of the biofilm are sensitive to lysis by complement or the antimicrobial protein gramicidin, but cells in the towers are relatively resistant. These results indicated that biofilm formation protects mycoplasmas from antimicrobial agents and the innate immune system. There are only minor reports of mycoplasmal biofilms formed *in vivo*. In their study on biofilms of *Mycoplasma pulmonis* Simmons and Dybvig observed that biofilms formed on the epithelium of trachea in tracheal organ culture and in experimental infected mice have a similar structure and biological characteristics as biofilms formed *in vitro* (111). The densely packed towers represented a substantial reservoir of mycoplasmas that are resistant to host immunity and that might display the source of chronic disease in *Mycoplasma* infection.

1.3 The vascular endothelium in health and disease

1.3.1 Structure and function

The vascular endothelium consists of a cell monolayer lining all blood vessels in the circulatory system providing a barrier between the vascular space and the surrounding tissue.

This cellular layer is an active and dynamic organ important in several housekeeping functions in health and disease, such as regulation of vascular tone, maintenance of blood circulation, fluidity, coagulation, and inflammatory responses (32, 68). Endothelial activation may result from a variety of insults such as disordered cytokine production, microbial infection or free radical formation. Several diseases contribute to vascular dysfunction, e.g. atherosclerosis, type-II diabetes mellitus, hypertension and inflammatory diseases (68, 91).

1.3.2 Microbial interactions with the vascular endothelium

Interactions of pathogens with the endothelium can occur via a variety of mechanisms. The first contact of pathogens with the endothelium is typically mediated by specific pathogen surface structures miming endogenous ligands and thereby permitting adhesion or uptake into the endothelium, e.g. the fibronectin-binding protein A of *Staphylococcus aureus* binding to the host cell integrin $\alpha 5\beta 1$ (47, 112).

Some bacteria are able to perturb membrane integrity of endothelial cells (ECs) by the secretion of exotoxins in the host environment (10, 47). A distinction is drawn between pore forming exotoxins integrating into the host cell membrane and bacterial exotoxins binding to EC receptors resulting in toxin translocation into the cytosol. Pore forming exotoxins create small holes in the plasma membrane of eukaryotic cells allowing uncontrolled ion fluxes that result in endothelial hyperpermeability and oedema formation. In addition, these toxins activate the expression of endothelial adhesion molecules on the cell surface resulting in enhanced endothelial-leukocyte interaction and inflammatory responses.

Furthermore, lipid A, the endotoxin component of lipopolysaccharide (LPS), a cell wall component of gram-negative bacteria, causes a systemic inflammatory response syndrome *in vivo* in which vascular injury displays the major pathophysiological change (9, 31, 33). LPS induces endothelial apoptosis and also interacts with neutrophils leading to an oxidative burst as well as the release of apoptosis-inducing substances from neutrophilic granula (45). Many pathogens are able to invade ECs (18, 118, 124), either via initiation of receptor-mediated endocytosis or via direct affection of the cytoskeleton by pathogen derived proteins (47). Inside the host cell pathogens either remain within a vacuole or escape into the cytoplasm, such as *Chlamydia* (118) and *Listeria* (47), respectively. Most of these interactions depend on alterations of the actin cytoskeleton (47) by bacterial effector molecules.

1.3.3 Inflammation of the vascular endothelium

Usually, adhesion of pathogens to the endothelial surface is enough to activate numerous signalling pathways. “Pattern recognition receptors” on the surface of ECs recognize conserved microbial structures, so called “pathogen-associated molecular patterns” (PAMPs), shared by different microbes (e.g. LPS, bacterial lipoproteins and peptidoglycan). The best known of these receptors belong to the family of *toll*-like receptors (TLR) consisting of TLR1-10 (123). Upon activation of TLRs complex signalling cascades are activated leading to the transformation of ECs into a pro-inflammatory phenotype (47). Pro-inflammatory responses include mediator release, leukocyte recruitment, pro-coagulant activity and breakdown of the endothelial barrier function (47). LPS, for instance, induces endothelial apoptosis by interaction with TLR 2 and 4 (4). Inflammatory mediators produced by ECs involve chemotactic cytokines, lipid mediators like prostaglandins or platelet-activated factor and complement factors (38, 47). In addition, expression of adhesion molecules [P-selectin, E-selectin, intercellular adhesion molecule-1 (ICAM-1), or vascular cellular adhesion molecule-1 (VCAM-1)] by the endothelium results in recruitment of leukocytes via interaction of the adhesion molecules with their ligands expressed on leukocytes (34). This cell-cell interaction results in subsequent rolling, adhesion and transmigration of leukocytes through the endothelium into the underlying tissue. By producing vasoactive substances, i.e. nitric oxide (NO), prostacyclin, and endothelins upon stimulation with inflammatory agents the endothelium has a great influence on blood pressure (127). As an example, NO is a potent vasodilator and is liberated in large quantities in the perivascular space upon pro-inflammatory stimulation. The resulting increase in local blood flow as well as reduction in velocity of blood flow enhances attachment of leukocytes to the adhesion molecules on the ECs. Furthermore, large amounts of NO may contribute to the killing of pathogens (47).

The quiescent endothelium provides an anti-thrombotic surface that inhibits the coagulation cascade by preventing activation of thrombin. Thrombin, once activated, stimulates coagulation by causing platelet activation and activation of several coagulation factors (68) bringing up a molecular fishing network for the immobilization of invading pathogens.

The hallmark of acute inflammatory reactions on the endothelium is the development of the aforementioned hyperpermeability resulting in oedema formation (116). Most of the activated signalling pathways lead to an increased actin-myosin interaction and contraction of ECs resulting in formation of intercellular gaps that break down the barrier function (116).

Furthermore, TNF-α or leukocyte-derived oxygen radicals and proteases can attack the endothelium promoting hyperpermeability by the direct degradation of cell-cell contacts or cell-matrix adhesions. As a consequence pathogens gain access to the sub-endothelial matrix and may colonise the host tissue (47, 69). In cases of severe systemic infections such as sepsis endothelial dysfunction contributes to the development of multiple organ failure. Moreover, loss of barrier function can result in oedema formation and distribution of pathogens in specially protected compartments like the brain by overcoming the blood-brain barrier (47).

1.3.4 Endothelium in apoptosis

Apoptosis is a mode of "programmed" cell death (PCD) leading to the genetically determined elimination of cells (23). It is a normal physiological process during development and aging and a homeostatic mechanism to maintain cell populations in tissues. PCD can also occur as a defence mechanism in immune reactions or when cells are damaged (88). Apoptosis leads to various morphologic changes including blebbing, loss of membrane asymmetry and attachment, cell shrinkage, nuclear fragmentation, chromatin condensation, and chromosomal DNA fragmentation (23). Apoptosis of ECs is responsible for organ failure in bacterial sepsis and *Plasmodium* (*P.*) *falciparum* caused malaria (44, 54). In malaria apoptosis can be induced by *P. falciparum*-parasitized RBCs carrying *P. falciparum* erythrocyte membrane protein-1 on their surface, which binds specific to receptors on ECs. In sepsis, bacterial products such as LPS can trigger endothelial apoptosis upon interaction with TLR2 and TLR4 (4).

Neutrophils contribute to a great extend to endothelial apoptosis in malaria and sepsis by direct interaction of leukocyte function antigen 1 (LFA1) on neutrophils with ICAM-1 on ECs. Furthermore, neutrophils, activated by microbial substances such as LPS, lipoteichoic acids, peptidoglycans or *P. falciparum* parasite antigens, release apoptosis-inducing reactive oxygen species (ROS) and proteases from neutrophil granula (45).

Cytokines such as TNF-α are known to sensitise ECs to undergo apoptosis via induction of signal transduction pathways involving the intracellular production of ROS (19). In addition, TNF-α influences EC viability by altering the balance of regulatory molecules that either induce or suppress apoptosis (95). Bacteria-activated platelets do not only promote pro-coagulative changes and pro-inflammatory responses. They also contribute to vascular damage and EC apoptosis through a variety of mechanisms such as direct cell-to-cell contact or the induction of EC production of ROS (60).

1.3.5 Wall structure of blood vessels

Blood vessels generally consist of three layers that are separated by internal and external elastic laminae: intima, media and adventitia. The tunica intima is the thinnest layer consisting of a single lining layer of ECs and a subendothelial fibrous tissue interlaced with a number of circularly arranged elastic bands called the internal elastic lamina. The tunica media is the thickest layer that is composed of multiple layers of smooth muscle cells separated by collagen and elastic fibres. The tunica adventitia is the connective tissue surrounding the vessel with bundles of collagen and loose bands of elastic tissue. Small blood vessels (*vasa vasorum*) are located in the adventitial layer and penetrate to varying depths into the outermost portion of the medial layer supplying oxygen and nutrients to the wall of the blood vessel (57). There are some basic structural differences between arteries and veins that are related to their specific function in the circulatory system. Arteries generally receive red oxygenated blood directly from the heart and must be able to withstand the immense blood pressure whereas veins carry bluish-red de-oxygenated blood towards the heart. In the arteries blood flows fast and in spurts, reflecting the rhythmic pumping action of the heart. In veins the blood flows more slowly and smoothly without big pressure. Therefore, arteries have thick and elastic muscular walls while veins have relatively thin and slightly muscular walls. Arteries have no valves. Veins, in contrast, possess internal valves along their length to prevent back flow of blood (126).

A

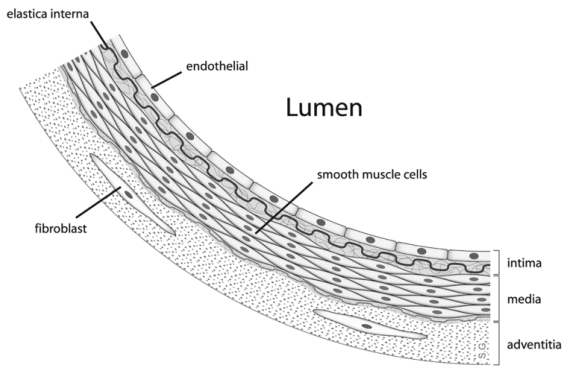

B

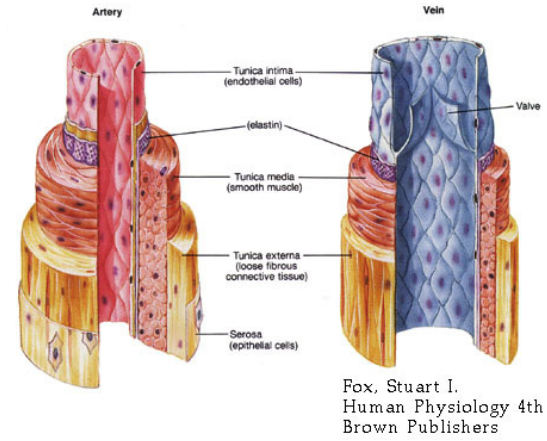

Figure 2: Anatomy overview of mammalian blood vessels. (**A**) Cross section of a human artery made for a PhD project (Maastricht, november 2005, Stijn A.I. Ghesquiere). This file is licensed under the Creative Commons Attribution-Share Alike 2.5 Generic license. Figure is copied from http://en.wikipedia.org/wiki/File:Anatomy_artery.png. (**B**) Diagram of human arteries and veins. Copied from http://www.nicksnowden.net/images/.

1.3.6 Haemorrhagic diatheses in IAP

There are repeated reports of haemorrhagic diatheses in IAP (1, 27, 43, 59, 94, 115). In their studies Plank and Heinritzi tried to characterise the type, extend and cause of *M. suis* induced bleeding diatheses. They detected a reduction of platelets as well as a prolongation of partial thromboplastin time and prothrombine time (PT Quick). Furthermore, a prolongation in reaction and clot building time was shown. Deviation from reference values was proportional to the number of erythrocytes infected with *M. suis.* The authors associated their findings with intravascular coagulation and subsequent consumption coagulopathy. However, a damage of the vasculature, a further risk factor for intravascular coagulation, has not been proved and there are no indices for infection of ECs by *M. suis*.

1.4 Objectives of this thesis

Basic research on HM is complicated due to the impossibility to cultivate these organisms. Therefore, high-resolution microscopic techniques should be applied on blood and tissue of *M. suis* infected pigs, in order to phenotypically describe the host-pathogen interactions and examine the dissemination of *M. suis* within the host. The specific aims of this thesis were the following:

(1) Examination of a putative intraerythrocytic life-style of *Mycoplasma suis* and
(2) Investigating the vasculature of infected pigs for morphologic changes and endothelial damages.

The hypothesis of an intracellular localisation of *M. suis* within the host erythrocytes was based on an increased incidence of acute IAP in feeder pigs with predominantly fatal outcome despite antibiotic therapy. In acridine orange-stained blood smears of those pigs only few *M. suis* particles were detected on and between the erythrocytes. This microscopic finding conflicted with the results of quantitative real-time PCR that detected high numbers of *M. suis* (10^9-10^{10} cells per mL) in the same blood samples. This striking difference between microscopy and PCR raised the issue of a putative intracellular localisation of *M. suis* within the erythrocytes. Verification of this hypothesis was carried out by means of experimental infection of splenectomised pigs with the said highly virulent *M. suis* strain 08/07 and microscopic analysis of infected RBCs using scanning- and transmission electron microscopy as well as confocal laser scanning microscopy. The results of this work are described in detail in the publication: Groebel, K., K. Hoelzle, M. M. Wittenbrink, U. Ziegler, and L. E. Hoelzle 2009. *Mycoplasma suis* invades porcine erythrocytes. Infect Immun 77:576-584.

The increased haemorrhagic diatheses in pigs with acute IAP, intravascular coagulation and subsequent consumption of platelets (94), as well as the strong deformation of infected erythrocytes and RBC aggregation indicate a damage of the vasculature in *M. suis* infected pigs which should be verified by means of light and electron microscopy. Histological examinations should be applied for an overall morphologic assessment of blood vessels and organs. These studies will also help to investigate if *M. suis* is able to infect and invade other host cells, such as ECs which could explain the long-life persistence of *M. suis* (and other HM). Furthermore, apoptosis assays should be carried out with cultures of porcine aortic endothelial cells incubated with serum and plasma of infected and control pigs.

2. Methods

2.1 Objective (1): Examination of a putative intracellular life-style of *M. suis*

All methods used for this objective are described in detail in the publication "Groebel, K., K. Hoelzle, M. M. Wittenbrink, U. Ziegler, and L. E. Hoelzle. 2009. *Mycoplasma suis* invades porcine erythrocytes. Infect Immun 77:576-584" presented in the section *Selected publication* on page 74.

2.2 Objective (2): Investigation of vascular damages in *M. suis* infections

2.2.1 Bacterial strains and experimental infection

Two different *M. suis* strains, discriminated by their virulence, i.e. moderate and high, were used for the experiments. The moderate strain, referred to as 3804 is not invasive, but is difficult to be controlled by means of antibiotics. However, pigs survive for several days. First clinical signs are observed as early as 10 dpi. The highly virulent strain is referred to as *M. suis* 08/07 being erythrocyte invasive and untreatable by means of tetracycline (36). An infected pig usually dies within 8 dpi despite antibiotic treatment. A splenectomised pig model was used for experimental infection of pigs with *M. suis* (41). Briefly, five- to ten week-old pigs were screened for *M. suis* negative status by quantitative PCR targeting the *g1* adhesin gene of *M. suis* and *M. suis* immunoblot as described earlier (48, 50). Pigs were splenectomised according to the method of Heinritzi (41)**.** For infection, two ml of the infected animal's blood was inoculated intramuscularly. Pigs were housed under controlled conditions and monitored for clinical signs of IAP. Clinical symptoms, feeding behaviour, and body temperature were monitored at least daily for each individual pig. Clinical diagnosis of acute IAP was confirmed by quantitative PCR and *M. suis* immunoblot as well as by microscopic detection of *M. suis* particles in blood smears stained with acridine orange (48, 75). At the time point of acute clinical attacks pigs infected with *M. suis* 08/07 were immediately euthanised (pigs 3806, 3807). Pigs infected with *M. suis* 3804 were either euthanised on the day of first appearance of high fever or treated with tetracycline (40 mg/kg body weight) and glucose (35 g glucose/l drinking water) to prevent death caused by *M. suis* induced hypoglycaemia and were then euthanised during the 3rd or 4th clinical attack.

2.2.2 Platelet count

Before experimental infection and during the course of the disease blood anticoagulated by EDTA was withdrawn for establishment of a differential haemogram. Platelet count was measued using a 3-DIFF analytical apparatus (ABX Micros CRP, AxonLab, Baden, Switzerland) according to the manufacturer's recommendations. Blood was tested within one hour of blood withdrawal.

2.2.3 Harvesting of blood vessels

Blood vessels (abdominal aorta, vein) were collected freshly and transported in pre-warmed phosphate-buffered saline (PBS) to the laboratory. After cleaning fat and adherent tissues, blood vessels were thoroughly rinsed in sterile PBS and fixed in 4 % phosphate-buffered formaldehyde for 24 h. Strips of five to eight mm (long axis of the blood vessel) were dissected on at least two different parts of the aorta and further processed for histochemistry staining as described below. The remaining parts of the blood vessel were post-fixed in 2.5 % phosphate-buffered glutaraldehyde (GA) for 24 h and stored in 0.1 M cacodylate buffer until further processing.

2.2.4 Light macroscopy and scanning electron microscopy of aortic vessels

Luminal surface ultrastructure of GA-fixed blood vessels from pigs acutely infected with *M. suis* and control pigs were examined by light macroscopy and SEM. Briefly, fixed blood vessels were sectioned into strips of 2 cm (long axis) and cut into halves for light macroscopic documentation on a Leica Z16 APO Macroscope (Leica Microsystems, Heerbrugg, Switzerland). Halves were post-fixed for 1 h at room temperature in 1 % osmium tetroxide (Fluka Chemie, Buchs, Switzerland) suspended in 0.1 M cacodylate buffer and then dehydrated with a graded ethanol series, and critical point dried (BAL-TEC CPD 030, Critical Point Dryer, Balzers, Liechtenstein). Finally, the samples were coated with 12 nm of platinum using the BAL-TEC MED 020 Coating system, mounted on aluminum stub and analysed on a Zeiss Supra 50 VP scanning electron microscope.

2.2.5 Transmission electron microscopy of aortic vessels and parenchymas

Blood vessels and parenchymas (liver, heart, kidney) were fixed in 4 % formaldehyde, cut in 1 mm - 2 mm wide segments and post-fixed in 2.5 % phosphate buffered GA solution (see above). Samples were washed in 0.05 M cacodylate buffer and stored until further processing.

Following postfixation in 2 % osmium tetroxide (Fluka Chemie, Buchs, Switzerland) in cacodylate buffer cells were washed once in 0.05 M cacodylate buffer. Samples were dehydrated in increasing concentrations of ethanol (70-100%) and then infiltrated by increasing concentrations (33 and 50 %) of Epon 812 (Fluka Chemie, Buchs, Switzerland) in ethanol for 1 h each. After incubation in a mixture of 75 % Epon and 25 % ethanol over night samples were infiltrated by fresh pure Epon for 2-3 h. Specimen were embedded in fresh epon in flat silicone rubber moulds and hardened for at least 12 h in an oven at 60°C. After preparation of ultrathin sections on an Ultracut E microtome (Reichert-Jung, Vienna, Austria) sections were placed on grids and contrasted consecutively with 4 % uranyl acetate (Fluka Chemie, Buchs, Switzerland) and lead citrate as described elsewhere (99) and were analysed with a Philips CM100 transmission electron microscope.

2.2.6 Histochemical staining of aortic vessels and parenchymas

Histochemical staining of parenchymas was done at the institute for veterinary pathology at the University in Leipzig, Germany. Briefly, formaldehyde fixed specimens were embedded in paraplast (Vogel, Giessen, Germany) using the Hypercenter XP enclosed tissue processor (Shandon, Frankfurt, Germany), sectioned into 3-4 µm slices with a sled microtome (Reichert-Jung, Vienna, Austria) and stained with haematoxylin and eosin (HE), as previously described (105). Samples were examined by light microscopy (Olympus, Hamburg, Germany).

2.2.7 TNF-α ELISA

The TNF-α concentration in sera of healthy and acutely diseased *M. suis* infected pigs was measured using a commercially available porcine TNF-α ELISA Kit (RayBiotech, Lucerne, Switzerland) according to the manufacturer's instructions. All standards and samples were run in duplicate. Briefly, different concentrations (50, 12.5, 3.125, 0.781, 0.196, 0.049, 0.012 and 0 ng/mL) of recombinant porcine TNF-α, used as standard, were prepared in Assay Diluent C. Sera of 8 healthy and 8 acutely diseased *M. suis* infected pigs were used undiluted. 100 µL of each standard and sample were added into appropriate wells of a 96-well plate coated with an antibody specific for TNF-α and incubated over night at 4 °C with gentle shaking. Solutions were discarded and the wells were washed four times with 300 µL of wash solution. 100 µL of solution with biotinylated anti-porcine TNF-α antibody was added in each well and incubated for 1 h at room temperature with gentle shaking. Solution was discarded

and wells were washed four times, as described above. 100 µL of HRP-Streptavidin solution was added to each well and incubated for 45 min at room temperature with gentle shaking. Wells were washed four times before 100 µL of TMB One-Step Substrate Reagent was added to each well. After 30 min incubation in the dark 50 µL of stop solution was added and absorbance was measured on a photometer reader (Tecan, Männedorf, Switzerland) at 450 nm.

2.2.8 Cell culture

Porcine aortic endothelial cells (PAECs) were purchased from the European Collection of Cell Cultures (Salisbury, UK) and maintained in Porcine Endothelial Growth Medium (CellMade, Archamps, France) containing penicillin (100 U/mL) and streptomycin (100 µg/mL).

For adhesion assays of *M. suis* to PAECs cell cultures were infected with plasma of acutely diseased pigs containing floating *M. suis* cells not attached to the surface of RBC's. To obtain plasma pools of healthy control pigs as well as of *M. suis* infected pigs, whole blood, anticoagulated with sodium citrate, of four healthy control pigs and acutely diseased *M. suis* infected pigs was centrifuged for 5 min at 300 × g for sedimentation of erythrocytes. Plasma containing supernatants were withdrawn carefully and stored in aliquots at -20°C. For quantification of *M. suis,* DNA was extracted from each plasma pool and analysed by quantitative PCR as described above. PAECs were used between the third and sixth passage and seeded on cover slips in 0.5 mL of medium with penicillin (100 U/mL) in 24-well tissue culture plates. Cells were incubated with 100 µL per well of the control plasma or the *M. suis* containing infected plasma for different time periods (5 min to 5 days), washed twice with PBS and fixed in 2.5 % phosphate buffered paraformaldehyde (PFA) for 2 h at 4 °C.

For apoptosis assays PAECs were used between the third and sixth subcultivation and seeded in 2 mL of medium into 6-well tissue culture plates (Greiner Bio-One, St. Gallen, Switzerland) or on cover slips in 0.5 mL of medium in 24-well tissue culture plates. PAECs were incubated with serum and plasma pools of at least four different acutely diseased *M. suis* infected pigs and four healthy control pigs, respectively. Plasma contains dissolved proteins, glucose, clotting factors, mineral ions, hormones, and, in the case of infected pigs, free floating *M. suis* cells not attached to the RBC surface. Blood serum is substantially free of fibrinogen and blood clotting factors and contains less *M. suis* particles.

Medium supplemented with recombinant porcine TNF-α (50 ng/mL) served as positive control for the induction of apoptosis. Each experiment was performed at confluence. The cells were washed twice with Dulbecco's phosphate buffered saline and incubated in Dulbecco's modified Eagle medium (DMEM) containing 30 % (v/v) of either control plasma, control serum, infected plasma or infected serum, respectively or with TNF-α for 24 h at 37 °C and 5 % CO_2.

2.2.9 Immunofluorescence staining of *M. suis* attached to PAECs

PFA-fixed PAECs on cover slips incubated with plasma of acutely diseased *M. suis*-infected pigs or healthy control pigs were washed with PBS and permeabilised with 0.2 % Triton X-100 (Sigma) for 2 min at 20-25°C. Cells were washed with PBS and non-reacted aldehydes were blocked with 0.1 M glycine (Carl Roth, Karlsruhe, Germany) in PBS for 20 min. Unspecific binding of antibodies was reduced by incubation of samples in blocking buffer (3 % BSA in PBS) for 30 min. Adhesion of *M. suis* to PAECs was visualized upon staining of *M. suis* with rabbit monospecific anti-HspA1 serum (1:100) for 1 h followed by TRITC-conjugated goat anti-rabbit IgG (Sigma-Aldrich, Buchs, Switzerland) for 1 h. PAECs were stained with FITC-phalloidine (1:80 in PBS, Invitrogen, Basel, Switzerland) and the nucleus was counterstained with DAPI (1:20'000). Confocal microscopy was performed on a Leica SP2 confocal microscope (Leica Microsystems, Mannheim, Germany).

2.2.10 Quantification of apoptosis by Annexin-V staining

To analyse EC death fluorescence staining was performed using Annexin-V-FLUOS Staining Kit (Roche, Rotkreuz, Switzerland) according to the manufacturer's instructions. Annexin-V binds to negatively charged phospholipids, specifically phosphatidylserine (PS), that are translocated during early stages of apoptosis from the inner part of the plasma membrane to the external surface. For discrimination of apoptotic from necrotic cells, which also expose PS due to the loss of membrane integrity, cells are simultaneously stained with the membrane impermeable DNA stain propidium iodide (PI). PI only detects leaky necrotic cells. PAECs incubated with 30 % (v/v) of either control plasma, control serum, infected plasma or infected serum or with TNF-α (50 ng/mL) were examined for cell death. Briefly, adherent cells from 6-well culture dishes were detached. Cells were washed twice with PBS and resuspended in 100 µL of Annexin-V-FLUOS labelling solution (Roche, Rotkreuz, Switzerland). After 10-15 min incubation at room temperature reaction was stopped by addition of 500 µL of

HEPES Buffer (10 mM HEPES, pH 7.4, 140 mM NaCl, 5 mM $CaCl_2$). Cells were immediately analysed by flow cytometry with a fluorescence activated cell sorting (FACS) device (FACSCalibur, BD Biosciences, Allschwil, Switzerland). 10'000 PAECs were recorded for quantification of cell death. Annexin-V stained cells were considered to be apoptotic whereas double-stained (Annexin-V and PI) cells were considered as necrotic. To set instrument parameters, cells fixed with 2 % PFA were used. These cells stain all positive with Annexin-V, a phenomenon described to occur as well in platelets fixed by means of PFA (132).

2.2.11 Statistical analysis

Data are expressed as the mean ± standard deviation. To test whether two groups differed significantly in apoptosis development; the *P*-values were calculated with the unpaired student t-test. Two groups were considered as significantly different if $P \leq 0.05$.

2.2.12 Analysis of DNA fragmentation

DNA fragmentation studies were done as previously described with slight modifications (95). In brief, PAECs were detached from culture plates by trypsinisation, washed twice with PBS and resuspended in 400 µL of lysis buffer (25 mM EDTA, 10 mM TRIS, 100 mM NaCl, 0.5 % SDS, 20 µg/mL RNase A and 0.1 mg/mL proteinase K), and incubated at 50 °C for 18 h. Samples were extracted twice with equal volumes of phenol and chloroform-isoamylalcohol. DNA was precipitated for 2 h at -80°C in 2 vol of ethanol, 0.1 vol of 3 M sodium acetate and centrifuged at 13'000 × g for 10 min. The pellet was washed with 70 % ethanol and resuspended in 50 µL of TE buffer (0.01 M Tris, pH 8.0, 1 mM EDTA). 2 µg DNA samples were electrophoretically separated on 1.5 % agarose gel containing ethidium bromide (0.4 µg/mL). DNA from apoptotic cells showed a typical banding pattern on agarose gels due to DNA fragmentation. DNA was visualised by a UV transilluminator at 302 nm (LTF Labortechnik, Wasserburg, Germany).

3. Results

3.1 Objective (1): Examination of a putative intracellular life-style of *M. suis*

Please refer to manuscript: Groebel, K., K. Hoelzle, M. M. Wittenbrink, U. Ziegler, and L. E. Hoelzle. 2009. *Mycoplasma suis* invades porcine erythrocytes. Infect Immun 77:576-584.

3.2 Objective (2): Investigation of vascular damages in *M. suis* infections

3.2.1 Light macroscopy and scanning electron microscopy of blood vessels

The luminal surface of blood vessels (abdominal aortas and veins) from healthy control pigs and acutely diseased *M. suis* infected pigs was assessed by means of light macroscopy and scanning electron microscopy (SEM). By using quantitative PCR the *M. suis* load of each pig was determined at the time of euthanasia from blood samples. Light macroscopy of aortic vessels of healthy pigs showed a smooth and even surface structure (Fig. 3A,B). Electron micrographs revealed a confluent layer of parallel arranged and spindle-shaped ECs of 5-8 µm in width and 10-25 µm in length (Fig. 3 C,D). High magnification of control vessels revealed holes on the surface of some ECs of 0.5-1 µm in diameter (Fig. 3E,F).

Three pigs (animal numbers 3807, 3806 and 5280) were infected with the highly virulent strain *M. suis* 08/07. Different peculiarities of vascular damage were observed in blood vessels of each pig examined.

Experimental pig 3807 was euthanised during an acute clinical attack at day 8 pi with a bacterial load of 1.65×10^9 *M. suis* cells/mL. The abdominal aorta did not show any abnormalities in the light macroscope (Fig. 4A,B). However, by SEM endothelial denudation was observed in wide areas of the aortic vessel, exposing the porous three-dimensional subendotelial structure of elastic laminae and collagen fibres (Fig. 4C-F). Most ECs were covered by numerous microvillis (Fig. 4D). A great number of leukocytes could be detected in some of the endothelial gaps (Fig. 4E), indicating an inflammatory response. RBCs adhered to the surface of the vessel wall (Fig. 4F-H). Arterial thrombi were identified by the presence of erythrocytes, leukocytes, and platelets embedded in a network of collagen fibres (Fig. 4G). On some of the erythrocytes *M. suis* cells could be identified (Fig. 4H). Eryptotic cells distinguished by characteristic changes as cell shrinkage, change in shape from discocytic to spherocytic and microvesiculation could be observed (Fig. 4H).

Experimental pig 3806 was euthanised during the first acute clinical attack at day 8 pi and had a bacterial load of $1x10^9$ *M. suis* cells/mL. Using light macroscopy blood vessels (abdominal aorta and jugular vein) displayed a fibrous change on the luminal side of the vessel wall with a red discolouration, indicating attached RBCs (Fig. 5A,B and Fig. 6A,B). By SEM a complete denudation of ECs could be detected on the aorta. The vascular wall was entirely covered with aggregated cell fragments probably containing RBC debris. In fragment free areas single RBCs embedded in a matrix of fibrin fibres as well as collagen and elastic fibres of the tunica media were visible (Fig. 5D). The vascular wall of the jugular vein of the same pig was to a great part covered with ECs (Fig. 6C,D). Large areas with endothelial gaps exposing the subendothelial matrix (Fig. 6C) indicated an initiating ablation of the endothelium. In addition, aggregated cell fragments or artefacts were seen on the surface of ECs (Fig. 6D).

Experimental pig 5280 was euthanised immediately at the time of the first clinical attack at day 12 pi. The bacterial load in the blood was $8.22x10^8$ *M. suis* cells/mL. By using light macroscopy areas with adherent blood were observed (Fig. 7A,B). With SEM those areas were identified as arterial thrombi by the presence of RBCs and platelets embedded in a network of fibrin fibres (Fig. 7G). Different parts of the aortic vessel showed distinct appearances of ECs that were irregular oriented and morphologically changed (Fig. 7C-E). In particular, many of the ECs appeared round (Fig. 7C) or had a cuboidal appearance protruding into the lumen of the vessel (Fig. 7D). In addition, a massive destruction of the endothelial layer characterised by large gaps exposing the subendothelial layer was detected (Fig. 7C-E). Bacterial biofilms of 3-6 µm in diameter were located on the surface of the vascular wall (Fig. 7E,F). These biofilms were characterised by round to elongated bacteria of 200-300 nm in size embedded in a three-dimensional granular matrix with micro-crystals. Smaller coccoid forms of less than 100 nm in size probably originated from budding-like mechanisms on the surface of the larger cells (Fig. 7F). *M. suis* cells on some of the RBCs were interconnected via small fibrils (Fig. 7H).

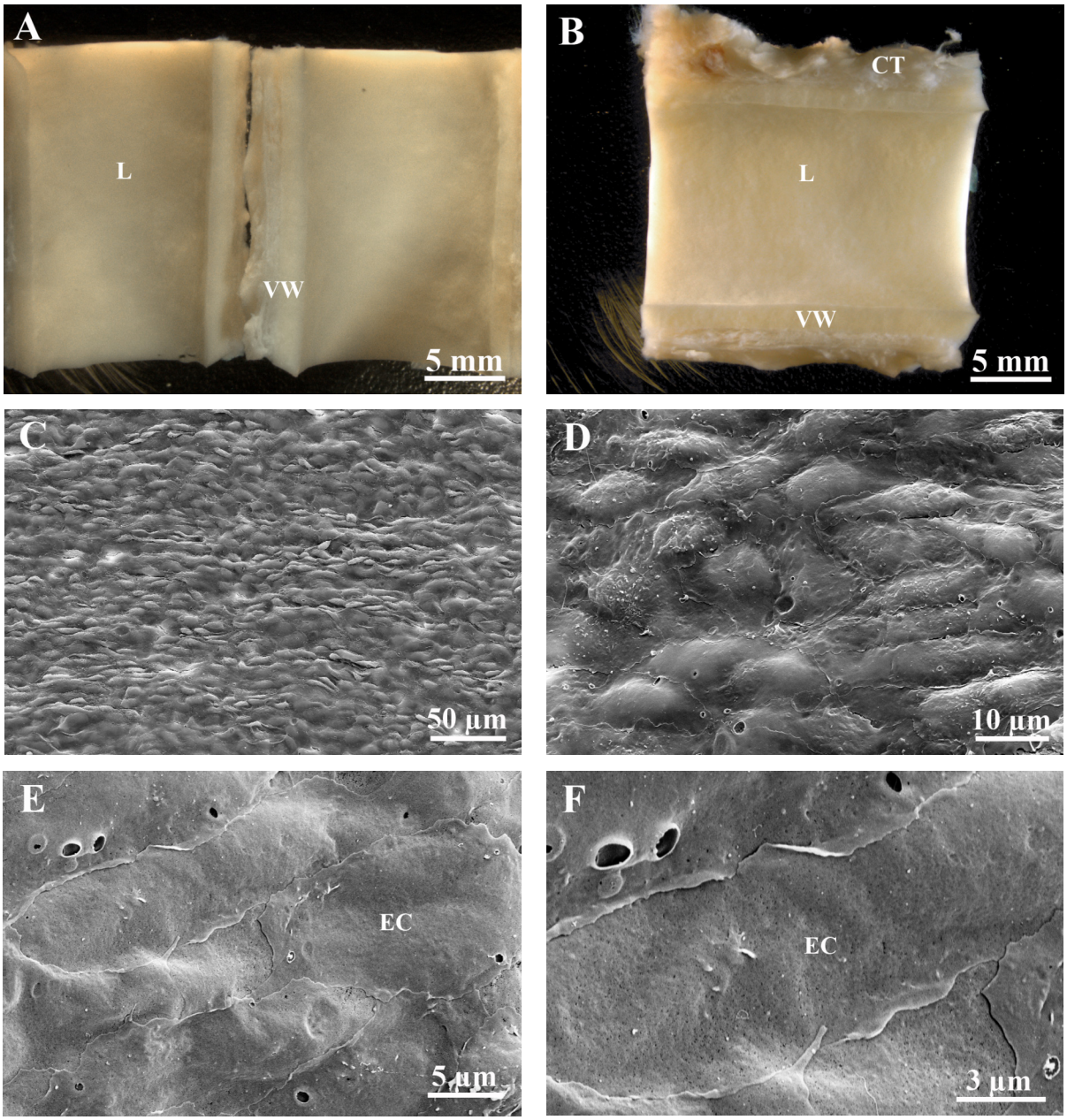

Figure 3: Healthy control pig: light macroscopic **(A,B)** and scanning electron microscopic images **(C-F)** of aortic vessels. Connective tissue (CT), Endothelial cell (EC), lumen (L), vessel wall (VW).

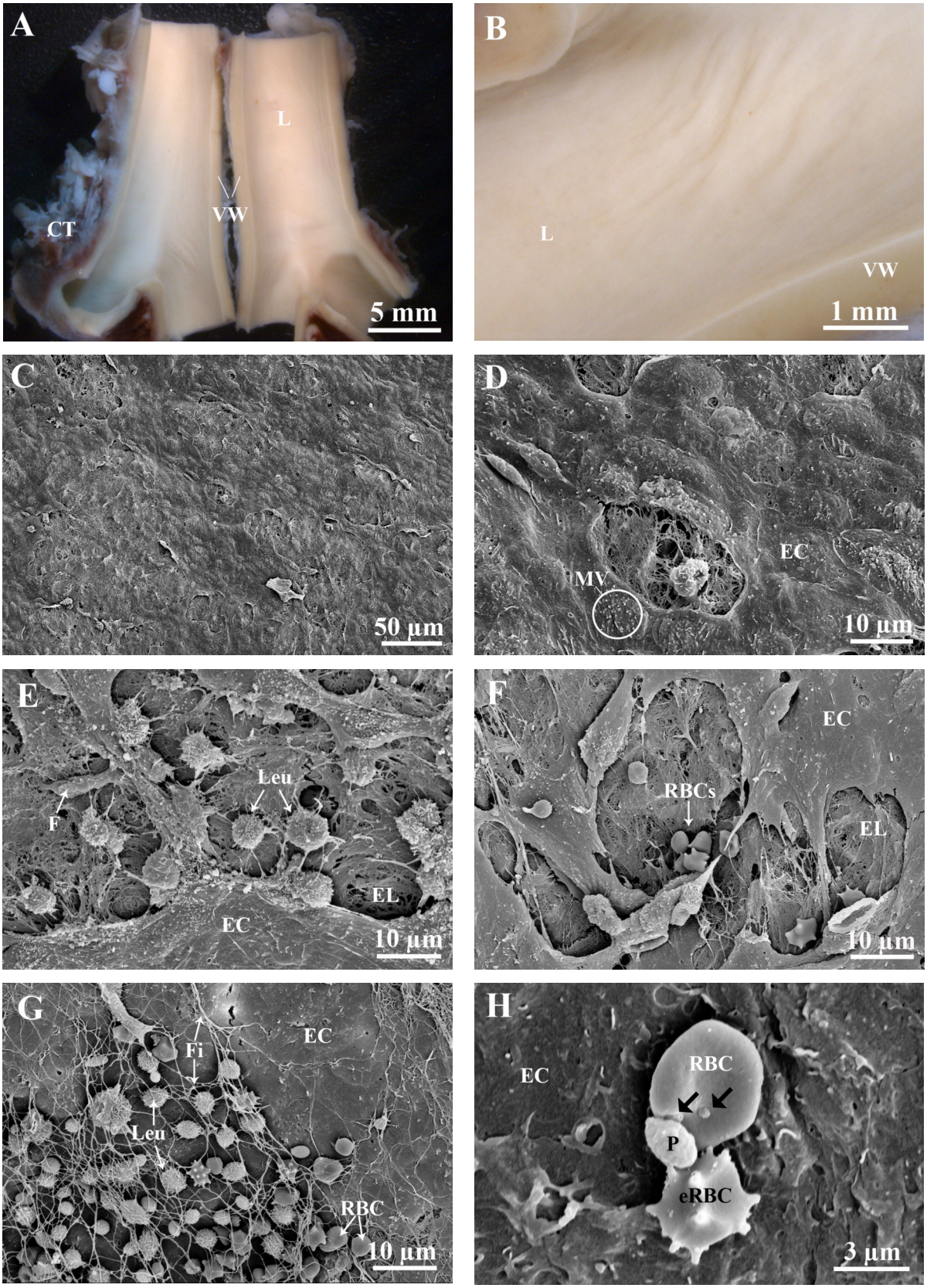

Figure 4: Experimental pig 3807 infected with *M. suis* 08/07: light macroscopic **(A,B)** and SEM images **(C-H)** of the aortic vessel. Endothelium was interrupted by large gaps **(C-F)**. Leukocytes (Leu) indicated an inflammatory reaction **(E,G)**. Red blood cells (RBCs) with attached *M. suis* cells (black arrows) and eryptotic RBCs (eRBC) adhered to the vascular wall **(H)**. Endothelial cell (EC), elastic laminae (EL), fibroblast (F), fibrinogen fibres (FI), microvilli (MV). Connective tissue (CT), lumen (L), vessel wall (VW).

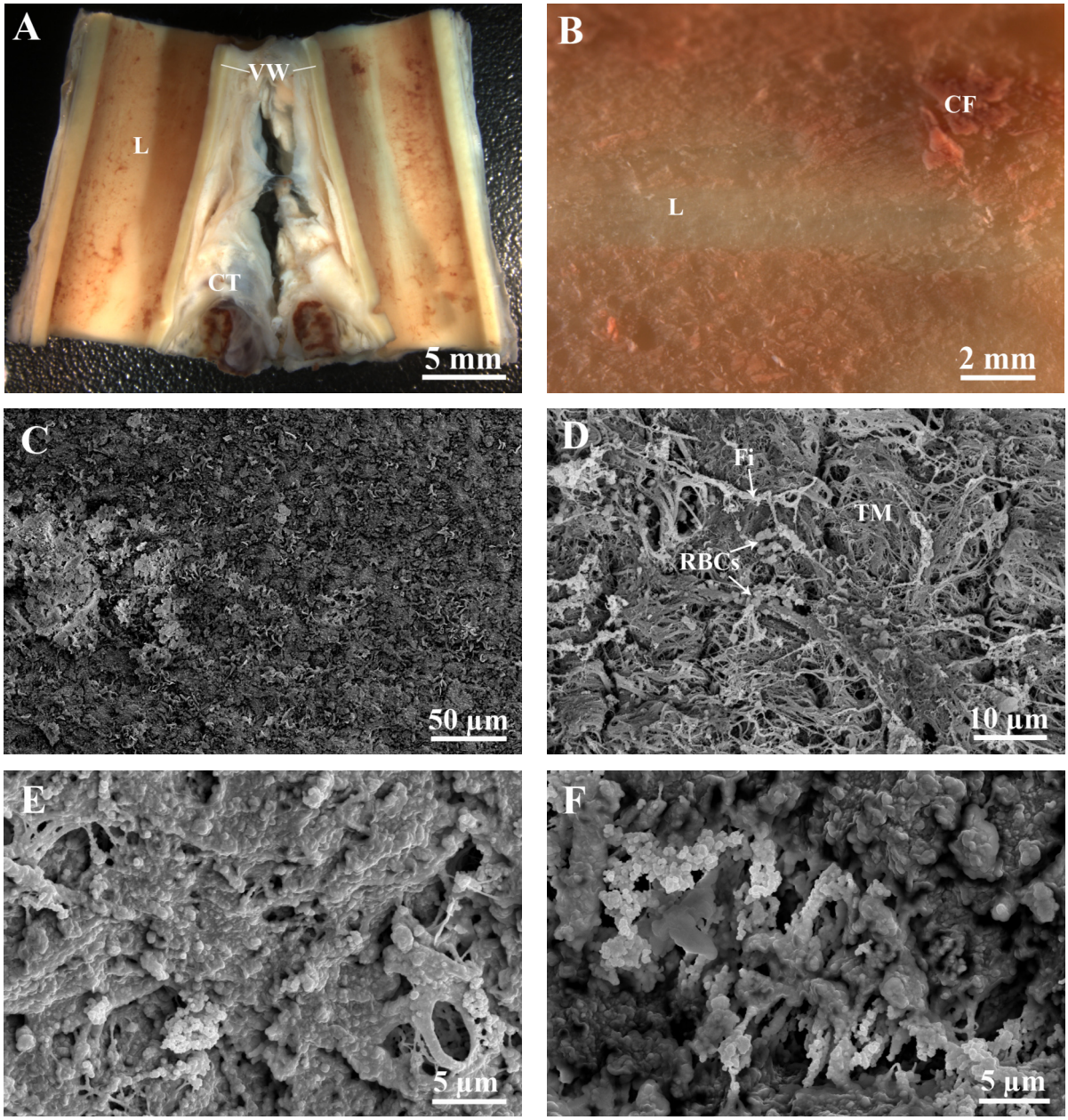

Figure 5: Experimental pig 3806 infected with *M. suis* 08/07: light macroscopic **(A,B)** and SEM images **(C-F)** of the aortic vessel. Endothelial cells and elastic laminae were absent exposing the collagen and elastic fibres of the tunica media (TM). Red blood cells (RBCs) and fibrin fibres (Fi) were detected on the subendothelial tissue **(D)**. The main part of the vascular wall was covered with aggregated cell fragments **(D-F).** cell fragments (CF), connective tissue (CT), lumen (L), vessel wall (VW).

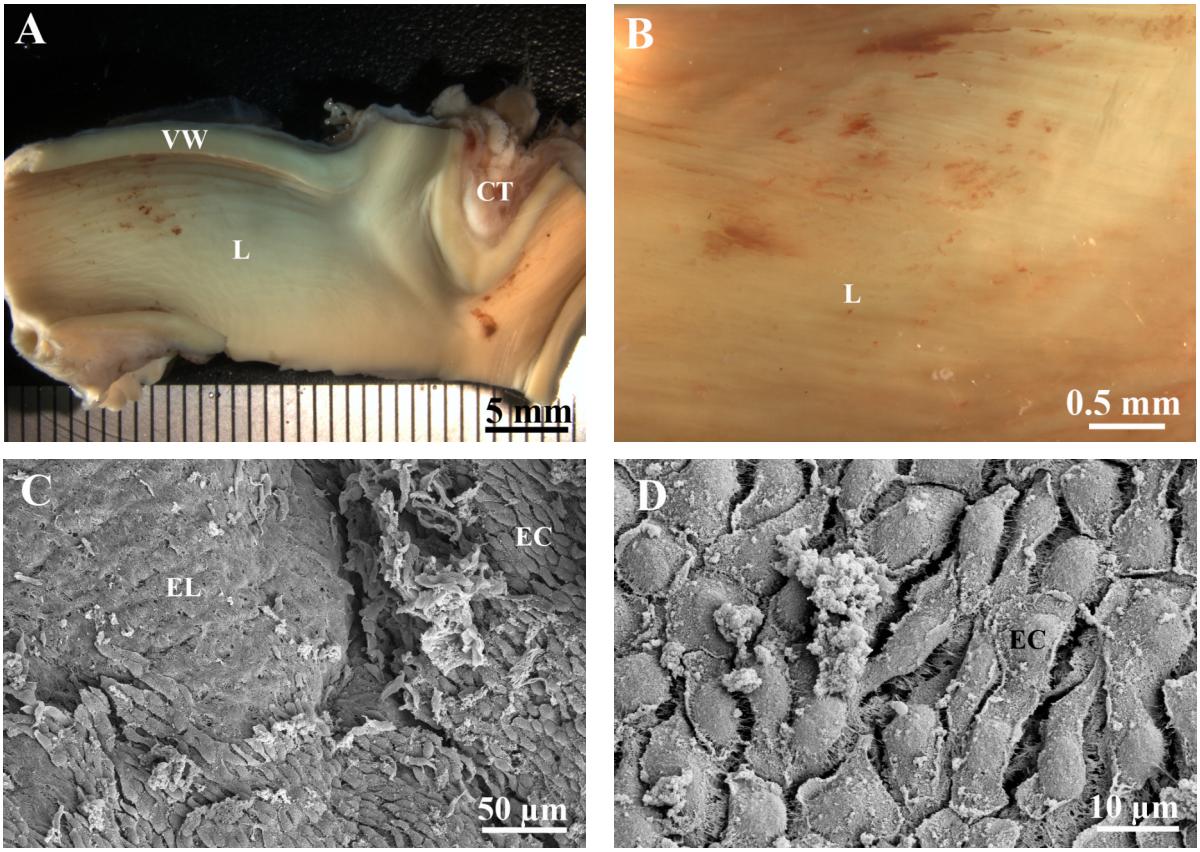

Figure 6: Experimental pig 3806 infected with *M. suis* 08/07: light macroscopic **(A,B)** and scanning electron microscopic images **(C,D)** of the jugular vein. RBC aggregates adhered to the vascular wall **(A,B)**. Endothelial cells (EC) were detached in certain areas **(C)** exposing the elastic laminae (EL). Aggregates are probably red blood cell debris or preparation artefacts **(D)**. Connective tissue (CT), lumen (L), vessel wall (VW).

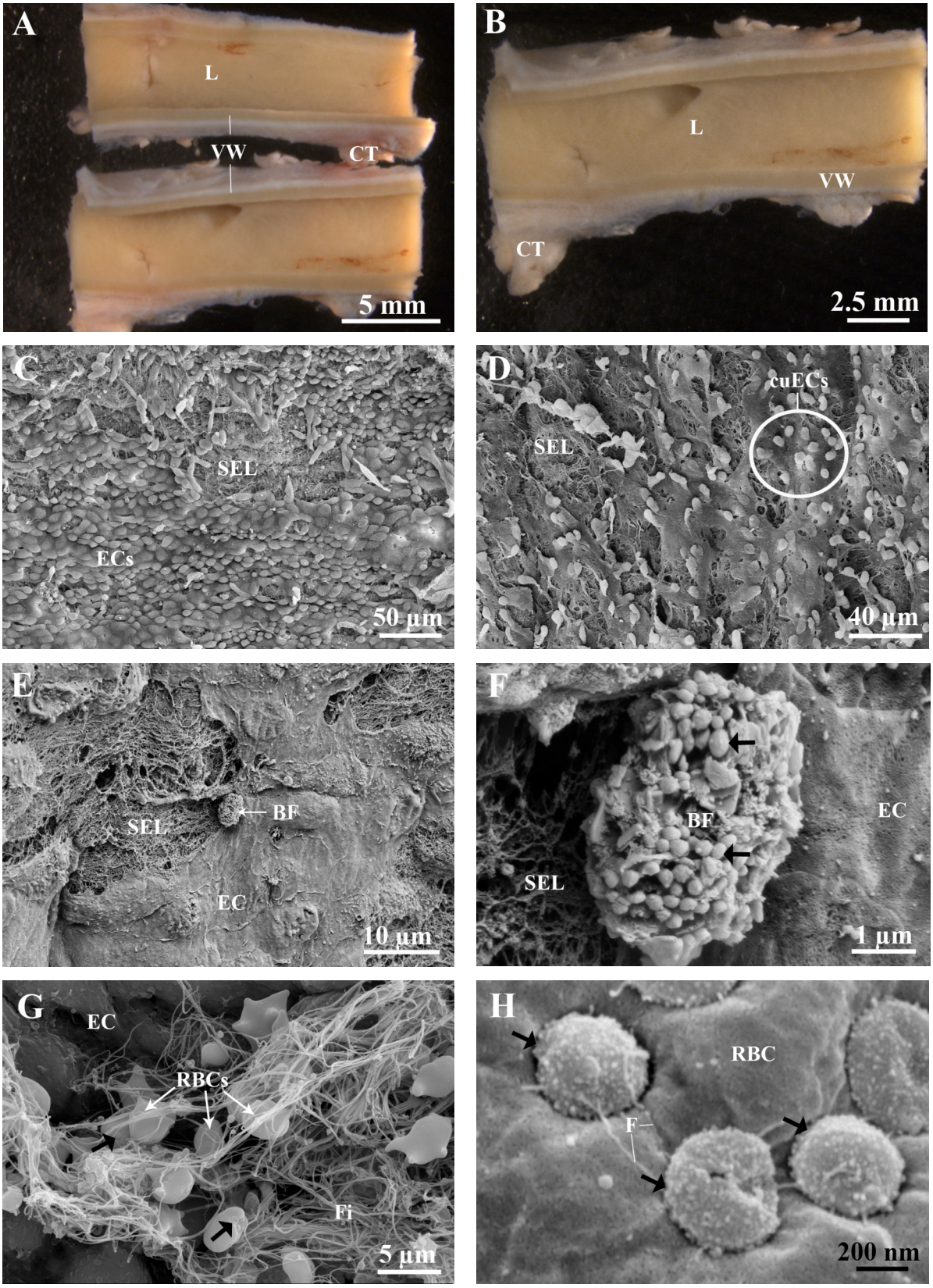

Figure 7: Experimental pig 5280 infected with *M. suis* 08/07: light macroscopic (**A,B**) and SEM images (**C-H**) of the abdominal aorta. Endothelial denudation (**C-E**) exposed subendothelial layer (SEL). Some endothelial cells (ECs) were round (**C**) or cuboidal (cuECs, **D**). Bacterial biofilms (BF) were observed (**E,F**). Arterial thrombi consisting of fibrin fibers (Fi), platelets and red blood cells (RBCs) were seen (**F**). Small fibrils (F) connected *M. suis* cells (black arrow) on the RBCs (**G,H**). Connective tissue (CT), lumen (L), vessel wall (VW).

Two pigs (experimental pigs 5275 and 3804) were infected with the moderate *M. suis* strain 3804. Experimental pig 5275 was euthanised immediately at the time of the first clinical attack at day 11 pi with a bacterial load of $5.58x10^9$ *M. suis* cells/mL. Light macroscopic pictures showed a fibrous change of the vascular wall that was covered to a great part with aggregated blood being attached to walls (Fig. 8A,B). By SEM adherent blood was identified as thrombi consisting of a densely packed fibrin-network embedding erythrocytes and platelets (Fig. 8E-G). Most ECs were parallel arranged and still had a spindle-shaped structure (Fig. 8C). However, numerous microvillis were detected on the surface of ECs and RBCs attached to the cells (Fig. 8D). *M. suis* cells on some of the RBCs were interconnected via small fibrils (Fig. 8H).

Figure 9 shows the aortic vessel of experimental pig 3804 that was chronically infected with *M. suis* strain 3804. Due to the high bacteraemia in the blood during the clinical attacks on day 20 ($4x10^{11}$ *M. suis* cells/mL) and day 35 ($2x10^{10}$ *M. suis* cells/mL) pi as well as due to the hypoglycaemia pig had to be treated with tetracycline and glucose. Subsequent attacks were milder and the pig recovered without treatment within 2 d. Pig was euthanised on day 58 pi during the 4^{th} clinical attack with a bacterial load of $1.31x10^6$ *M. suis* cells/mL. Light-macroscopic examination of abdominal aortic vessel showed anomalies on the endothelial surface structure (Fig. 9A,B) such as perforations in the vessel wall resulting in bleedings into the surrounding connective tissue. Scanning electron microscopic analysis of the vascular wall revealed a denudation of the endothelium exposing elastic laminae (Fig. 9C). In other parts of the aorta the vascular wall was completely destroyed exposing collagen and elastic fibres of the tunica media (Fig. 9D,E). Large bacterial colonies of about 30-50 µm in diameter were detected on the surface of the vessel wall (Fig. 9F). Most of these colonies were in direct contact with RBC aggregates indicating that these colonies are *M. suis* (Fig. 9F,G). Colonies consisted of a three-dimensional network of crosslinked cells with 200-400 nm in size (Fig. 9G,H).

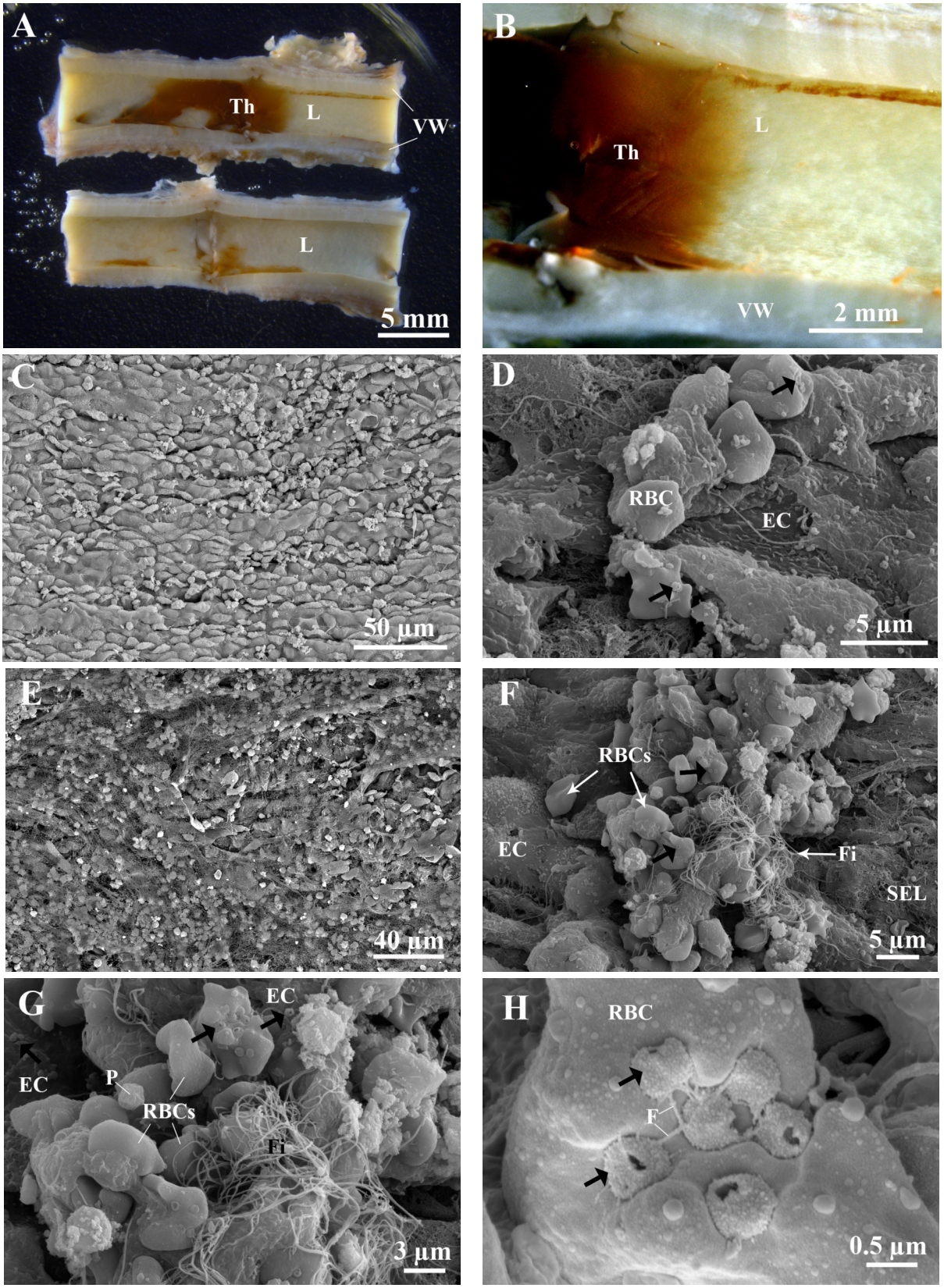

Figure 8: Experimental pig 5275 infected with *M. suis* 3804: light macroscopic (**A,B**) and SEM images (**C-H**) of the abominal aorta. Endothelial cells (ECs) were spindle-shaped and parallel arranged (**C**). Vascular wall was covered with blot clots (**D-G**) consisting of red blood cells (RBCs) and platelets (P) embedded in a matrix of fibrin fibers (Fi*). M. suis* cells, marked with a black arrow (**F-H**), were found being attached to the RBCs. *M. suis* cells (H) are interconnected via small fibrils (F). Connective tissue (CT), lumen (L), thrombus (Th), vessel wall (VW).

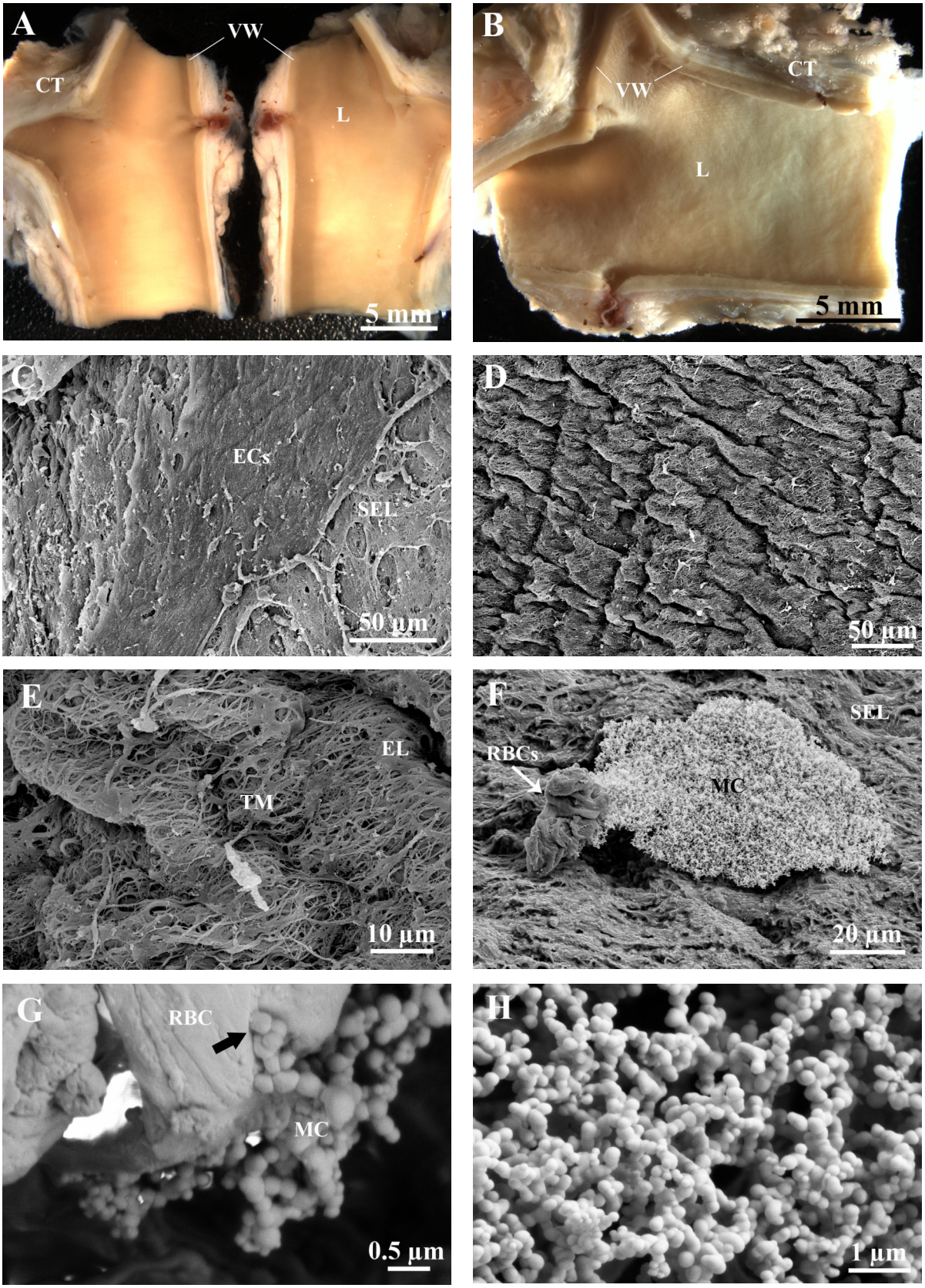

Figure 9: Experimental pig 3804 infected with *M. suis* 3804: light macroscopic **(A,B)** and SEM images **(C-H)** of the abominal aorta. Endothelial cells (ECs) were to the most part detached **(C-E)** exposing subendothelial layers (SEL) including elastic laminae (EL) and the tunica media (TM). Bacterial microcolonies (MC) being in direct contact with red blood cell (RBC) aggregates were observed on the vascular wall **(F-H).** Connective tissue (CT), lumen (L), vessel wall (VW).

3.2.2 Transmission electron microscopy of aortic sections

In Figure 10 aortic sections of a healthy control pig (Fig. 10A,B) and two *M. suis* infected pigs (Fig. 10C-F) submitted to transmission electron microscopic examination are displayed. The vascular wall of the healthy control pig was characterised by a continuous layer of ECs (Fig. 10A,B). Structural organelles such as cytosolic plasmalemma vesicles, nuclei and nuclear membranes showed a normal ultrastructure.

ECs of the abdominal aorta of experimental pig 5280, infected with the highly virulent *M. suis* strain 08/07 showed ultrastructural changes such as microvilli formation (Fig. 10C). In some ultrathin sections no ECs could be detected (Fig. 10D) which is consistent with the SEM micrographs taken from the aorta of the same pig (see Fig. 7C-E). Occasionally, cells of 5-10 µm in size with intracellular vacuoles could be detected (Fig. 10D).

ECs of the aorta of pig 5275 (Fig. 10E,F), infected with the moderate *M. suis* strain 3804, also showed morphologic changes and microvilli formation.

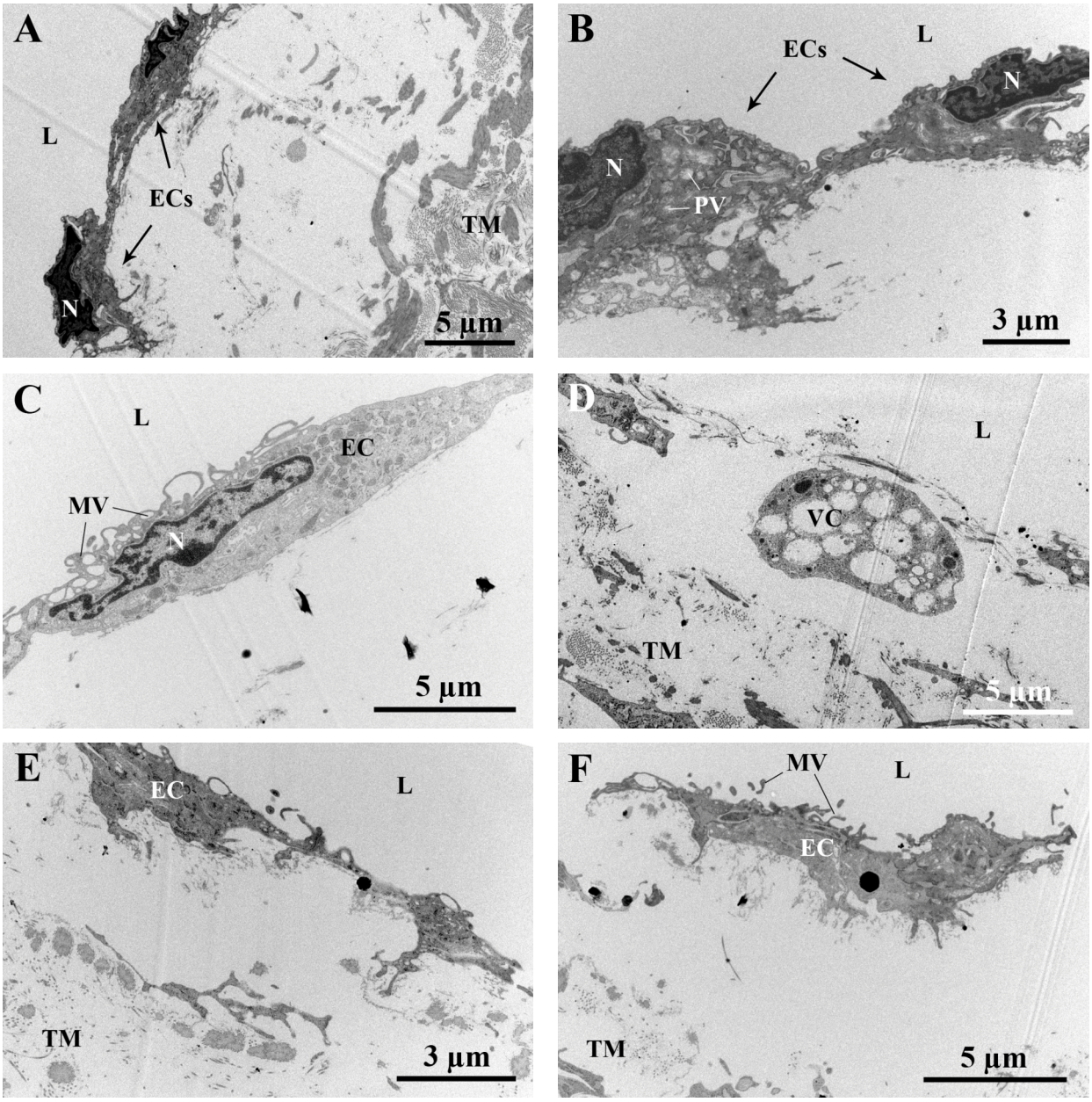

Figure 10: Transmission electron micrographs of aortic sections of a healthy pig **(A,B)** and two *M. suis* infected pigs **(C-F)**. Endothelial cells (ECs) of the control pig have a normal ultrastructure. ECs of *M. suis* infected pigs are characterised by intense microvilli (MV) formations. Lumen (L), plasmalemma vesicle (PV), tunica media (TM), vacuolic cell (VC).

3.2.3 Transmission electron microscopy of parenchymas

Parenchymas (liver, heart, kidney) of a healthy control pig and experimental pig 5275 infected with the moderate *M. suis* strain 3804 were prepared for transmission electron microscopic examination with focus on capillaries. The aim was to examine organ biopsies for morphologic changes, intravascular coagulation in capillaries and endothelial alterations.

Figure 11 shows liver preparations of the control pig (Fig. 11A,B) and the *M. suis* positive pig (Fig. 11C-F). Liver cells (hepatocytes) in both preparations had a normal polygonal structure and contacted at least one microvascular channel (sinusoid) in the liver parenchyma. Some organelles (endoplasmic reticulum, mitochondria) are shown. Bile canaliculi, thin tubes collecting bile secreted by hepatocytes, are displayed. Plasma in sinusoids of the control pig had a homogenous appearance and erythrocytes were separated from the vessel wall (Fig. 11A,B).

In the sinusoids of the *M. suis* infected pig aggregated RBCs were detected being embedded in an electron dense matrix indicating intravascular coagulation (Fig. 11C,D). RBCs attached to the vascular wall with apparent blockage of sinusoids (Fig. 11C). In addition, some ECs lining the capillary had big intracellular vacuoles containing electron dense structures. In Figure 11D an *M. suis* cell is displayed being in close contact with one of the vacuoles.

In Figure 12 transmission electron micrographs of heart biopsies from the *M. suis* negative control pig (Fig. 12A,B) and the *M. suis* infected pig (Fig. 12C-F) are shown. A cardiac muscle is composed of numerous elongate cells called muscle fibres or myofibres. Each myofibre contains many bundles of contractile myofilaments called myofibrils. Cardiac muscle cells of the control pig, being approximately 100 µm in length and 25 µm in diameter, were striated and exhibited a characteristic banding pattern with alternating light and dark bands, termed I and A bands, respectively (Fig. 12A,B). I bands were bisected by the linear Z-line. Sarcomeres, forming the basic functional unit of striated muscles, were parallel arranged and extended between adjacent Z-lines. Myofibrils were separated by stripes of regularly arranged mitochondria (Fig. 12A). Intercalated disks, containing adherens and communicating junctions, are membrane specialisations and were located between adjacent cells.

Myofibrils in cardiac muscle cells of the *M. suis* infected pig were disarranged and destructed. Mitochondria that are usually located in large numbers between each myofibril were reduced in numbers and were located disordered in the heart tissue of the *M. suis* infected pig.

Sarcomeres appeared unequal and shrunk in many parts of the tissue (Fig. 12C,D). The ECs lining the capillaries of the *M. suis* positive pig were irregular in shape with localised swellings and finger-like pseudopodia (Fig. 12D-F) whereas ECs in the control pig had a regular pattern (Fig. 12A,B). In capillaries of the *M. suis* positive pig RBCs adhered to the endothelium (Fig. 12D-F) and endothelial pseudopodia surrounded the adherent RBCs (Fig. 12D,F). Most RBCs had attached *M. suis* cells on the cell surface (Fig. 12C-F). Some of the mycoplasma cells were attached at the same time to the RBCs as well as to the ECs in the capillaries (Fig. 12D-F). In the control pig no RBCs were found to be attached to the vessel wall and no *M. suis* particles could be detected.

In kidney capillaries of the *M. suis*-infected pig an agglutination of RBCs as well as adhesion to the vessel walls could be confirmed (Fig. 13C-F). Plasma appeared electron dense and compact. In addition, some crystalline structures could be found in capillaries of the IAP-infected pig that might represent uric acid- or calcium oxalate crystals. The kidney of the control pig showed a normal ultrastructure and non-aggregated RBCs that were separated from the vessel wall (Fig. 13A,D).

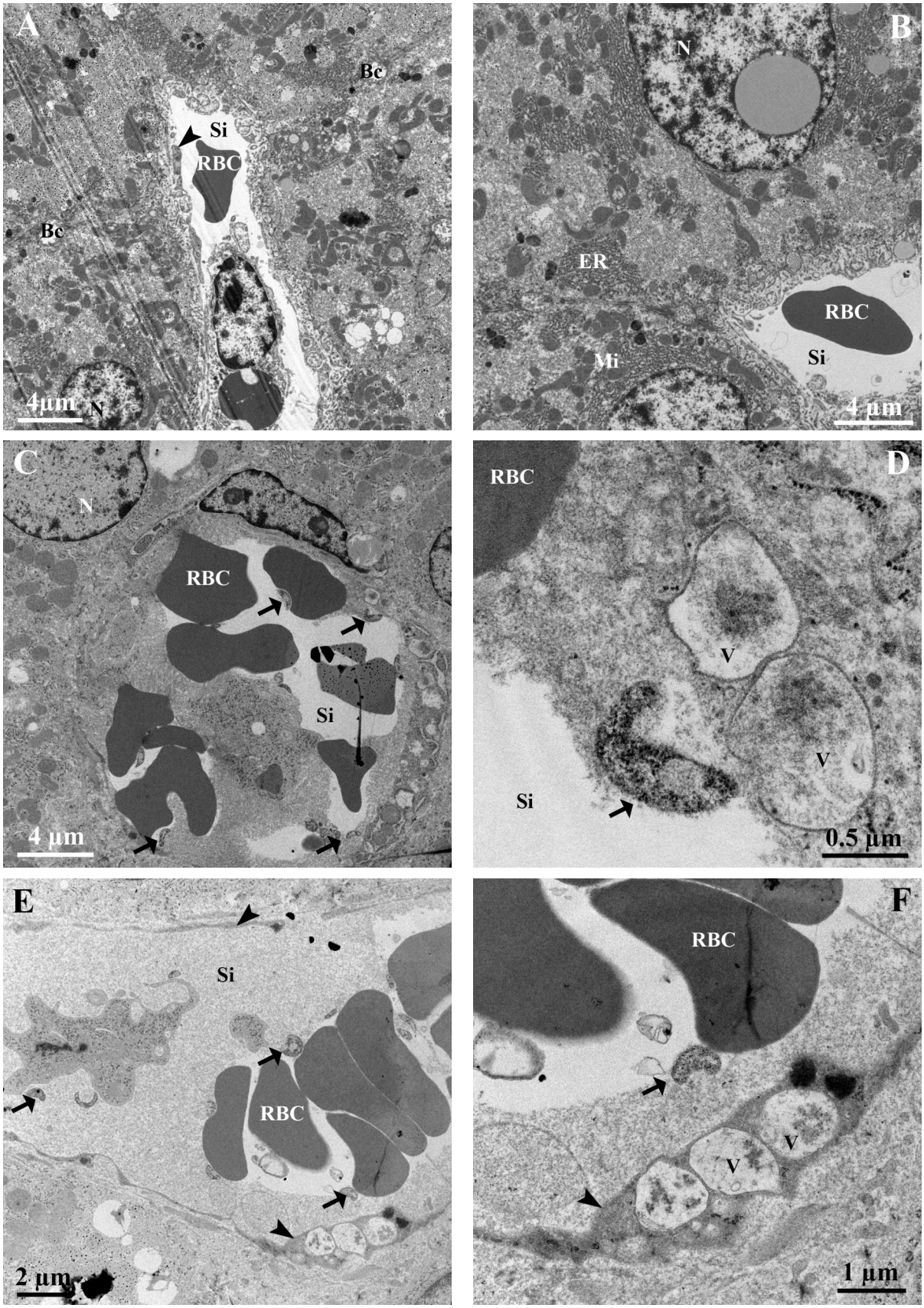

Figure 11: TEM micrographs of liver preparations of an *M. suis* negative control pig **(A,B)** and an *M. suis* infected pig **(C-F)**. *M. suis* cells are marked with a black arrow and endothelial cells (ECs) of sinusoids (Si) with an arrowhead. Red blood cells (RBCs) are aggregated (**C,E,F**) and adhere to ECs (**C**). Some ECs have large intracellular vacuoles (V). Bc (bile canaliculi), ER (endoplasmic reticulum), Mi (mitochondria).

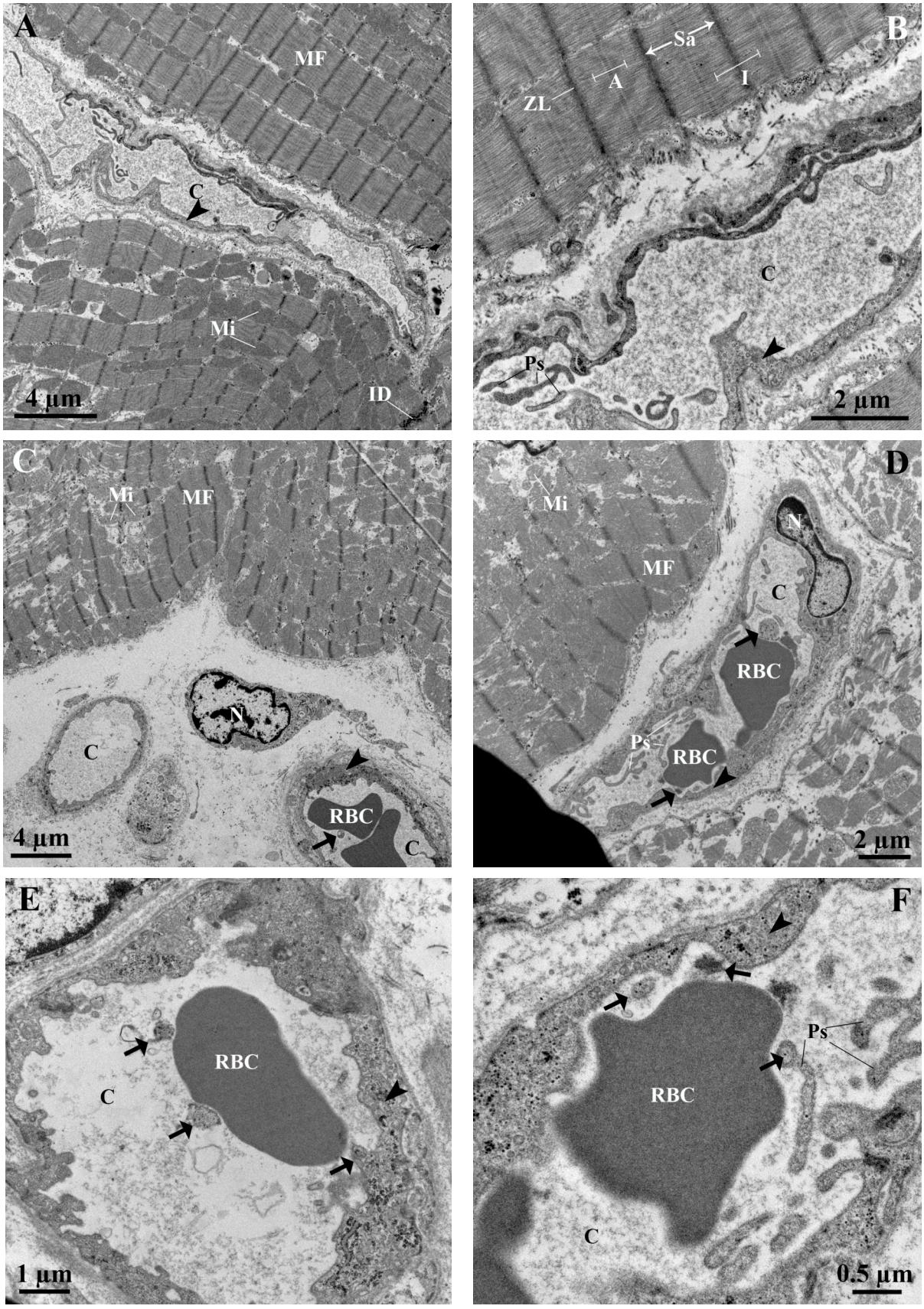

Figure 12: TEM micrographs of heart biopsies of a control pig **(A,B)** and an *M. suis* infected pig **(C-F)**. Myofibrils (MF) of the control pig show typical banding patterns with alternating A and I bands while MF of the infected pig are disarranged. *M. suis* cells are marked with a black arrow and thin endothelial cells of capillaries (c) with an arrowhead. Mitochondria (Mi), nucleus (N), pseudopodia (Ps), red blood cell (RBC).

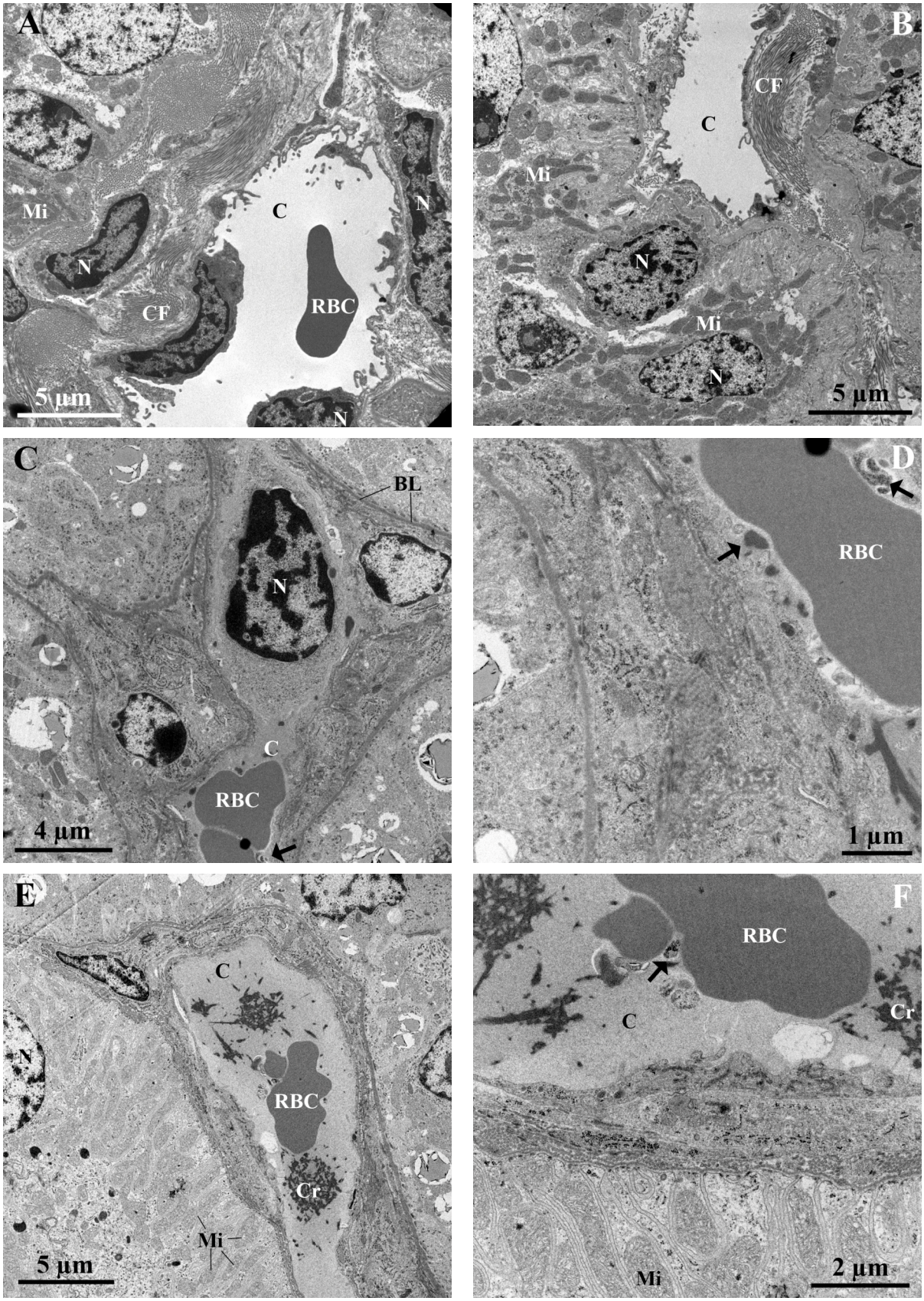

Figure 13: TEM micrographs of kidney biopsies of a control pig **(A,B)** and an *M. suis* infected pig **(C-F)**. Red blood cells (RBCs) in capillaries (C) of the IAP-infected pig are aggregated (**C,E,F**) and attach to the vascular wall (**C,D**). black arrow (*M. suis*), BL (basal laminae), CF (collagen fibres), Cr (crystals), Mi (mitochondria), N (nucleus).

3.2.4 Histochemical staining of parenchymas

Parenchymas (lung, liver) were prepared for histochemistry analyses. 5-6 µm sections were stained with hematoxylin and eosin for the assessment of the general micro-morphology (Fig. 14). The lung of the infected pig showed endothelial alterations within a vein (Fig. 14A). In addition, intravascular coagulopathy and erythrocytes being attached to the endothelium were detected. The kidney of the same pig was characterised by strong endothelial alterations in arterial blood vessels as well as attachment of RBCs to the vessel wall (Fig. 14B).

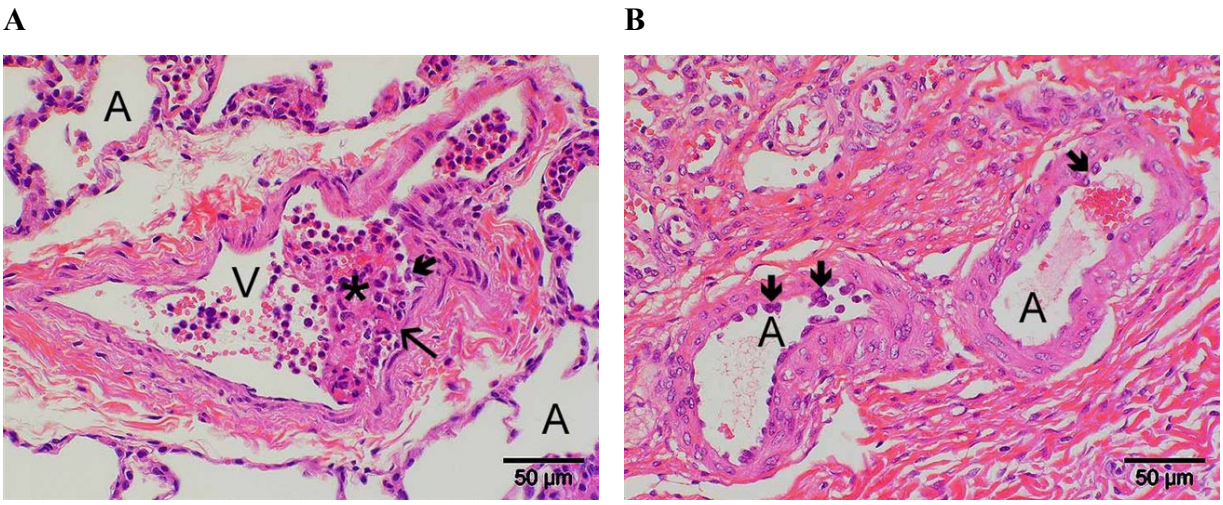

Figure 14: Hematoxylin and eosin stained sections of parenchymas. **(A)** Lung biopsy of an *M. suis* infected pig. Endothelial alterations (thick arrow) within a vein (V) with intravascular coagulopathy (star) and endothelial attachment of red blood cells (thin arrow). A: alveole. **(B)** Kidney of an *M. suis* infected pig. Distinct endothelial alterations (thick arrow) were detected in arterial blood vessels (A).

3.2.5 Measurement of TNF-α concentration in porcine sera

Cytokines such as TNF-α are known to sensitise ECs to undergo apoptosis. We evaluated if EC death in aortas of *M. suis*-infected pigs was due to increased TNF-α levels in the blood. TNF-α concentration in serum samples of 8 healthy and 8 acutely diseased *M. suis* infected pigs was measured using a commercially available porcine TNF-α ELISA kit. A standard curve using recombinant porcine TNF-α was run in parallel with concentrations ranging from 50-0.012 ng/mL. No TNF-α could be measured in any of the samples. Although the relative absorbance during read out on the photometer reader was slightly higher in serum samples of two diseased pigs when compared to the serum levels of the same pigs before the artificial infection the values were below the detection range of the standard. Therefore, results could not be interpreted.

3.2.6 Platelet count

In their studies on increased bleeding tendencies in IAP-infected pigs Plank and Heinritzi detected a reduction of platelets during the course of the infection (94). To confirm the platelet reduction in our experimental pigs the platelet count in the blood was followed before and after artificial infection using an analytical apparatus. Three pigs (animal no. 5264, 5271 and 5275) were infected with the moderate *M. suis* strain 3804 and experimental pig 5280 with the highly virulent *M. suis* strain 08/07.

Experimental pig 5264 developed acute IAP at day 8 pi and was euthanised three days later. The platelet count had fluctuations from 336-493x10^3 platelets/mm^3 before the infection and decreased to 53x10^3 platelets/mm^3 at day of euthanasia (Fig. 15A). Pig 5275 showed the first symptoms at day 11 pi and was euthanised one day later. The platelet count had fluctuations from 218-206x10^3 platelets/mm^3 and decreased to 71x10^3 platelets/mm^3 at day of euthanasia (Fig. 15B). The platelet count in the blood of experimental pig 5271 was relatively constant between 462 and 516 x 10^3 platelets/mm^3. Rapidly after the infection the concentration decreased to 129x10^3 platelets/mm^3 (Fig. 15C). Pig 5280 developed acute IAP 12 days pi. Platelet count decreased constantly from 441 to 92x10^3 platelets/mm^3 (Fig. 15D).

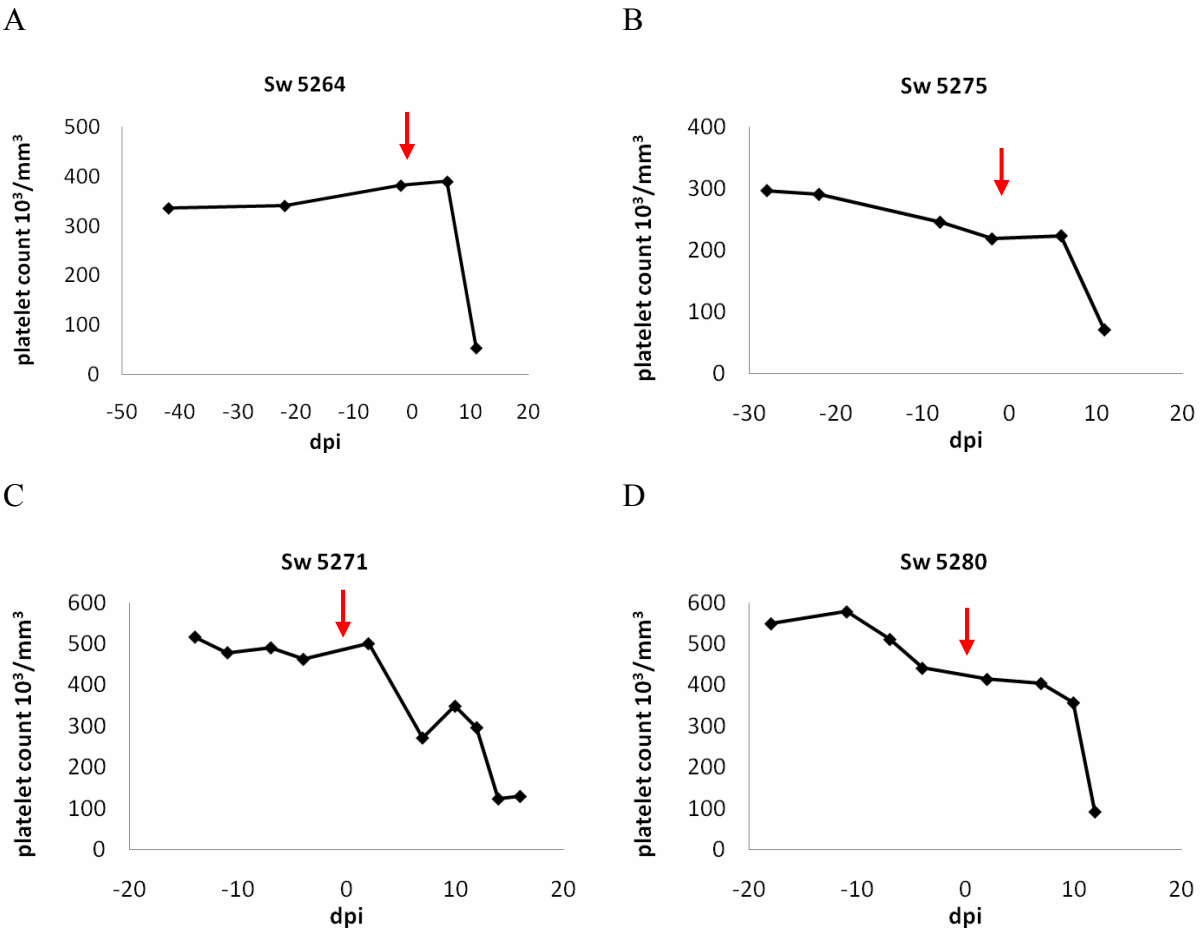

Figure 15: Platelet counts of four *M. suis* infected pigs. Red arrow indicates day of infection. days post-infectionem (dpi), animal number (Sw).

3.2.7 Adhesion of *Mycoplasma suis* to porcine aortic endothelial cells

To examine the ability of *M. suis* to attach to ECs *in vitro*, PAECs were infected with plasma of acutely diseased pigs. At the point of infection PAECs were grown to 50 % confluence on cover slips in 24-well plates. 100 µL of plasma with a bacterial load of 10^4 *M. suis* cells/mL were added to each well. As a control, wells were incubated with plasma of healthy pigs. After 5, 10, 30, 90 and 360 min (6 h) as well as after 4 days non-attached *M. suis* cells were removed after several washing steps before fixation of endothelial monolayers with PFA. Actin cytoskeleton of PAECs was stained green with FITC-phalloidin and bacteria were stained red using an *M. suis* specific antisera and a TRITC-labelled secondary antibody. Endothelial nuclei and bacteria were counterstained with DAPI.

M. suis was detected in form of aggregates on the surface of ECs after 90 min of incubation (Fig. 16B) until the end of the experiment 4 days pi (Fig. 16D). Actin condensation was observed at the point of attachment of bacteria with ECs (Fig. 16B-D). Thereby, condensed

actin always colocalised with bacterial aggregates. A propagation of *M. suis* on the surface of ECs could not be observed during the time course of infection. On day 4 pi nuclei of some cells that were in contact with *M. suis* aggregates appeared apoptotic due to chromatin condensation and marginalisation (Fig. 16 D). No *M. suis* cells were detected on PAECs incubated with control plasma.

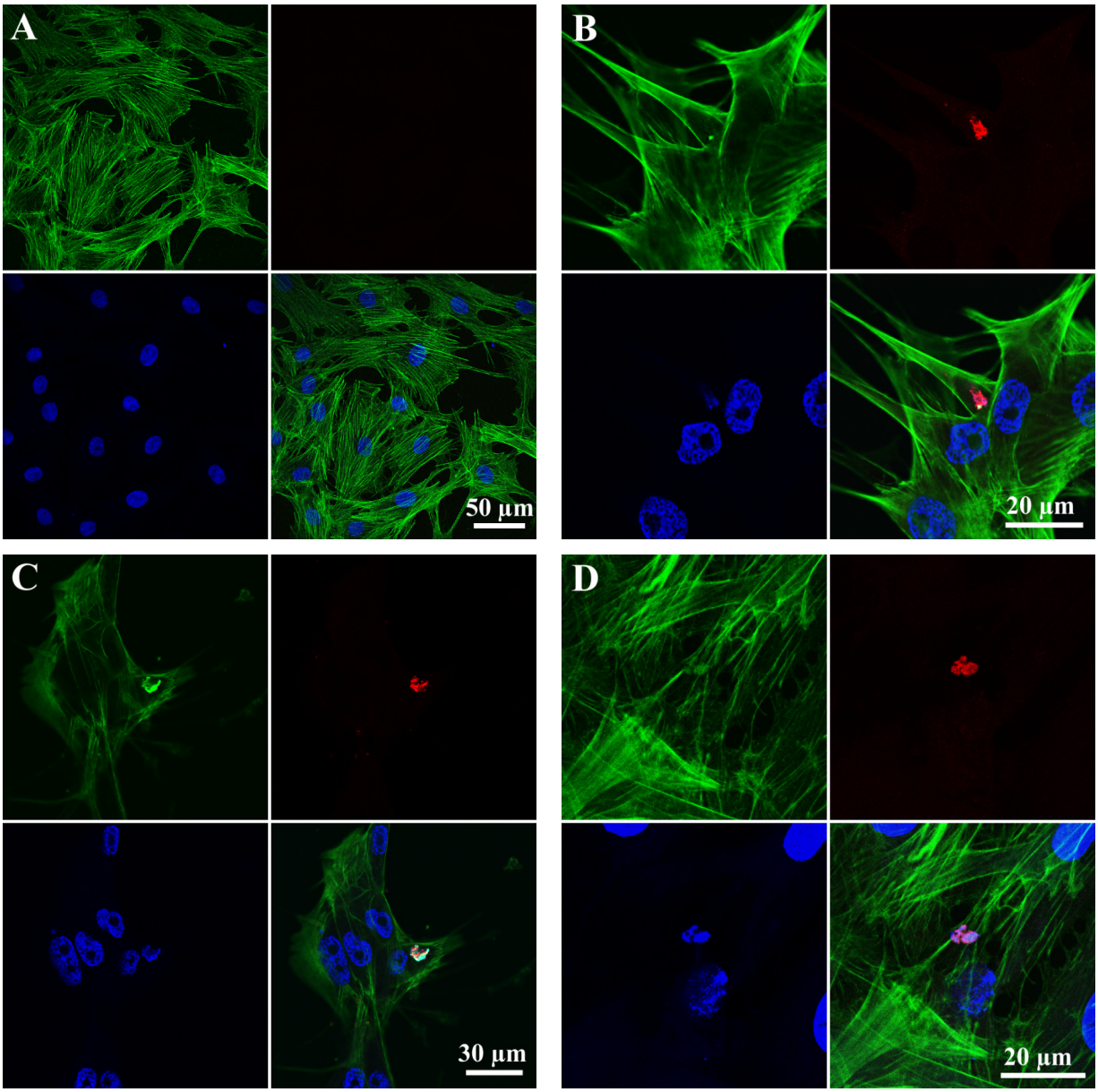

Figure 16: Confocal laser scanning micrographs of PAECs incubated with plasma of IAP-diseased pigs. Actin cytoskeleton is stained green with FITC-phalloidine. *M. suis* cells were stained red using anti-HspA1 antiserum and TRITC-labelled secondary antibodies. Nuclei and bacteria were counterstained blue with DAPI. The lower right quarter in each illustrate represents overlay of all fluorescent channels. (**A**) Before infection. (**B**) 90 min pi. (**C**) 6 hours pi. (**D**) 4 days pi.

3.2.8 Apoptosis detection in cell cultures

To examine EC death *in vitro* cell monolayers of PAECs were incubated with serum pools (serum infected) or plasma pools (plasma infected) of acutely diseased *M. suis* infected pigs. As a control PAECs were incubated with serum pools (serum control) or plasma pools (plasma control) of healthy control pigs. Medium supplemented with recombinant porcine TNF-α served as positive control for the induction of apoptosis (not shown). Cells were detached from the culture plates and stained in solution with Annexin-V-FLUOS and propidium iodide (PI) for quantification of EC death by flow cytometry. Apoptotic cells are single stained with Annexin-V which binds to surface-exposed phosphatidylserines while necrotic cells that have lost membrane integrity are also counterstained with the membrane impermeable DNA stain PI. PFA-fixed cells, staining positive with Annexin-V, were used to perform instrument settings. 10'000 ECs were taken into consideration and measurements were repeated 5 times for each sample. The amount of cells single-stained with Annexin-V was recorded for quantification of apoptosis. A difference was regarded as significant when the P-value was below 0.05. In PAECs incubated with "plasma infected" apoptosis rate was with 3.46 % (±0.44) significantly higher (P = 0.00065) than in PAECs incubated with "plasma control" showing an apoptosis rate of 1.74 % (±0.33). There was also a significant difference (P = 0.02333) in necrosis rate. However, the discrepancy in necrotic cell death between control cells (5.04 % ± 0.16) and cells incubated with "plasma infected" (5.95 % ± 0.75) was much lower than in apoptosis. PAECs incubated with "serum infected" showed an apoptosis rate of 4.80 % ± 0.60 that was significantly higher (P = 0.00875) than in PAECs incubated with "serum control" (2.95 % ± 0.22). The necrosis rate between cells incubated with "serum infected" (5.71 % ± 0.68) or "serum control" (5.29 % ± 0.75) was not significantly different (P = 0.26047).

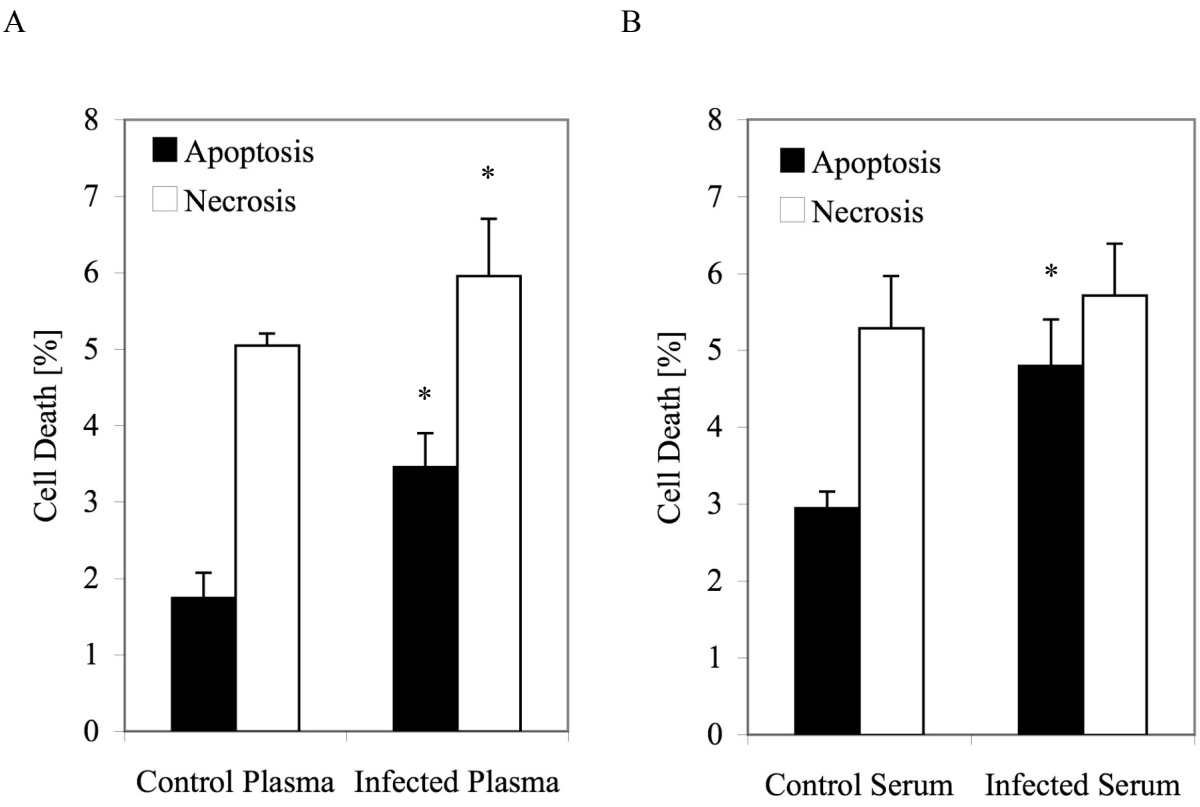

Figure 17: Apoptosis (black bars) and necrosis rates (white bars) of porcine aortic endothelial cells incubated with **(A)** plasma pools of healthy ("Control Plasma") and *M. suis* infected pigs ("Infected plasma") or **(B)** serum pools of healthy ("Control Serum") and *M. suis* infected pigs ("Infected Serum"). Stars represent significance: *p≤0.05;.

During apoptosis nuclear DNA is cleaved due to activation of endogenous endonucleases into fragments of ~200 bp and multiples thereof. To confirm apoptosis rates from *in vitro* assays genomic DNA, extracted from PAECs, incubated with sera and plasma of healthy or infected pigs, was separated by agarose gel electrophoresis (Fig. 18). A 100 bp ladder was run in parallel to visualize fragmented DNA of 200 bp and multiples thereof. No DNA laddering could be demonstrated in genomic DNA of ECs.

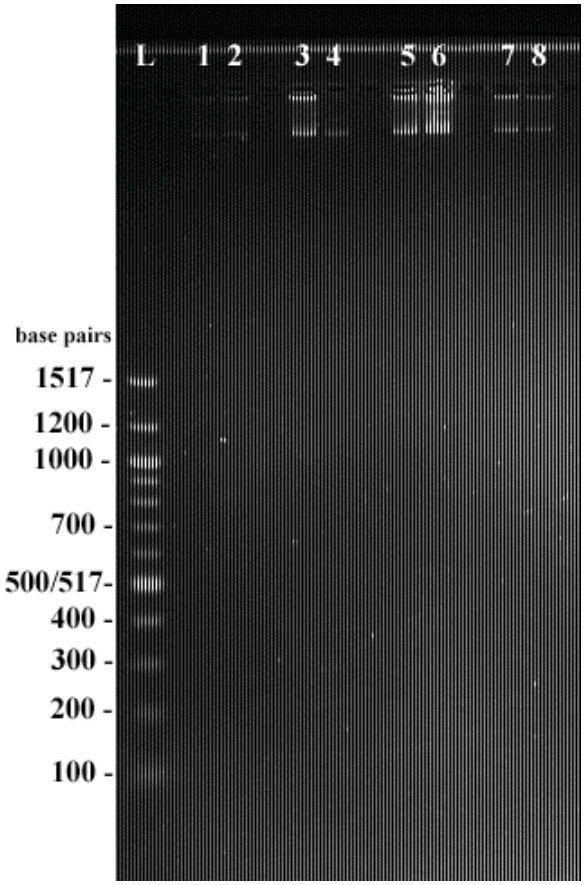

Figure 18: Results of agarose gel electrophoresis showing nuclear DNA of porcine aortic endothelial cells incubated with "control plasma" (lanes 1 and 2), "infected plasma" (lanes 3 and 4), "control serum" (lanes 5 and 6) and "infected serum" (lanes 7 and 8). L (ladder)

4. Discussion

4.1 Objective (1): Examination of a putative intracellular life-style of *M. suis*

The results of this objective are discussed in detail in the publication of section "selected publications": Groebel, K., K. Hoelzle, M. M. Wittenbrink, U. Ziegler, and L. E. Hoelzle. 2009. *Mycoplasma suis* invades porcine erythrocytes. Infect Immun 77:576-584.

4.2 Objective (2): Investigation of vascular damages in *M. suis* infections

Infectious anaemia in pigs caused by *Mycoplasma suis* is a disease which is accompanied by haemorrhagic diatheses (1, 27, 59, 115), RBC abnormalities (75), and blood clotting (49). In their study, Plank and Heinritzi (94) observed a reduced efficiency of the coagulation pathway in the blood of *M. suis*-infected pigs and a reduced platelet count. The authors explained their findings by intravascular coagulation and subsequent consumption of platelets. To which extend a damage of the vascular endothelium contributed to the activation of intravascular coagulation could not be evaluated. However, the authors suspected an indirect damage of the endothelium because of the hypoglycaemic-hypoxic-acidotic metabolic status during acute IAP (92). Endothelial activation can potentially break down the endothelial barrier function, leading to the formation of haemorrhages.

Several working groups proved that blood clotting can lead to a local obstruction of blood flow and vascular dysfunction (72) as well as to an altered vasomotor tonus (5). Furthermore, abnormalities of RBCs can lead to an increased adhesion to ECs and endothelial activation, which was already observed in various diseases such as sickle cell anaemia, diabetes or malaria (40, 104, 130). During *M. suis* bacteraemia a change in erythrocyte morphology as well as agglutination of RBCs can be observed in the blood of infected pigs.

Nevertheless nothing is known of the capacity of *M. suis* to cause endothelial aberrations and pathologic changes. Therefore, we examined the blood vessels and capillaries in parenchymas of IAP-infected pigs for said changes.

A wide spectrum of alterations of the endothelial layer in blood vessels of *M. suis*-infected pigs was presented by using scanning and transmission electron microscope techniques. The extend of the morphologic anomalies were different in each infected pig, probably depending on the immune status, severity of infection as well as the bacterial load in the blood. The damages of the vascular endothelium were in any case severe, regardless whether pigs were

infected with a moderate or a highly virulent *M. suis* strain.

We confirmed an increased RBC adhesion to the endothelium in IAP-infected pigs, which may result from different adhesion mechanisms. In sickle cell anaemia a great variety of adhesion molecules being expressed on both cell types as well as intervening bridging molecules [e.g. von Willebrand Factor (vWF) and thrombospondin] contribute to increased RBC-EC interaction: For example, endothelial phosphatidylserine (PS) receptors detect the abnormally displayed PS on sickle RBCs. The latter is probably a consequence of abnormal distribution of glycoproteins on sickle RBCs. In addition, α4β1 integrin on sickle RBCs can interact with VCAM on ECs (39). In malaria attachment of *P. falciparum* infected erythrocytes (Pf-IRBCs) to the cerebral endothelium is also mediated by specific endothelial receptor molecules such as ICAM-1 (85, 96, 120, 122). Tripathi and co-workers even discovered that Pf-IRBCs induce a dose- and time-dependent increase in ICAM-1 expression on HBMEC (120). It remains to be elucidated, if an increased expression of adhesion molecules such as ICAM-1 in IAP-activated ECs is also responsible for sequestration of RBCs to vascular ECs.

Increased adhesion of *M. suis* infected RBCs to ECs may trigger various pathological observations made in this study, i.e. vasoocclusion, endothelial activation, and initiation of the coagulation cascade. Vasoocclusion or the tightness of packing of RBCs in capillaries, especially in the liver, displays a strong correlation between vascular pathology and IAP. Leakage of blood plasma from small vessels might result from the local obstruction of blood flow and local oedema would be expected to occur in organs with tightly packed capillaries. Using TEM or histochemical staining, no oedematous areas were observed in the examined samples, probably due to the small size of samples. However, we found ascites in infected pigs indicating a transition of fluid through changed vessels (data not shown).

In this study we found morphological changes of the endothelium in the porcine vessels during IAP (microvilli formation, change in overall appearance from flat to a round or cuboidal) indicating an activation of ECs. The formation of microvilli protrusions has been observed on isolated human brain microvascular endothelial cells (HBMEC) incubated with *P. falciparum* infected erythrocytes (120) as well as in microvessels of brain and other tissue samples from patients dying from *P. falciparum* malaria (71). Clark and co-workers described the development of pseudopodia during cerebral malaria as a manifestation of endothelial damage caused by active oxygen metabolites such as hydrogen peroxide, superoxide anion,

and the hydroxyl radical (17). Such metabolites may be released during acute IAP by neutrophils and activated macrophages. Furthermore, production of hydrogen peroxide is probably a contributory factor to the pathogenicity of mycoplasmas (13, 28, 56). Interestingly, we detected that *E. coli* cells expressing recombinant MSG1 on their surface display a higher tolerance to elevated H_2O_2 concentrations than control cells (unpublished data). MSG1 is an *M. suis* specific protein that was shown earlier to be involved in the attachment of *M. suis* to porcine RBCs (52) and has probably additional functions such as protection of the organisms to active oxygen metabolites.

Other authors described the development of pseudopodia by cerebral endothelium in malaria as a non-specific response to injurious stimuli (71). In addition, the development of microvillis on ECs generates a greater endothelial surface area and might further increase the frequency of adherent RBCs in blood vessels of IAP-infected pigs. The high degree of red cell adhesion seen in liver sinusoids as well as in heart and kidney capillaries may therefore be a result of a combination of activated ECs expressing adhesion molecules, an altered RBC membrane, and an increased adhesiveness caused by pseudopodia.

The next change of ECs found in connection with IAP is a cuboidal morphology. This changed morphology of ECs as a result of cell activation was already suggested by other authors in connection with atherosclerosis (128). Activated ECs are characterised by an increased expression of proinflammatory cytokines leading to the activation of NF-kB and expression of adhesion molecules such as ICAM-1, P-selectin and E-selectin (47). This increased level of protein biosynthesis may contribute to cell hypertrophy. Further studies applying immuno-histochemical staining on aortic sections of healthy and *M. suis*-infected pigs with antibodies, e.g. to ICAM-1 or E-selectin should be carried out to confirm elevated expression of pro-inflammatory and pro-thrombotic markers.

An adhesion of pathogens to the endothelial surface is usually enough to activate numerous signalling pathways by the interaction of microbial structures with TLRs on ECs (47). The detection of bacterial microcolonies and biofilms on the endothelium of IAP-infected pigs therefore supports the assumption that a cuboidal shape of the ECs cells reflects a pathogen-activated cell phenotype.

The accumulation of arterial thrombi consisting of fibrin fibres, leukocytes, RBCs, and platelets on the endothelial surface found in this study point to diminished anti-thrombotic and anti-adhesive properties of the endothelium which confirm the dysfunctional activated

endothelium in IAP. Furthermore, the physical presence of fibrin in almost all examined aortic vessels is a typical hallmark of inflammation and vascular disease and functions as a haemostatic plug in lesions and as a provisional matrix in inflammation and wound healing (98). This coagulation cascade may have been initiated upon endothelial injury during acute IAP which led to EC death and denudation. To avoid the breakdown of the endothelial barrier function platelets may have been activated, forming a platelet plug, which stopped the bleeding (6, 62). In parallel, soluble fibrinogen was converted to a network of insoluble fibrin fibers that was stabilising the platelet plug by a receptor-mediated interaction with activated platelets (62).

After infection of our experimental pigs with *M. suis* we detected a dramatic decrease of platelets in the blood. This decrease was accompanied by the detection of numerous blot clots in aortas of *M. suis*-infected pigs. These observations confirm the hypothesis of Plank and Heinritzi (94) that the platelet reduction must be a consequence of intravascular coagulation and the subsequent consumption coagulopathy.

The presence of fibrin fibres on the vascular wall of IAP-infected pigs observed in this study might further strengthen the process of RBC adhesion to the endothelium. Fibrinogen, among other plasma factors, has been identified to enhance adhesion of pathological RBCs to ECs (108, 129), probably by acting as ligand, cross-linking receptors on both cell types. In addition, plasma fibrinogen is an acute-phase protein and is primarily synthesised in the liver during early stages of inflammation (37). The process is regulated by cytokines, such as interleukin (IL)-6, IL-1β, and glucocorticoids (86). TNF-α, in particular, is released by activated platelets and macrophages and is also known to sensitise ECs to undergo apoptosis via induction of signal transduction pathways involving the intracellular production of reactive oxygen species (ROS) (19). Furthermore, TNF-α influences EC viability by altering the balance of regulatory molecules that either induce or suppress apoptosis (95). Many *Mycoplasma spp*. have been shown to activate monocytes and macrophages and induce secretion of the proinflammatory cytokines such as TNF-α, IL-1 and IL-6 (107). Therefore, we suggested that TNF-α may be a contributory factor to EC inflammation and apoptosis in IAP-infected pigs. However, we did not detect soluble TNF-α in serum samples of IAP-infected pigs. It is possible that TNF-α remains cell surface-associated, where it could still contribute to EC inflammation and apoptosis. Furthermore, it is most likely that other cytokines, such as IL-6, contribute to vascular pathogenesis in IAP.

Studies have shown that fibrin and fibrinogen metabolites not only bind to activated platelets but also to vascular ECs (24), induce vWF release (100) and activate ECs, e.g. by inducing leukocyte chemotactic activity (98). As a consequence, phagocytes are infiltrated into the injured tissue soon after formation of the fibrin clot and eliminate contaminating bacteria via phagocytosis (62). We could confirm the presence of leukocytes in some of the blot clots in our scanning electron microscopic pictures. In addition, phagocytic cells could be detected in aortic sections via transmission electron microscopy.

Denudation of ECs in blood vessels of *M. suis* infected pigs is a result from EC death. ECs may have undergone necrotic cell death due to direct damage or apoptosis, a form of programmed cell death. Most apoptotic cells lose their surface attachments and detach into the surrounding extracellular space (134). Furthermore, it cannot be excluded that ECs in certain areas became detached during harvesting of blood vessels at autopsy or during the course of specimen preparation. In the control vessels, however, denudation of ECs was only seen rarely and was limited to small areas. Therefore, endothelial denudation can be regarded as a pathological finding in IAP. We assume that apoptotic cell death in ECs of IAP-infected pigs is triggered by diverse mechanisms:

Intravascular haemolysis may release oxyhaemoglobin (OxyHb), which is the main component of erythrocytes and is known to induce apoptosis in cultured ECs (89). OxyHb has been documented to have cytotoxic effects on ECs due to autooxidation from OxyHb to methaemoglobin which releases free radicals, such as superoxide and hydrogen peroxide that may cause damage and detachment of ECs (78). In a similar way acute haemolytic anaemia in pigs may lead to endothelial apoptosis.

Activated neutrophils may release apoptosis-inducing ROS and proteases from neutrophilic granula. Neutrophils are part of the innate immune system and can be activated by parasite or bacterial products (45). In malaria and bacterial sepsis neutrophils contribute to a great extend to endothelial apoptosis, both by their secretory products and by binding to ECs via direct interaction of LFA1 on neutrophils with ICAM-1 on ECs. It remains to be elucidated if activated neutrophils contribute to EC apoptosis in IAP.

Bacteria-activated platelets are also known to induce EC apoptosis. In some specimens we observed a direct contact between *M. suis*-infected RBCs, platelets and ECs. Kuckleburg and co-workers have demonstrated that a direct contact between *Haemophilus somnus*-activated platelets and ECs induces significant levels of apoptosis via activation of caspases 8 and 9

(60). In addition, activated platelets induce EC production of ROS (54) which contributes to vascular damage. Furthermore, *M. suis* cells on the surface of RBCs may interact with the host cell in a way that results in expression of bacterial proteins on the surface of RBCs. This may further enhance attachment of RBCs to ECs and lead to EC apoptosis. In malaria, EC apoptosis can be induced by *P. falciparum*-parasitized RBCs expressing the multivariant parasite-derived *P. falciparum* erythrocyte membrane protein-1 on their surface which binds specific to receptors, such as CD36, ICAM-1, P-selectin, and VCAM-1, E-selectin and chondroitin sulphate.

Interestingly, we also found bacterial cells being directly attached to the vascular wall, either single cells or smaller to larger microcolonies having a size up to 30–50 μm in diameter. So, a direct damage of the ECs by *M. suis* is possible. Several pathogenic *Mycoplasma* species are known to interact with ECs. However, there are no reports of haemotrophic mycoplasmas infecting vascular ECs. Large colony (LC) strains of *Mycoplasma mycoides* subsp. m*ycoides* causing septicaemia with vasculitis and coagulation disturbances in goats can adhere to caprine ECs (125). Scanning electron micrographs of goat aorta tissue treated with at least 10^6 CFU/mL of *M. mycoides* subsp. *mycoides* D44 revealed a severe damage of ECs exposing subendothelial collagen (106). In addition, coagulopathy with increased blood fibrinogen, prolonged prothrombin time, and decreased platelet count can be detected in septicaemic goats – symptoms similar to those observed in pigs with acute IAP. Furthermore, haemorrhages and thrombosis can be observed in lung, liver, and kidneys at necropsy. The authors related coagulopathy with endothelial damage caused by the *Mycoplasma* that would expose subendothelial collagen, and result in aggregation and activation of platelets. An interaction of *M. suis* with porcine endothelial cells may similarly lead to endothelial damage and coagulation disturbances.

To get further insight into the molecular mechanisms leading to EC damage by *M. suis*, we investigated this interaction also *in vitro.* For this, we used primary cell cultures of porcine aortic endothelial cells (PAECs) incubated with plasma of acutely diseased *M. suis* infected pigs containing 10^3 *M. suis* cells/mL. Adhesion assays revealed the attachment of *M. suis* aggregates on the surface of ECs after 90 min of incubation. Interestingly, actin condensation was observed at the point of attachment of bacteria with ECs. These data correlate with the finding that MSG1, an *M. suis* specific protein that was shown earlier to be involved in the attachment of *M. suis* to porcine RBCs (52) can interact with cytoskeletal β-actin of eucarytic

cells, specifically RBCs (25, 26). In addition, Felder and co-workers reported that autoreactive IgG antibodies up-regulated during IAP recognise actin. The authors hypothesised that *M. suis* is able to dissolve the RBC plasma membrane by enzymatic activity. Due to this membrane damage RBC actin that is usually cryptic, gets accessible to interaction with *M. suis*. They further suggested that the strongly β-actin-binding antibodies identified do not only affect RBCs since β-actin is part of the cytoskeleton in many eukaryotic cells. Interaction of *M. suis* with endothelial actin may therefore in a similar way lead to cytoskeletal rearrangement in ECs.

In order to verify apoptotic processes of PAECs *in vitro* we incubated the cells with plasma and serum pools of acutely diseased *M. suis*-infected pigs or with corresponding controls of healthy pigs, respectively. The application of both, plasma and serum, in this assay should help identifying the factors contributing to EC apoptosis in *M. suis* infections. After 24 h of incubation PAECs were stained with Annexin-V and propidium iodide to discriminate apoptotic from necrotic cells. Using this approach it was detected that the apoptosis rate was twofold higher in PAECs incubated with *M. suis*-positive plasma than in the control cells. Similar results were obtained when PAECs were incubated with sera of *M. suis*-infected pigs. In contrast, the necrosis rate remained constant in all experiments indicating that endothelial cell death in PAECs is rather due to apoptosis than to necrosis.

We further tried to verify EC apoptosis by DNA fragmentation assays. During apoptosis nuclear DNA is cleaved due to activation of endogenous endonucleases into fragments of approximately 200 bp and multiples thereof which can be made visible after separation of nuclear DNA on an agarose gel. We did not detect any fragmented DNA on the gel. DNA concentration was set to 2 µg per well for each sample examined. However, apoptosis rates of PAECs showed only a maximum of 3.46 % when incubated with *M. suis* containing plasma and 4.8 % after incubation with sera of diseased pigs as detected by Annexin-V quantification. For 2 µg genomic DNA applied to the gel that would correspond to 70-10 ng fragmented DNA which would be below the detection range of an ethidium bromide stained agarose gel.

Even though we detected a significant difference in apoptosis rates in PAECs incubated with plasma and serum of infected pigs compared to the control, measured apoptosis rates were too low to explain the severe endothelial damage seen *in vivo*. If apoptosis is the main mechanism leading to endothelial cell damage further factors that are not contained in the serum or

plasma components, such as *M. suis* parasitized erythrocytes, are necessary to reconstruct the *in vivo* apoptosis cascade also *in vitro*. Furthermore, endothelial cell apoptosis *in vivo* may occur due to direct interaction of *M. suis* with the host cell. The reduced or inhibited proliferation capacity of the organism, when grown *in vitro*, may be responsible for the low rate of apoptosis in cell culture experiments. Furthermore, the multiplicity of infection (MOI) may have been too low to result in elevated apoptosis rates and experiments should be carried out with higher plasma concentrations.

Interestingly, we found two different phenotypic morphologies of mycoplasmal microcolonies on the vascular wall. One type consisted of homogenous crosslinked cells of 200-400 nm in size forming a three-dimensional network. These colonies were in direct contact with RBC aggregates indicating that these cells are *M. suis*. The other microcolony type differed from the first one by the compact appearance and the presence of a granular matrix with microcrystals in which the bacteria were embedded. Smaller coccoid forms of less than 100 nm appeared on the surface of the larger cells of 200-400 nm in size and probably originated from budding-like mechanisms. A budding-like mechanism of replication has already been proposed for HM (135) as well as for other mycoplasmas (29, 90). The coccoid forms including smaller budding bacteria strongly resemble propagating *M. suis* cells found on erythrocytes. We suggested that the two morphologies represent different stages of biofilm formation in *M. suis*. Adhesion of *M. suis*-infected RBCs to the ECs may mediate initial attachment of *M. suis* to the endothelium. During progression of disease bacteria may propagate on the surface of the endothelium and RBCs disappear due to haemolysis. It is known that soon after attachment of planctonic cells to a surface and subsequent division bacteria start to produce extracellular polymeric substances (EPS). By this cells adhere irreversibly to the substrate (117). The granular matrix and microcrystals we have found in biofilms of the vascular endothelium may therefore represent EPS. By additional EPS production, cellular motility and reproduction, the biofilm may further differentiate to produce a mature, thick and spatially structured biofilm.

There are only few publications concerning biofilm formation of mycoplasma species. McAuliffe and co-workers have proven that many mycoplasmas (e.g. *Mycoplasma putrefaciens, M. cottewii, M. yeatsii, M. agalactiae and M. bovis*) are able to form prolific biofilms (74). Furthermore, it was shown by immunofluorescence microscopy that *in vitro* formed mycoplasmal biofilms contain all of the highly differentiated structural features, such

as honeycombed regions and areas of outgrowths referred to as mushrooms or towers, found in biofilms that are formed by other bacteria (74, 109-111). In addition, *M. pulmonis* biofilms formed on the epithelium of trachea in tracheal organ culture and in experimental infected mice have a similar structure and biological characteristics as biofilms formed *in vitro* (110). The microcolonies or biofilms found on the endothelium in *M. suis*-infected pigs using SEM techniques did not contain any mushrooms or towers. Considering the fact that euthanasia was carried out between days 8 and 12 pi for most of the experimental pigs it is likely that the period of infection was too short for the development of a differentiated biofilm. It is possible that these biofilms were in a beginning stage of biofilm formation.

Recent studies have indicated that biofilm formation protects mycoplasmas from antimicrobial agents and the innate immune system (110). The endothelial biofilm may therefore represent a substantial reservoir of *M. suis* cells that are resistant to host immunity and that might display the source of chronic disease in IAP infections. We concluded that the formation of mycoplasmal biofilms on the endothelium in IAP infected pigs may contribute to the persistence of *M. suis* in the host. Prior to the onset of acute infection, the endothelium may display the primary niche, where the pathogen propagates before being released into the bloodstream to parasitize the erythrocytes.

One further interesting feature of this study was the cardiac muscle damage. Cardiac muscles cells were disarranged and destructed. Mitochondria were drastically reduced in numbers and located disordered in the heart tissue of the *M. suis* infected pig. Sarcomeres appeared unequal and shrunk in many parts of the tissue. These changes can be explained by RBC aggregation in blood vessels of *M. suis*-infected pigs with subsequent occlusion of capillaries leading to ischaemia (interruption of blood supply). The resulting oxygen shortage may have finally caused cardiac cells to die.

Ischaemia is central to a number of pathologies including myocardial infarction. In myocardial infarction ischaemia can be caused by rupture of atherosclerotic lesions in coronary arteries. The contents of the lesions enter the bloodstream and can occasionally lead to the formation of a thrombus. Thrombotic occlusions are often followed by restoration of blood flow (reperfusion) due to clot lysis. During reperfusion ROS are generated, which can further trigger an inflammatory response and irreversible cell damage (70).

Furthermore, disarranged muscle cells can be a result from a loss of function in actin-myosin contraction. It was proven by members of our group that the *M. suis* protein MSG1 can

interact with cytoskeletal β-actin (unpublished data). It may be possible that *M. suis* can also interact with α-actin of muscle cells, leading to a loss of function. Further studies are, however, necessary to verify these hypotheses.

Another interesting observation was the formation of small fibrils interconnecting several *M. suis* cells on the surface of RBCs being attached to the vascular wall. Similar fibrils are known to connect *M. suis* with the host erythrocyte (48, 97, 135). However, a physical contact between mycoplasmal cells that is mediated via fibrillar structures has not been reported so far. Interconnecting appendages have been noted only for a few prokaryotes including *Pyrodictium abyssi.* The cells of this archaeon are connected to each other in a matrix of extracellular tubules that maintain the cells in close proximity to each other (101). In addition, the vegetative cells of the gram-negative bacterium *Myxococcus xanthus* form extensive fibrillar interconnections, which is necessary for the manifestation of their characteristic social behaviour. The fibrils of *M. xanthus* are composed of approximately equal amounts of protein and polysaccharide and cell-cell contact is mediated by the action of a fibrillar ADP-ribosyl transferase (22). As interconnected *M. suis* cells were solely found on the surface of RBCs being attached to the endothelium this type of specialised cell to cell communication may be necessary for the development of an endothelial biofilm. Further studies are necessary to characterise the composition of the *M. suis* fibrils.

This is the first study showing that infections with HM are accompanied by a widespread endothelial damage, RBC adhesiveness to the endothelium, and vascular occlusion. These vascular alterations may lead to the development of haemorrhages, ascites, oedema and organ failure. In addition, the ability of *M. suis* to form endothelial biofilms in which the organisms are protected from killing by antibiotics as well as from the host's immune system may contribute to the persistence of HM.

5. Milestones and outlook

The mechanisms of interaction of *M. suis* with the infected host are very complex and not yet fully understood. In this thesis important milestones, summarised in Figure 19, were set for a better understanding of the pathogenesis in *M. suis* infections. Both, the intracellular infection of erythrocytes as well as the biofilm formation on ECs may thwart the host's immune system and antibiotic treatment leading to persistence of the organism. Endothelial inflammation and cell death as well as circulatory disorders may explain the severe clinical symptoms in acute IAP infections.

Taken together, these data indicate that lots of further pathogenicity mechanisms exist which contribute to the severity of acute and chronic IAP infection and are the basis for clarification of further questions:

- This study has shown that the cell tropism of *Mycoplasma suis* is not solely confined to erythrocytes. The organism is also able to attach to endothelial cells and form microcolonies on the latter. Therefore, a further topic of research at the moment is the analysis of the *M. suis* cell tropism using epithelial cells, macrophages and leucocytes.
- During IAP an increased number of erythrocytes is attached to the endothelium. An upregulation of EC adhesion molecules may explain the increased adhesiveness. To address this question immune fluorescence staining with antibodies to adhesion molecules (e. g. VCAM-1, ICAM-1) will be applied on cultured porcine aortic endothelial cells incubated with *M. suis* containing plasma or on histological sections of aortic vessels of diseased pigs.
- Elevated plasma levels of von Willebrand factor (vWF) are indices of chronic and acute endothelial cell perturbation (73). Therefore the vWF concentration is measured in the plasma of control pigs and acutely diseased IAP-infected pigs using a commercially available ELISA kit.

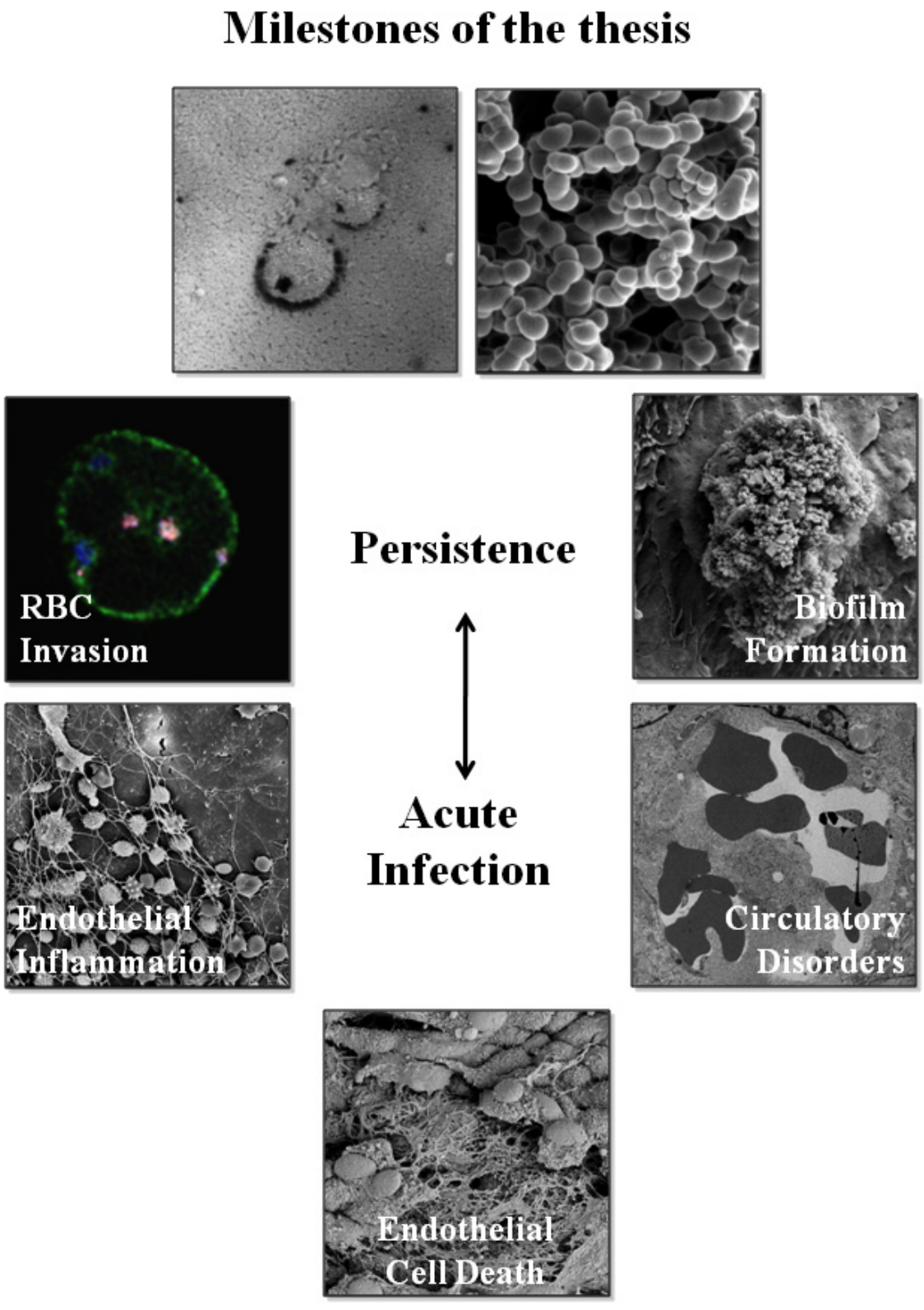

Figure 19: Milestones of the thesis. Endothelial inflammation and cell death as well as circulatory disorders may explain the severe clinical symptoms in acute IAP infections. Furthermore, the capability of RBC invasion and biofilm formation may contribute to the persistence of the organism in chronic *M. suis* infections.

6. References

1. **Adams, E. W., D. I. Lyles, and K. O. Cockrell.** 1959. Eperythrozoonosis in a herd of purebred Landrace pigs. J Am Vet Med Assoc **135:**226-228.
2. **Archer, G. L., P. H. Coleman, R. M. Cole, R. J. Duma, and C. L. Johnston, Jr.** 1980. Hemotropic bacteria. N Engl J Med **302:**1151-1152.
3. **Balaban, N. Q., J. Merrin, R. Chait, L. Kowalik, and S. Leibler.** 2004. Bacterial persistence as a phenotypic switch. Science **305:**1622-1625.
4. **Bannerman, D. D., and S. E. Goldblum.** 2003. Mechanisms of bacterial lipopolysaccharide-induced endothelial apoptosis. Am J Physiol Lung Cell Mol Physiol **284:**L899-914.
5. **Baskurt, O. K., O. Yalcin, S. Ozdem, J. K. Armstrong, and H. J. Meiselman.** 2004. Modulation of endothelial nitric oxide synthase expression by red blood cell aggregation. Am J Physiol Heart Circ Physiol **286:**H222-229.
6. **Baum, C. L., and C. J. Arpey.** 2005. Normal cutaneous wound healing: clinical correlation with cellular and molecular events. Dermatol Surg **31:**674-686; discussion 686.
7. **Berent, L. M., and J. B. Messick.** 2003. Physical map and genome sequencing survey of Mycoplasma haemofelis (Haemobartonella felis). Infect Immun **71:**3657-3662.
8. **Berent, L. M., J. B. Messick, and S. K. Cooper.** 1998. Detection of Haemobartonella felis in cats with experimentally induced acute and chronic infections, using a polymerase chain reaction assay. Am J Vet Res **59:**1215-1220.
9. **Bernardini, C., A. Zannoni, M. E. Turba, P. Fantinati, C. Tamanini, M. L. Bacci, and M. Forni.** 2005. Heat shock protein 70, heat shock protein 32, and vascular endothelial growth factor production and their effects on lipopolysaccharide-induced apoptosis in porcine aortic endothelial cells. Cell Stress Chaperones **10:**340-348.
10. **Bhakdi, S., F. Grimminger, N. Suttorp, D. Walmrath, and W. Seeger.** 1994. Proteinaceous bacterial toxins and pathogenesis of sepsis syndrome and septic shock: the unknown connection. Med Microbiol Immunol **183:**119-144.
11. **Bigger, J. W.** 1944. Treatment of staphylococcal infections with penicillin. Lancet **ii:**497-500.
12. **Black, D. S., A. J. Kelly, M. J. Mardis, and H. S. Moyed.** 1991. Structure and organization of hip, an operon that affects lethality due to inhibition of peptidoglycan or DNA synthesis. J Bacteriol **173:**5732-5739.
13. **Brennan, P. C., and R. N. Feinstein.** 1969. Relationship of hydrogen peroxide production by Mycoplasma pulmonis to virulence for catalase-deficient mice. J Bacteriol **98:**1036-1040.
14. **Brooun, A., S. Liu, and K. Lewis.** 2000. A dose-response study of antibiotic resistance in Pseudomonas aeruginosa biofilms. Antimicrob Agents Chemother **44:**640-646.
15. **Bugnowski, H., F. Horsch, D. Muller, and V. Zepezauer.** 1990. [Infection model for the reproduction of eperythrozoonosis in splenectomized SPF primary piglets]. Arch Exp Veterinarmed **44:**627-637.
16. **Christensen, S. K., M. Mikkelsen, K. Pedersen, and K. Gerdes.** 2001. RelE, a global inhibitor of translation, is activated during nutritional stress. Proc Natl Acad Sci U S A **98:**14328-14333.
17. **Clark, I. A., and N. H. Hunt.** 1983. Evidence for reactive oxygen intermediates

causing hemolysis and parasite death in malaria. Infect Immun **39:**1-6.
18. **Dehio, C.** 2001. Bartonella interactions with endothelial cells and erythrocytes. Trends Microbiol **9:**279-285.
19. **Deshpande, S. S., P. Angkeow, J. Huang, M. Ozaki, and K. Irani.** 2000. Rac1 inhibits TNF-alpha-induced endothelial cell apoptosis: dual regulation by reactive oxygen species. Faseb J **14:**1705-1714.
20. **dos Santos, A. P., R. P. dos Santos, A. W. Biondo, J. M. Dora, L. Z. Goldani, S. T. de Oliveira, A. M. de Sa Guimaraes, J. Timenetsky, H. A. de Morais, F. H. Gonzalez, and J. B. Messick.** 2008. Hemoplasma infection in HIV-positive patient, Brazil. Emerg Infect Dis **14:**1922-1924.
21. **Duarte, M. I., M. S. Oliveira, M. A. Shikanai-Yasuda, O. N. Mariano, C. F. Takakura, C. Pagliari, and C. E. Corbett.** 1992. Haemobartonella-like microorganism infection in AIDS patients: ultrastructural pathology. J Infect Dis **165:**976-977.
22. **Dworkin, M.** 1999. Fibrils as extracellular appendages of bacteria: their role in contact-mediated cell-cell interactions in Myxococcus xanthus. Bioessays **21:**590-595.
23. **Elmore, S.** 2007. Apoptosis: a review of programmed cell death. Toxicol Pathol **35:**495-516.
24. **Erban, J. K., and D. D. Wagner.** 1992. A 130-kDa protein on endothelial cells binds to amino acids 15-42 of the B beta chain of fibrinogen. J Biol Chem **267:**2451-2458.
25. **Felder, K.** 2010. Analysis of the Pathogenesis of Severe Anaemia of Pigs due to Mycoplasma suis Infection. PhD thesis. University of Zurich, Zurich.
26. **Felder, K. M., K. Hoelzle, K. Heinritzi, M. Ritzmann, and L. E. Hoelzle.** 2010. Antibodies to actin in autoimmune haemolytic anaemia. BMC Vet Res **6:**18.
27. **Foote, L. E., W. E. Brock, and B. Gallaher.** 1951. Ictero-anemia, eperythrozoonosis, or anaplasmosis-like disease of swine proved to be caused by a filtrable virus. North Am Vet **32:**17-23.
28. **Frey, J.** 2002. Mycoplasmas of animals, p. 82. In S. Razin and R. Herrmann (ed.), Molecular biology and pathogenicity of mycoplasmas. Kluwer Academic/ Plenum Publishers.
29. **Furness, G., and J. Whitescarver.** 1975. Adaptation of Mycoplasma hominis to an obligate parasitic existence in monkey kidney cell culture (BSC-1). Proc Soc Exp Biol Med **149:**427-432.
30. **Fux, C. A., J. W. Costerton, P. S. Stewart, and P. Stoodley.** 2005. Survival strategies of infectious biofilms. Trends Microbiol **13:**34-40.
31. **Goddard, C. M., M. F. Allard, J. C. Hogg, and K. R. Walley.** 1996. Myocardial morphometric changes related to decreased contractility after endotoxin. Am J Physiol **270:**H1446-1452.
32. **Gonzalez, M. A., and A. P. Selwyn.** 2003. Endothelial function, inflammation, and prognosis in cardiovascular disease. Am J Med **115 Suppl 8A:**99S-106S.
33. **Gotloib, L., A. Shostak, P. Galdi, J. Jaichenko, and R. Fudin.** 1992. Loss of microvascular negative charges accompanied by interstitial edema in septic rats' heart. Circ Shock **36:**45-56.
34. **Granger, D. N., and P. Kubes.** 1994. The microcirculation and inflammation: modulation of leukocyte-endothelial cell adhesion. J Leukoc Biol **55:**662-675.
35. **Gresham, A., J. Rogers, H. Tribe, and L. P. Phipps.** 1994. Eperythrozoon suis in weaned pigs. Vet Rec **134:**71-72.
36. **Groebel, K., K. Hoelzle, M. M. Wittenbrink, U. Ziegler, and L. E. Hoelzle.** 2009. Mycoplasma suis invades porcine erythrocytes. Infect Immun **77:**576-584.

37. **Guadiz, G., L. A. Sporn, and P. J. Simpson-Haidaris.** 1997. Thrombin cleavage-independent deposition of fibrinogen in extracellular matrices. Blood **90:**2644-2653.
38. **Hack, C. E., and S. Zeerleder.** 2001. The endothelium in sepsis: source of and a target for inflammation. Crit Care Med **29:**S21-27.
39. **Hebbel, R. P.** 2008. Adhesion of sickle red cells to endothelium: myths and future directions. Transfus Clin Biol **15:**14-18.
40. **Hebbel, R. P., O. Yamada, C. F. Moldow, H. S. Jacob, J. G. White, and J. W. Eaton.** 1980. Abnormal adherence of sickle erythrocytes to cultured vascular endothelium: possible mechanism for microvascular occlusion in sickle cell disease. J Clin Invest **65:**154-160.
41. **Heinritzi, K.** 1984. [A contribution on splenectomy in swine]. Tierarztl Prax **12:**451-454.
42. **Heinritzi, K.** 1990. [The diagnosis of Eperythrozoon suis infection]. Tierarztl Prax **18:**477-481.
43. **Heinritzi, K., I. Wentz, and W. Bollwahn.** 1984. [Hematologic findings in acute eperythrozoonosis of swine]. Berl Munch Tierarztl Wochenschr **97:**404-407.
44. **Hemmer, C. J., H. A. Lehr, K. Westphal, M. Unverricht, M. Kratzius, and E. C. Reisinger.** 2005. Plasmodium falciparum Malaria: reduction of endothelial cell apoptosis in vitro. Infect Immun **73:**1764-1770.
45. **Hemmer, C. J., A. Vogt, M. Unverricht, R. Krause, M. Lademann, and E. C. Reisinger.** 2008. Malaria and bacterial sepsis: similar mechanisms of endothelial apoptosis and its prevention in vitro. Crit Care Med **36:**2562-2568.
46. **Henry, S. C.** 1979. Clinical observations on eperythrozoonosis. J Am Vet Med Assoc **174:**601-603.
47. **Hippenstiel, S., and N. Suttorp.** 2003. Interaction of pathogens with the endothelium. Thromb Haemost **89:**18-24.
48. **Hoelzle, L. E.** 2008. Haemotrophic mycoplasmas: recent advances in Mycoplasma suis. Vet Microbiol **130:**215-226.
49. **Hoelzle, L. E.** 2007. [Significance of haemotrophic mycoplasmas in veterinary medicine with particular regard to the Mycoplasma suis infection in swine]. Berl Munch Tierarztl Wochenschr **120:**34-41.
50. **Hoelzle, L. E., M. Helbling, K. Hoelzle, M. Ritzmann, K. Heinritzi, and M. M. Wittenbrink.** 2007. First LightCycler real-time PCR assay for the quantitative detection of Mycoplasma suis in clinical samples. J Microbiol Methods **70:**346-354.
51. **Hoelzle, L. E., K. Hoelzle, A. Harder, M. Ritzmann, H. Aupperle, H. A. Schoon, K. Heinritzi, and M. M. Wittenbrink.** 2007. First identification and functional characterization of an immunogenic protein in unculturable haemotrophic Mycoplasmas (Mycoplasma suis HspA1). FEMS Immunol Med Microbiol **49:**215-223.
52. **Hoelzle, L. E., K. Hoelzle, M. Helbling, H. Aupperle, H. A. Schoon, M. Ritzmann, K. Heinritzi, K. M. Felder, and M. M. Wittenbrink.** 2007. MSG1, a surface-localised protein of Mycoplasma suis is involved in the adhesion to erythrocytes. Microbes Infect **9:**466-474.
53. **Hoelzle, L. E., K. Hoelzle, M. Ritzmann, K. Heinritzi, and M. M. Wittenbrink.** 2006. Mycoplasma suis antigens recognized during humoral immune response in experimentally infected pigs. Clin Vaccine Immunol **13:**116-122.
54. **Hotchkiss, R. S., K. W. Tinsley, P. E. Swanson, and I. E. Karl.** 2002. Endothelial cell apoptosis in sepsis. Crit Care Med **30:**S225-228.
55. **Jayaraman, R.** 2008. Bacterial persistence: some new insights into an old

phenomenon. J Biosci **33:**795-805.
56. **Kannan, T. R., and J. B. Baseman.** 2000. Hemolytic and hemoxidative activities in Mycoplasma penetrans. Infect Immun **68:**6419-6422.
57. **Kassab, G. S.** 2006. Biomechanics of the cardiovascular system: the aorta as an illustratory example. J R Soc Interface **3:**719-740.
58. **Keren, I., D. Shah, A. Spoering, N. Kaldalu, and K. Lewis.** 2004. Specialized persister cells and the mechanism of multidrug tolerance in Escherichia coli. J Bacteriol **186:**8172-8180.
59. **Korn, G., and M. Mussgay.** 1968. [A case of eperythrozoonosis suis and its differential diagnostic significance in relation to suspected swine fever]. Zentralbl Veterinarmed B **15:**617-630.
60. **Kuckleburg, C. J., R. Tiwari, and C. J. Czuprynski.** 2008. Endothelial cell apoptosis induced by bacteria-activated platelets requires caspase-8 and -9 and generation of reactive oxygen species. Thromb Haemost **99:**363-372.
61. **Kussell, E., R. Kishony, N. Q. Balaban, and S. Leibler.** 2005. Bacterial persistence: a model of survival in changing environments. Genetics **169:**1807-1814.
62. **Laurens, N., P. Koolwijk, and M. P. de Maat.** 2006. Fibrin structure and wound healing. J Thromb Haemost **4:**932-939.
63. **Levin, B. R., and D. E. Rozen.** 2006. Non-inherited antibiotic resistance. Nat Rev Microbiol **4:**556-562.
64. **Lewis, K.** 2008. Multidrug tolerance of biofilms and persister cells. Curr Top Microbiol Immunol **322:**107-131.
65. **Lewis, K.** 2005. Persister cells and the riddle of biofilm survival. Biochemistry (Mosc) **70:**267-274.
66. **Lewis, K.** 2007. Persister cells, dormancy and infectious disease. Nat Rev Microbiol **5:**48-56.
67. **Lewis, K.** 2001. Riddle of biofilm resistance. Antimicrob Agents Chemother **45:**999-1007.
68. **Limaye, V., and M. Vadas.** 2007. The vascular endothelium: structure and function, p. 1-11. In R. Fitridge and M. Thompson (ed.), Mechanisms of Vascular Disease: A Textbook for Vascular Surgeons, 1 ed. Cambridge University Press, Cambridge.
69. **Ljungh, A., and T. Wadstrom.** 1996. Interactions of bacterial adhesins with the extracellular matrix. Adv Exp Med Biol **408:**129-140.
70. **Loubele, S. T., H. Ten Cate, and H. M. Spronk.** Anticoagulant therapy in critical organ ischaemia/reperfusion injury. Thromb Haemost **104**.
71. **MacPherson, G. G., M. J. Warrell, N. J. White, S. Looareesuwan, and D. A. Warrell.** 1985. Human cerebral malaria. A quantitative ultrastructural analysis of parasitized erythrocyte sequestration. Am J Pathol **119:**385-401.
72. **Maharshak, N., Y. Arbel, I. Shapira, S. Berliner, R. Ben-Ami, S. Yedgar, G. Barshtein, and I. Dotan.** 2009. Increased strength of erythrocyte aggregates in blood of patients with inflammatory bowel disease. Inflamm Bowel Dis **15:**707-713.
73. **Mannucci, P. M.** 1998. von Willebrand factor: a marker of endothelial damage? Arterioscler Thromb Vasc Biol **18:**1359-1362.
74. **McAuliffe, L., R. J. Ellis, K. Miles, R. D. Ayling, and R. A. Nicholas.** 2006. Biofilm formation by mycoplasma species and its role in environmental persistence and survival. Microbiology **152:**913-922.
75. **Messick, J. B.** 2004. Hemotrophic mycoplasmas (hemoplasmas): a review and new insights into pathogenic potential. Vet Clin Pathol **33:**2-13.
76. **Messick, J. B., G. Smith, L. Berent, and S. Cooper.** 2000. Genome size of

Eperythrozoon suis and hybridization with 16S rRNA gene. Can J Microbiol **46:**1082-1086.

77. **Messick, J. B., P. G. Walker, W. Raphael, L. Berent, and X. Shi.** 2002. 'Candidatus mycoplasma haemodidelphidis' sp. nov., 'Candidatus mycoplasma haemolamae' sp. nov. and Mycoplasma haemocanis comb. nov., haemotrophic parasites from a naturally infected opossum (Didelphis virginiana), alpaca (Lama pacos) and dog (Canis familiaris): phylogenetic and secondary structural relatedness of their 16S rRNA genes to other mycoplasmas. Int J Syst Evol Microbiol **52:**693-698.
78. **Misra, H. P., and I. Fridovich.** 1972. The generation of superoxide radical during the autoxidation of hemoglobin. J Biol Chem **247:**6960-6962.
79. **Moulder, J. W.** 1974. Order I. Rickettsiales, p. 882-890. In R. E. Buchanan and N. E. Gibbons (ed.), Bergey's Manual of Determinative Bacteriology, 8 ed. The Williams & Wilkins Co, Baltimore, MD.
80. **Moyed, H. S., and K. P. Bertrand.** 1983. hipA, a newly recognized gene of Escherichia coli K-12 that affects frequency of persistence after inhibition of murein synthesis. J Bacteriol **155:**768-775.
81. **Moyed, H. S., and S. H. Broderick.** 1986. Molecular cloning and expression of hipA, a gene of Escherichia coli K-12 that affects frequency of persistence after inhibition of murein synthesis. J Bacteriol **166:**399-403.
82. **Neimark, H., K. E. Johansson, Y. Rikihisa, and J. G. Tully.** 2001. Proposal to transfer some members of the genera Haemobartonella and Eperythrozoon to the genus Mycoplasma with descriptions of 'Candidatus Mycoplasma haemofelis', 'Candidatus Mycoplasma haemomuris', 'Candidatus Mycoplasma haemosuis' and 'Candidatus Mycoplasma wenyonii'. Int J Syst Evol Microbiol **51:**891-899.
83. **Neimark, H., K. E. Johansson, Y. Rikihisa, and J. G. Tully.** 2002. Revision of haemotrophic Mycoplasma species names. Int J Syst Evol Microbiol **52:**683.
84. **Neimark, H., and K. M. Kocan.** 1997. The cell wall-less rickettsia Eperythrozoon wenyonii is a Mycoplasma. FEMS Microbiol Lett **156:**287-291.
85. **Newbold, C., P. Warn, G. Black, A. Berendt, A. Craig, B. Snow, M. Msobo, N. Peshu, and K. Marsh.** 1997. Receptor-specific adhesion and clinical disease in Plasmodium falciparum. Am J Trop Med Hyg **57:**389-398.
86. **Nguyen, M. D., and P. J. Simpson-Haidaris.** 2000. Cell type-specific regulation of fibrinogen expression in lung epithelial cells by dexamethasone and interleukin-1beta. Am J Respir Cell Mol Biol **22:**209-217.
87. **Nonaka, N., B. J. Thacker, T. W. Schillhorn van Veen, and R. W. Bull.** 1996. In vitro maintenance of Eperythrozoon suis. Vet Parasitol **61:**181-199.
88. **Norbury, C. J., and I. D. Hickson.** 2001. Cellular responses to DNA damage. Annu Rev Pharmacol Toxicol **41:**367-401.
89. **Ogihara, K., A. Y. Zubkov, D. H. Bernanke, A. I. Lewis, A. D. Parent, and J. H. Zhang.** 1999. Oxyhemoglobin-induced apoptosis in cultured endothelial cells. J Neurosurg **91:**459-465.
90. **Panangala, V. S., J. S. Stringfellow, K. Dybvig, A. Woodard, F. Sun, D. L. Rose, and M. M. Gresham.** 1993. Mycoplasma corogypsi sp. nov., a new species from the footpad abscess of a black vulture, Coragyps atratus. Int J Syst Bacteriol **43:**585-590.
91. **Panus, C., M. Mota, D. Vladu, L. Vanghelie, and C. L. Raducanu.** 2003. The endothelial dysfunction in diabetes mellitus. Rom J Intern Med **41:**27-33.
92. **Peteranderl, W.** 1988. Untersuchungen über den Glucose-, Lactat- und Pyruvatgehalt sowie den Säure-Basenhaushalt im venösen Blut bei der Eperythrozoonose des Schweines. Vet.-med. Diss. LMU München, München.

93. **Peters, I. R., C. R. Helps, L. McAuliffe, H. Neimark, M. R. Lappin, T. J. Gruffydd-Jones, M. J. Day, L. E. Hoelzle, B. Willi, M. Meli, R. Hofmann-Lehmann, and S. Tasker.** 2008. RNase P RNA gene (rnpB) phylogeny of Hemoplasmas and other Mycoplasma species. J Clin Microbiol **46:**1873-1877.
94. **Plank, G., and K. Heinritzi.** 1990. [Disseminated intravascular coagulation in eperythrozoonosis of swine]. Berl Munch Tierarztl Wochenschr **103:**13-18.
95. **Polunovsky, V. A., C. H. Wendt, D. H. Ingbar, M. S. Peterson, and P. B. Bitterman.** 1994. Induction of endothelial cell apoptosis by TNF alpha: modulation by inhibitors of protein synthesis. Exp Cell Res **214:**584-594.
96. **Porta, J., A. Carota, G. P. Pizzolato, E. Wildi, M. C. Widmer, C. Margairaz, and G. E. Grau.** 1993. Immunopathological changes in human cerebral malaria. Clin Neuropathol **12:**142-146.
97. **Pospischil, A., and R. Hoffmann.** 1982. Eperythrozoon suis in naturally infected pigs: a light and electron microscopic study. Vet Pathol **19:**651-657.
98. **Qi, J., and D. L. Kreutzer.** 1995. Fibrin activation of vascular endothelial cells. Induction of IL-8 expression. J Immunol **155:**867-876.
99. **Reynolds, E. S.** 1963. The use of lead citrate at high pH as an electron-opaque stain in electron microscopy. J Cell Biol **17:**208-212.
100. **Ribes, J. A., F. Ni, D. D. Wagner, and C. W. Francis.** 1989. Mediation of fibrin-induced release of von Willebrand factor from cultured endothelial cells by the fibrin beta chain. J Clin Invest **84:**435-442.
101. **Rieger, G., R. Rachel, R. Hermann, and K. O. Stetter.** 1995. Ultrastructure of the Hyperthermophilic Archaeon Pyrodictium abyssi. J Struct Biol **115:**78-87.
102. **Rikihisa, Y., M. Kawahara, B. Wen, G. Kociba, P. Fuerst, F. Kawamori, C. Suto, S. Shibata, and M. Futohashi.** 1997. Western immunoblot analysis of Haemobartonella muris and comparison of 16S rRNA gene sequences of H. muris, H. felis, and Eperythrozoon suis. J Clin Microbiol **35:**823-829.
103. **Ristic, M., and J. P. Kreier.** 1979. Hemotropic bacteria. N Engl J Med **301:**937-939.
104. **Robert, C., S. Peyrol, B. Pouvelle, F. Gay-Andrieu, and J. Gysin.** 1996. Ultrastructural aspects of Plasmodium falciparum-infected erythrocyte adherence to endothelial cells of Saimiri brain microvasculature. Am J Trop Med Hyg **54:**169-177.
105. **Romeis, B.** 1989. Mikroskopische Technik, 17 ed. Verlag Urban und Schwarzenberg, München, Wien.
106. **Rosendal, S.** 1984. Effect of the caprine variant of Mycoplasma mycoides subsp mycoides on endothelium, monocytes, and complement of guinea pig, calf, sheep, and goat serum. Am J Vet Res **45:**2396-2402.
107. **Rottem, S.** 2003. Interaction of mycoplasmas with host cells. Physiol Rev **83:**417-432.
108. **Shiu, Y. T., and L. V. McIntire.** 2003. In vitro studies of erythrocyte-vascular endothelium interactions. Ann Biomed Eng **31:**1299-1313.
109. **Simmons, W. L., J. R. Bolland, J. M. Daubenspeck, and K. Dybvig.** 2007. A stochastic mechanism for biofilm formation by Mycoplasma pulmonis. J Bacteriol **189:**1905-1913.
110. **Simmons, W. L., and K. Dybvig.** 2007. Biofilms protect Mycoplasma pulmonis cells from lytic effects of complement and gramicidin. Infect Immun **75:**3696-3699.
111. **Simmons, W. L., and K. Dybvig.** 2009. Mycoplasma biofilms ex vivo and in vivo. FEMS Microbiol Lett **295:**77-81.
112. **Sinha, B., P. P. Francois, O. Nusse, M. Foti, O. M. Hartford, P. Vaudaux, T. J. Foster, D. P. Lew, M. Herrmann, and K. H. Krause.** 1999. Fibronectin-binding

protein acts as Staphylococcus aureus invasin via fibronectin bridging to integrin alpha5beta1. Cell Microbiol **1:**101-117.

113. **Smith, A. R.** 1992. Eperythrozoonosis, p. 470-474. In W. L. Mengeling, S. D. D-Allaire, and D. J. Taylor (ed.), Diseases of swine, 7 ed. Iowa State University Press, Ames, IA.
114. **Smith, J. E., J. E. Cipriano, and S. M. Hall.** 1990. In vitro and in vivo glucose consumption in swine eperythrozoonosis. Zentralbl Veterinarmed B **37:**587-592.
115. **Splitter, E. J.** 1950. Eperythrozoon suis, the etiologic agent of ictero-anemia or an anaplasmosis-like disease in swine. Am J Vet Res **11:**324-330.
116. **Stevens, T., J. G. Garcia, D. M. Shasby, J. Bhattacharya, and A. B. Malik.** 2000. Mechanisms regulating endothelial cell barrier function. Am J Physiol Lung Cell Mol Physiol **279:**L419-422.
117. **Stoodley, P., K. Sauer, D. G. Davies, and J. W. Costerton.** 2002. Biofilms as complex differentiated communities. Annu Rev Microbiol **56:**187-209.
118. **Summersgill, J. T., R. E. Molestina, R. D. Miller, and J. A. Ramirez.** 2000. Interactions of Chlamydia pneumoniae with human endothelial cells. J Infect Dis **181 Suppl 3:**S479-482.
119. **Tanaka, H., W. T. Hall, J. B. Sheffield, and D. H. Moore.** 1965. Fine structure of Haemobartonella muris as compared with Eperythrozoon coccoides and Mycoplasma pulmonis. J Bacteriol **90:**1735-1749.
120. **Tripathi, A. K., D. J. Sullivan, and M. F. Stins.** 2006. Plasmodium falciparum-infected erythrocytes increase intercellular adhesion molecule 1 expression on brain endothelium through NF-kappaB. Infect Immun **74:**3262-3270.
121. **Tully, J. G., J. M. Bové, F. Laigret, and R. F. Whitcomb.** 1993. Notes: Revised Taxonomy of the Class Mollicutes: Proposed Elevation of a Monophyletic Cluster of Arthropod-Associated Mollicutes to Ordinal Rank (Entomoplasmatales ord. nov.), with Provision for Familial Rank To Separate Species with Nonhelical Morphology (Entomoplasmataceae fam. nov.) from Helical Species (Spiroplasmataceae), and Emended Descriptions of the Order Mycoplasmatales, Family Mycoplasmataceae. Int J Syst Bacteriol **43:**378-385.
122. **Turner, G. D., H. Morrison, M. Jones, T. M. Davis, S. Looareesuwan, I. D. Buley, K. C. Gatter, C. I. Newbold, S. Pukritayakamee, B. Nagachinta, and et al.** 1994. An immunohistochemical study of the pathology of fatal malaria. Evidence for widespread endothelial activation and a potential role for intercellular adhesion molecule-1 in cerebral sequestration. Am J Pathol **145:**1057-1069.
123. **Underhill, D. M., and A. Ozinsky.** 2002. Toll-like receptors: key mediators of microbe detection. Curr Opin Immunol **14:**103-110.
124. **Valbuena, G., H. M. Feng, and D. H. Walker.** 2002. Mechanisms of immunity against rickettsiae. New perspectives and opportunities offered by unusual intracellular parasites. Microbes Infect **4:**625-633.
125. **Valdivieso-Garcia, A., S. Rosendal, and S. Serebrin.** 1989. Adherence of Mycoplasma mycoides subspecies mycoides to cultured endothelial cells. Zentralbl Bakteriol **272:**210-215.
126. **Van De Graaff, K. M.** 2001. Human Anatomy, 6th ed. McGraw-Hill Education.
127. **Vanhoutte, P. M., and J. V. Mombouli.** 1996. Vascular endothelium: vasoactive mediators. Prog Cardiovasc Dis **39:**229-238.
128. **Walski, M., S. Chlopicki, R. Celary-Walska, and M. Frontczak-Baniewicz.** 2002. Ultrastructural alterations of endothelium covering advanced atherosclerotic plaque in human carotid artery visualised by scanning electron microscope. J Physiol Pharmacol

53:713-723.

129. **Wautier, J. L., M. P. Wautier, D. Pintigny, F. Galacteros, A. Courillon, P. Passa, and J. P. Caen.** 1983. Factors involved in cell adhesion to vascular endothelium. Blood Cells **9:**221-234.
130. **Wautier, J. L., M. P. Wautier, A. M. Schmidt, G. M. Anderson, O. Hori, C. Zoukourian, L. Capron, O. Chappey, S. D. Yan, J. Brett, and et al.** 1994. Advanced glycation end products (AGEs) on the surface of diabetic erythrocytes bind to the vessel wall via a specific receptor inducing oxidant stress in the vasculature: a link between surface-associated AGEs and diabetic complications. Proc Natl Acad Sci U S A **91:**7742-7746.
131. **Wolfson, J. S., D. C. Hooper, G. L. McHugh, M. A. Bozza, and M. N. Swartz.** 1990. Mutants of Escherichia coli K-12 exhibiting reduced killing by both quinolone and beta-lactam antimicrobial agents. Antimicrob Agents Chemother **34:**1938-1943.
132. **Wong, K., X. Li, and Y. Ma.** 2006. Paraformaldehyde induces elevation of intracellular calcium and phosphatidylserine externalization in platelets. Thromb Res **117:**537-542.
133. **Yang, D., X. Tai, Y. Qiu, and S. Yun.** 2000. Prevalence of Eperythrozoon spp. infection and congenital eperythrozoonosis in humans in Inner Mongolia, China. Epidemiol Infect **125:**421-426.
134. **Young, D. S., M. Kadokura, I. Brockhausen, V. Kashef, and J. G. Coles.** 1996. Human serum-induced porcine endothelial cell apoptosis--another pathway to xenograft rejection. Transplant Proc **28:**611-612.
135. **Zachary, J. F., and E. J. Basgall.** 1985. Erythrocyte membrane alterations associated with the attachment and replication of Eperythrozoon suis: a light and electron microscopic study. Vet Pathol **22:**164-170.
136. **Zachary, J. F., and A. R. Smith.** 1985. Experimental porcine eperythrozoonosis: T-lymphocyte suppression and misdirected immune responses. Am J Vet Res **46:**821-830.

Selected Publication

In this section, a published manuscript including results associated with this Ph.D. thesis is presented:

Mycoplasma suis invades porcine erythrocytes.

Infection and Immunity. 2009; 77:576-584.

Groebel, K., K. Hoelzle, M. M. Wittenbrink, U. Ziegler, and L. E. Hoelzle.

This work was cited in Nature *Reviews Microbiology* as a *Research Highlight* within the *In Brief* section to bacterial pathogenesis:

Mycoplasma suis invades porcine erythrocytes.

Nature Reviews Microbiology 7, 4 (January 2009)

Groebel, K., K. Hoelzle, M. M. Wittenbrink, U. Ziegler, and L. E. Hoelzle.

This publication is the first to show that *Mycoplasma suis* 08/07, a member of the haemotrophic mycoplasmas, is able to invade erythrocytes. This finding has implications for the detection, pathogenesis and treatment of the *M. suis* infection.

I established the experimental set-up, performed fluorescence staining procedures, examined samples using confocal laser scanning microscopy, prepared and examined samples using scanning- and transmission electron microscopy and wrote the manuscript.

INFECTION AND IMMUNITY, Feb. 2009, p. 576–584 Vol. 77, No. 2
0019-9567/09/$08.00+0 doi:10.1128/IAI.00773-08

Mycoplasma suis Invades Porcine Erythrocytes▽

K. Groebel,[1] K. Hoelzle,[1] M. M. Wittenbrink,[1] U. Ziegler,[2] and L. E. Hoelzle[1]*

Institute of Veterinary Bacteriology, Vetsuisse Faculty, University of Zurich, Winterthurerstrasse 270, 8057 Zurich, Switzerland,[1] and Center for Microscopy and Image Analysis, University of Zurich, Gloriastrasse 30, 8006 Zurich, Switzerland[2]

Received 19 June 2008/Returned for modification 7 August 2008/Accepted 6 November 2008

Mycoplasma suis **belongs to the hemotrophic mycoplasma group and causes infectious anemia in pigs. According to the present state of knowledge, this organism adheres to the surface of erythrocytes but does not invade them. We found a novel *M. suis* isolate that caused severe anemia in pigs with a fatal disease course. Interestingly, only marginal numbers of the bacteria were visible on and between the erythrocytes in acridine orange-stained blood smears for acutely diseased pigs, whereas very high loads of *M. suis* were detected in the same blood samples by quantitative PCR. These findings indicated that *M. suis* is capable of invading erythrocytes. By use of fluorescent labeling of *M. suis* and examination by confocal laser scanning microscopy, as well as scanning and transmission electron microscopy, we proved that the localization of *M. suis* was intracellular. This organism invades erythrocytes in an endocytosis-like process and is initially surrounded by two membranes, and it was also found floating freely in the cytoplasm. In conclusion, we were able to prove for the first time that a member of the hemotrophic mycoplasma group is able to invade the erythrocytes of its host. Such colonization should protect the bacterial cells from the host's immune response and hamper antibiotic treatment. In addition, an intracellular life cycle may explain the chronic nature of hemotrophic mycoplasma infections and should serve as the foundation for novel strategies in hemotrophic mycoplasma research (e.g., treatment or prophylaxis).**

Mycoplasma suis is a member of the family *Mycoplasmataceae*. This organism belongs to a group of uncultivable highly specialized bacteria which parasitize the surface of erythrocytes of a variety of mammals (34). These species represent a distinct new cluster in the genus *Mycoplasma* and have been given the trivial name hemotrophic mycoplasmas (HM). Infections with HM are identified clinically by overt life-threatening hemolytic anemia or by subtle chronic anemia characterized by infertility, immune suppression, and greater susceptibility to infections (34). It is noteworthy that organisms that morphologically resemble HM have also been detected in the blood of humans (1, 8, 42, 50).

M. suis causes febrile acute icteroanemia in pigs (IAP), which is accompanied by high numbers of *M. suis* cells in the blood, as confirmed by microscopy as well as by PCR (18, 21, 34). Clinical symptoms are successfully cured by treatment with tetracycline. Nevertheless, once pigs are infected with *M. suis*, they remain lifelong carrier animals and therefore are epidemiologically important (19). Chronic *M. suis* infections result in reproductive disorders in sows, growth retardation in piglets, and increased susceptibility to respiratory and enteric infections in feeder pigs. *M. suis* occurs worldwide, and chronic IAP, in particular, is of major economic importance (19).

Contrary to the well-established clinical picture of IAP (i.e., high morbidity and low mortality), we recently observed an increased incidence of acute IAP in feeder pigs with a predominantly fatal outcome despite antibiotic therapy. And contrary to the expected high numbers of *M. suis* cells on and between the erythrocytes in acridine orange-stained blood smears (the established diagnostic feature of acute IAP), only marginal numbers of bacterial cells were observed. This microscopic finding conflicted with the results of quantitative real-time PCR, which detected high numbers of *M. suis* cells (10^9 to 10^{10} cells per ml of blood) in the same blood samples. The striking difference between the microscopy and PCR results raises the issue of putative intracellular localization of a novel *M. suis* isolate within the erythrocytes.

To date, several *Mycoplasma* species are known to invade cells (2, 28, 33, 46); for example, *M. penetrans* invades the epithelial cells of the human urogenital tract (28), and *M. genitalium* infects human lung fibroblasts (2, 33). *M. gallisepticum* can invade nonphagocytic cell lines, such as HeLa cells and chicken embryo fibroblasts (49), and is the only known *Mycoplasma* species that is able to invade erythrocytes (47). The general advantages associated with invasion of eukaryotic cells by bacterial pathogens include protection from the immune system, reduction in the efficacy of antibiotics during treatment, and nutritional benefits. The intraerythrocytic localization of *M. suis* might provide the organism with a supply of iron, large amounts of which can be found inside the red blood cells (RBCs) in the form of hemin, or other trace metals (47). It is known that hemin can support the growth of invasive bacteria, such as *Bartonella quintana* (43). Moreover, the persistence of some *Bartonella* species is directly linked to nonhemolytic erythrocyte parasitism (43). However, no influence of hemin on the growth of mycoplasmas has been demonstrated so far.

It is interesting that hemotrophic mycoplasmas have a tendency to establish chronic infections that often are not apparent clinically (34). The long persistence of *M. suis* (and other HM) might be linked to their ability to invade the cytoplasm of host cells. Dallo and Basemann (6) assumed that the chronic nature of mycoplasma infections (*M. pneumoniae*, *M. penetrans*, *M. genitalium*) can be explained by a subpopulation of mycoplasmas that enter mammalian cells, where they can per-

* Corresponding author. Mailing address: Institute of Veterinary Bacteriology, Winterthurerstrasse 270, 8057 Zurich, Switzerland. Phone: 41-44-6358613. Fax: 41-44-6358912. E-mail: lhoelzle@vetbakt.uzh.ch.
▽ Published ahead of print on 17 November 2008.

sist in a latent or nongrowth maintenance form. Such biological latency would circumvent the killing action of antimicrobials. The usual establishment of chronic disease in *M. gallisepticum*-infected birds and the limited effects of antibiotic treatments (44) have also been linked to the ability of this agent to enter nonphagocytic host cells (35, 49).

In order to confirm our hypothesis that *M. suis* invades blood cells, splenectomized pigs were experimentally infected with a novel *M. suis* isolate. The clinical course was monitored, and blood samples were taken during the experiments. Furthermore, we used fluorescent labeling of *M. suis* coupled to confocal laser scanning microscopy (CLSM), as well as scanning electron microscopy (SEM) and transmission electron microscopy (TEM), in order to investigate the intracellular life cycle of *M. suis*.

MATERIALS AND METHODS

Bacterial isolate and experimental infection. *M. suis* isolate 08/07 originated from a representative pig in a stock of feeder animals that had severe IAP infections with high mortality. The pig used suffered from acute IAP. A splenectomized pig model was used to maintain the new *M. suis* isolate, as described elsewhere (16). Briefly, 5-week-old pigs ($n = 10$) were screened to make sure that they were *M. suis* negative by quantitative PCR and *M. suis* immunoblotting as described previously (18, 20). Pigs were splenectomized by using the method of Heinritzi (16). For infection, 2 ml of the infected animal's blood was inoculated intramuscularly. Clinical symptoms, feeding behavior, and body temperature were monitored at least daily for each pig. Blood samples were taken prior to infection (day 0) and then weekly until necropsy, as well as when there were clinical attacks. Clinical diagnosis of acute IAP was confirmed by quantitative PCR and *M. suis* immunoblotting, as well as by microscopic detection of *M. suis* cells in blood smears stained with acridine orange. Briefly, blood smears obtained using anticoagulated blood were fixed in ethanol for 1 min and air dried. Staining was done by using an acridine orange solution (0.25 μg/ml) for 1 h in the dark. The slides were rinsed with water and air dried. *M. suis* cells on and between the erythrocytes were detected using UV light excitation with a fluorescence microscope. When there were acute clinical attacks, pigs were treated with tetracycline (40 mg/kg of body weight) and glucose (35 g glucose/liter of drinking water) to prevent death caused by *M. suis* 08/07-induced hypoglycemia.

Hematological investigations. The erythrocyte counts, hemoglobin concentrations, and hematocrit levels of acutely diseased pigs infected with *M. suis* 08/07 were determined using blood that was anticoagulated by EDTA and an automatic blood cell counter (Celltek; Bayer Diagnostics, Munich, Germany). Serum was obtained by centrifugation of a serum monovette (Hettich Rotixa/AP; Hettich, Tuttlingen, Germany). Glucose and bilirubin levels were determined in the laboratory of the farm animal clinic of Ludwig Maximilians University of Munich by using a selective, discrete, multiple-analysis system (Hitachi 911; Roche, Mannheim, Germany). The values obtained were compared to data obtained from classical *M. suis* infections (17). Reference values (erythrocyte counts, hematocrit levels, hemoglobin concentrations) for healthy pigs were obtained from previously published data of Kraft and coworkers (25). Reference ranges for bilirubin and blood glucose levels were obtained from the data of Kixmoeller et al. (24).

Quantitative real-time PCR. *M. suis* DNA was quantified using the LightCycler 2.0 system (Roche Diagnostics, Rotkreuz, Switzerland), as described previously (20). Primers *msg*1-Fw (5′-ACAACTAATGCACTAGCTCCTATC-3′) and *msg*1-Rv (5′-GCTCCTGTAGTTGTAGGAA TAATTGA-3′), as well as probes 5′-TTCACGCTTTCACTTCTGACCAAAGAC-fluorescein-3′ and 5′-LCRed-640-CAAGACTCTCCTCACTCTGACCTAAGAAGAGC-3′, were purchased from Metabion (Martinsried, Germany). Real-time PCR was performed using a LightCycler Fast Start DNA Master^{PLUS} hybridization probe kit (Roche Diagnostics) with 0.5 μM of each primer, as well as 0.2 μM of each probe. For quantification, *M. suis* genomic DNA was extracted from experimentally infected pigs and quantified as described previously (20).

Antibody reagents. Polyclonal monospecific antisera for the detection of *M. suis* by immunostaining were obtained by immunization of rabbits with recombinant HspA1, as described elsewhere (21). HspA1 is a surface protein of *M. suis* (21).

CLSM. For staining of the erythrocyte surface and differential staining of intracellular and extracellular *M. suis*, a modified version of the double-immunofluorescence (DIF) method adapted for use with erythrocytes (47) was used, with the following modifications. Peripheral anticoagulated blood samples (40 μl) were diluted in 2.5 ml phosphate-buffered saline (PBS) containing 10 mM glucose and 0.1% bovine serum albumin (BSA). Cells were fixed in 4% PBS-buffered paraformaldehyde (Sigma-Aldrich, Steinheim, Germany) containing 0.01% glutaraldehyde (grade I; Sigma-Aldrich, Buchs, Switzerland) and seeded onto poly-L-lysine-coated glass slides (SuperFrost; Menzel, Braunschweig, Germany). Nonreacted aldehydes were blocked with 0.1 M glycine (Carl Roth, Karlsruhe, Germany) in PBS for 20 min. Nonspecific binding of antibodies was reduced by incubation of samples in blocking buffer (3% BSA in PBS) for 30 min. The erythrocyte surface and extracellular *M. suis* cells were stained with purified mouse anti-pig CD235a (glycophorin A) monoclonal antibody (1:100; PharMingen, BD Biosciences, Europe) and rabbit monospecific anti-HspA1 serum (1:100) for 1 h, followed by tetramethyl rhodamine isocyanate (TRITC)-conjugated goat anti-mouse immunoglobulin G (IgG) (1:100, Sigma) and fluorescein isothiocyanate (FITC)-conjugated goat anti-rabbit IgG (Sigma), respectively, for 1 h. The cells were permeabilized with 0.1% Triton X-100 (Sigma) in PBS for 10 s and incubated in blocking buffer for 30 min. Intracellular *M. suis* cells were detected after incubation with rabbit monospecific anti-HspA1 serum for 1 h and Alexa Fluor 405-labeled goat anti-rabbit IgG (Molecular Probes, Basel, Switzerland) for 1 h. The staining procedure resulted in Alexa Fluor 405-labeled intracellular bacteria (blue) and FITC- and Alexa Fluor 405-labeled extracellular bacteria (blue and green). Confocal microscopy was performed with a Leica SP2 confocal microscope (Leica Microsystems, Mannheim, Germany).

Colocalization measurement. Colocalization of two labels indicates that they are located close enough to each other in the sample that they cannot be resolved optically. The colocalization of two labels was measured using the "Colocalization" module of Imaris 5.0.2 (64-bit version; Bitplane AG, Switzerland) (www.bitplane.com). When this application was used, extracellular *M. suis* cells appeared to be white since they were double labeled with both secondary fluorescent conjugates, as described above. Intracellular bacteria were stained with a single stain and were blue.

TEM. Blood samples were diluted in PBS containing 10 mM glucose and 0.1% BSA and fixed in a 1% glutaraldehyde solution. Cells were washed consecutively in PBS and 0.05 M cacodylate buffer and suspended in the latter buffer. Following postfixation in a mixture of 1% osmium tetroxide (Fluka Chemie, Buchs, Switzerland) and 1.5% potassium ferrocyanide (Fluka), cells were washed once in 0.05 M cacodylate buffer. Samples were embedded in molten 2.5% agar (Difco Laboratories, Detroit, MI) for dehydration using increasing concentrations of ethanol (70 to 100%) and propylene oxide (Fluka Chemie). During further processing samples were embedded in Epon 812 (Fluka Chemie) and sectioned. Grids with ultrathin sections were contrasted consecutively with 4% uranyl acetate (Fluka Chemie) and lead citrate as described elsewhere (41) and were analyzed with a Philips CM100 transmission electron microscope.

SEM. Blood samples were diluted in PBS containing 10 mM glucose and 0.1% BSA and fixed in a 1% glutaraldehyde solution. Cells were settled on carbon-coated coverslips (Assistant, Sondheim, Germany) using a Cytospin 2 (Shandon, Dako-Diagnostica, Zug, Switzerland) centrifuge, followed by dehydration using increasing concentrations of acetone and critical point drying (BAL-TEC CPD 030 critical point dryer; Balzers, Liechtenstein). Finally, the samples were sputter coated with 3 nm of gold using the BAL-TEC MED 020 coating system and analyzed with a Zeiss Supra 50 VP scanning electron microscope.

Array tube hybridization. *M. suis* genomic DNA was extracted from experimentally infected pigs and quantified, as previously described (20). To exclude the possibility that there were bacterial contaminants in the blood, the 16S rRNA gene was amplified using universal primers and sequenced (26). The sequences obtained were compared with data bank entries.

Genomic DNA (10 to 100 ng) was labeled by using a random primed polymerization reaction and Sequenase (version 2.0; USB Corporation, Cleveland, OH) as described previously (39). The protocol used for the labeling reaction was a modified protocol (modified by the DeRisi Laboratory, University of California, San Francisco, in June 2001) based on the method of Bohlander and coworkers (4). All reactions were carried out using an Eppendorf Mastercycler gradient (Vaudaux-Eppendorf, Schönenbuch, Switzerland). The DNA microarray used to detect 90 antibiotic resistance genes of gram-positive bacteria (39) was kindly provided by Vincent Perreten, Institute of Veterinary Bacteriology, University of Bern. DNA hybridization was carried out with a Thermomixer comfort instrument (Eppendorf AG, Hamburg, Germany), and the peroxidase staining procedure and online detection were performed using an *atr01* array tube reader (Clondiag, Jena, Germany) as described by Perreten and coworkers (39). The data were analyzed and processed using the Iconoclust software (Clondiag).

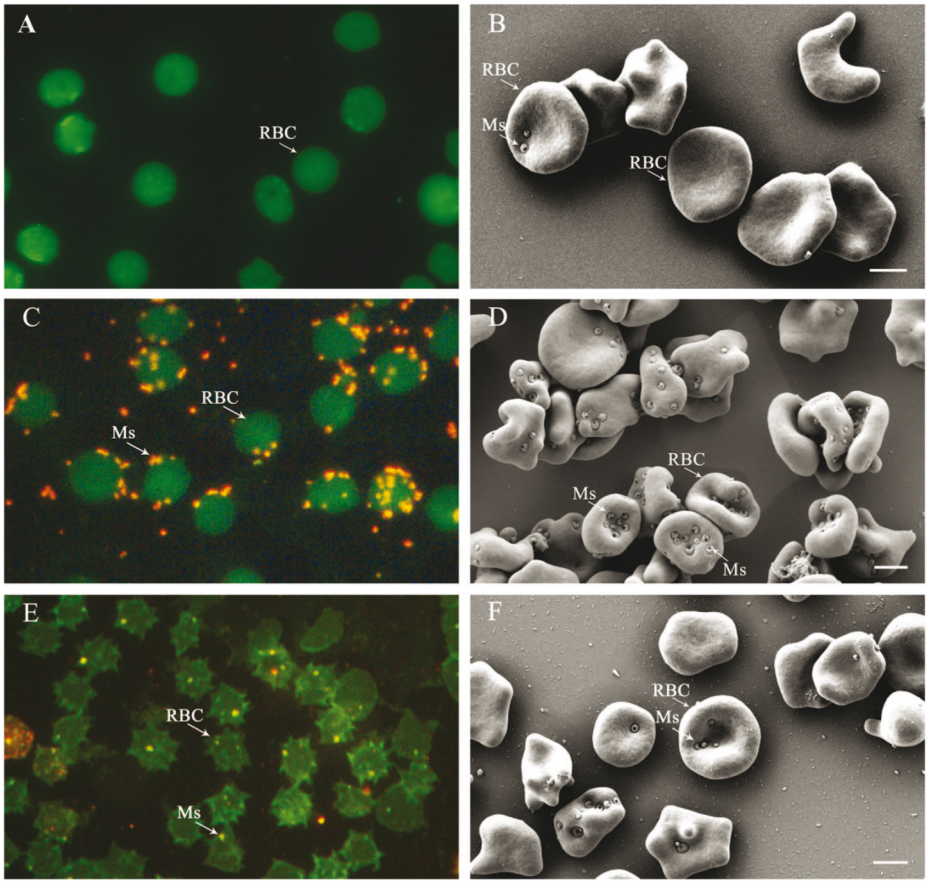

FIG. 1. Acridine orange-stained blood smears from pigs infected with *M. suis* 08/07 (A, C, and E) and corresponding SEM images (B, D, and F). On day 3 p.i. no mycoplasmas were detected in acridine orange-stained (A) blood smears, whereas in SEM single *M. suis* cells were visible (B). During acute clinical attack on day 7 p.i. numerous *M. suis* cells were identified on the erythrocytes by fluorescence microscopy (C) and SEM (D). Both methods revealed a significant reduction in the number of *M. suis* cells on the surface of RBCs on day 11 p.i. (E and F). Ms, *M. suis*. (A, C, and E) Magnification, ×1,000. (B, D, and F) Bar = 2 μm.

RESULTS

Clinical manifestations and bacteriology of *M. suis* novel isolate 08/07. For blood samples taken from experimental pigs on day 3 postinfection (p.i.), no *M. suis* cells were found in acridine orange-stained blood smears examined microscopically (Fig. 1A). In SEM, only single erythrocytes were marked by sporadically attached *M. suis* 08/07 cells (Fig. 1B). These microscopic findings corresponded both to the lack of symptoms in the animals and to the PCR detection of low numbers of *M. suis* cells (approximately 10^3 bacterial cells per ml of blood). With the clinical onset of acute IAP on day 7 p.i., numerous *M. suis* particles were found on and between the erythrocytes in acridine orange-stained blood smears, as well as by SEM (Fig. 1C and D). Two different morphological forms of *M. suis* were detected: smaller coccoid cells ranging from 0.2 to 0.4 μm in diameter and large rounded flattened cells up to 1 μm in diameter (Fig. 2). In SEM, larger forms had one or two conspicuous invaginations in the cell membrane (Fig. 2A and B). In TEM, these invaginations appeared to be vacuole-like structures (Fig. 2C and D). Smaller coccoid forms often appeared as a cluster of cells and might have resulted from cell division on the erythrocyte surface (Fig. 2A). In this stage of severe bacteremia, the animals suffered from febrile anemia, hypoglycemia, and bilirubinemia, as shown in Table 1. Quantification by real-time PCR revealed a bacterial load of 10^{10} to 10^{11} *M. suis* cells per ml of blood.

Due to the life-threatening effect of the IAP attack, tetracycline therapy and glucose infusion over a 5-day period were inevitable. The animals, however, did not respond to the therapy, and the severe clinical IAP continued. To examine the cause of this therapy failure, we performed a microarray-based detection assay used to screen for antibiotic resistance genes in gram-positive bacteria. However, hybridization analysis of *M. suis* 08/07 genomic DNA with the microarray revealed no common tetracycline resistance genes.

Especially remarkable on day 11 p.i. were the different sizes (anisocytosis) of the erythrocytes and the formation of echinocytes, as observed by fluorescent examination. Compared to

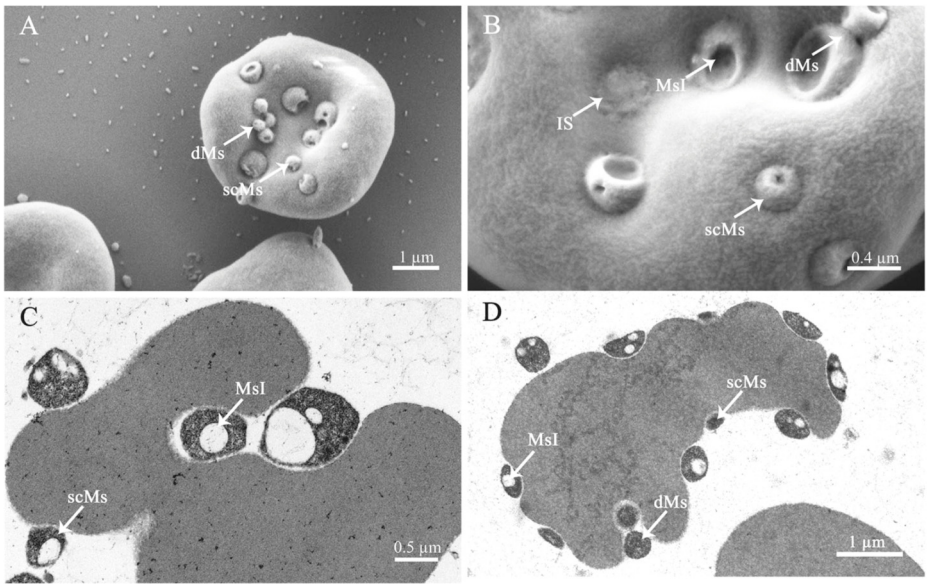

FIG. 2. SEM (A and B) and TEM (C and D) micrographs of *M. suis* 08/07-infected RBCs. The different morphological forms and features of *M. suis* 08/07 are shown. dMs, dividing *M. suis*; scMs, small coccoid *M. suis*; MsI, *M. suis* invagination; IS, invasion scar.

blood samples taken on day 7 p.i., blood samples taken from diseased animals on day 11 p.i. showed a clear reduction in the number of visible *M. suis* cells in acridine orange-stained smears, as well as in SEM (Fig. 1E and F). As determined by real-time PCR, the high bacterial loads (10^{10} to 10^{11} *M. suis* cells per ml of blood) persisted. The striking discrepancy between the microscopy results on the one hand and the PCR results on the other hand suggests that *M. suis* 08/07 might enter the erythrocytes after day 7 p.i., thus escaping detection by surface scanning microscopy.

Localization of *M. suis* within porcine erythrocytes. In order to investigate whether *M. suis* 08/07 is able to invade porcine erythrocytes, blood samples from experimental pigs were analyzed in detail by using SEM, TEM, and CLSM.

The interaction of *M. suis* and erythrocytes is marked by the formation of invaginations of variable depth in the erythrocyte membrane (Fig. 2A to D and 3A). In addition to superficially attached *M. suis* cells, the agents were also found in shallow pits. It is noteworthy that deep invaginations in which *M. suis* was surrounded almost completely by the erythrocyte membrane (Fig. 2C and D and 3A) occurred sporadically. In addition, in the *M. suis*-containing sections with deep invaginations, as shown by TEM, there were vacuoles in which the organism was entirely enclosed and therefore located in the RBC cytoplasm (Fig. 3A and D). *M. suis* cells in deep invaginations were covered by membrane material (Fig. 2B and 3B and C), leading to the formation of invasion scars (Fig. 2B).

We also detected intracellular mycoplasma cells which were not surrounded by the vacuole membrane (Fig. 3E), indicating that these bacterial cells were free in the cytoplasm. These free intracellular *M. suis* cells were approximately 300 to 500 nm in diameter, like extracellular attached *M. suis* cells (Fig. 3F), and they had a similar morphology.

The intracellular localization of *M. suis* was confirmed by a DIF technique (Fig. 4). Using this method, extra- and intracellular mycoplasmas were distinguished by consecutive incubation of infected erythrocytes with *M. suis*-specific antisera and different fluorescently labeled secondary antibodies before and after chemical permeabilization of the erythrocyte membrane. Bacteria with both green and blue marks were extracellular bacteria, whereas bacteria that stained only blue were intracellular (Fig. 4.). In superimposed images (Fig. 4D) green and blue fluorescence signals appeared to be light blue. By using this method we clearly showed that *M. suis* invaded the porcine erythrocytes. Uninfected porcine erythrocytes that were stained in parallel and served as negative controls did not exhibit any fluorescence signals (data not shown). Figure 5 shows erythrocytes that had a green label (FITC) due to glycophorin A. We used the Imaris Colocalization software to analyze whole stacks of confocal sections of erythrocytes that were double labeled for extra- and intracellular *M. suis* cells. When this method was used, extracellular *M. suis* cells stained red and blue with TRITC and Alexa Fluor 405 appeared to be white, while intracellular *M. suis* cells were blue. This method allowed definite discrimination of double-stained (extracellular) and single-stained mycoplasmas, confirming the intraerythrocytic localization of *M. suis*.

DISCUSSION

Our clinical data for experimentally infected splenectomized pigs revealed that *M. suis* 08/07 is more virulent than "classical" *M. suis* isolates. All infected pigs developed severe life-threatening hemolytic anemia (significant lower erythrocyte counts and hemoglobin and hematocrit levels), which was not affected by the antibiotic therapy. Despite the fact that as determined

TABLE 1. Hematological investigation of pigs infected either with the "classical" isolate or with *M. suis* 08/07

Reference range or isolate	Erythrocyte count (10^{12} cells/liter)		Hemoglobin concn (mmol/liter)		Hematocrit concn (liter/liter)		Glucose concn (mmol/liter)		Bilirubin concn (μmol/liter)		*M. suis* load (cells/ml blood)	
	Reference range	Mean (SD)	Reference range	Mean (SD)	Reference range	Mean (SD)	Reference range	Mean (SD)	Reference range	Mean (SD)	Reference range	Mean (range)
Reference range	5.80–8.10[a]		6.70–9.18[a]		0.33–0.45[a]		3.80–6.70[b]		<4.3[b]		0	
"Classical" isolate		2.58 (0.288)[c]		3.81 (0.313)[c]		0.21 (0.025)[c]		2.40 (0.93)[c]		9.06 (4.81)[c]		1.5×10^6 (3.50×10^4 to 7.90×10^8)[d,e]
M. suis 08/07[f]		1.76 (0.582)		2.98 (0.857)		0.12 (0.053)		0.60 (1.523)		24.50 (10.709)		1.8×10^{11} (1.73×10^9 to 8.85×10^{12})[e]

[a] Reference range according to Kraft and coworkers (25).
[b] Reference range according to Kixmoeller and coworkers (24).
[c] Value for pigs infected with a classical *M. suis* isolate according to Heinritzi (17) ($n = 42$).
[d] Value according to Hoelzle and coworkers (20).
[e] The standard deviation was not determined.
[f] Data from this study ($n = 10$).

by SEM the number of extraerythrocytic attached *M. suis* cells on day 11 was less than the number on day 7, the bacterial load (10^{10} to 10^{11} *M. suis* cells per ml of blood) was the same. These findings strongly indicated that there was intraerythrocyte localization of *M. suis*. The HM have previously been described as exclusively epicellular organisms (18, 40, 42), which was the basis for their initial designation as *Eperythrozoon suis* before they were reclassified in the genus *Mycoplasma* (37, 38, 45).

In order to define the localization of bacteria inside eukaryotic cells, the two approaches generally used are (i) the gentamicin invasion assay (9, 23, 49), which is a semiquantitative method for comparison of the invasion frequencies of different mycoplasma populations, and (ii) the DIF labeling technique (47, 49) coupled to CLSM, which provides simple and accurate differentiation between intracellular and extracellular mycoplasmas. As the gentamicin invasion assay cannot be used for examination of uncultivable bacteria, such as *M. suis*, for verification of an intracellular life cycle we had to rely on the DIF assay combined with CLSM, as well as on SEM and TEM. By using these methods we showed for the first time that a member of the HM group is able to invade erythrocytes. The reproducibility of the DIF assay was proved by the results of several repeated experiments performed with the blood of *M. suis* 08/07-infected pigs, and the data left no doubt concerning the intracellular localization of this bacterium.

Given the fact that acridine orange is a cell-permeable nucleic acid stain, one would expect intraerythrocytic *M. suis* to be detected by this technique. However, against the intense autofluorescence background of erythrocytes after chemical fixation with ethanol and staining with acridine orange, it is virtually impossible to differentiate the restrained light emission of intracellular *M. suis*.

Erythrocytes are markedly nonendocytic cells (15) and therefore are suitable hosts for studying intracellular parasitism and potential alternative pathways. In our case, entry of *M. suis* into the RBCs seemed to begin with invagination of the erythrocyte membrane. As invasion progressed, the depression in the erythrocyte deepened and conformed to the shape of the pathogen. Upon entry, the orifice of the invaginated erythrocyte membrane apparently fused. As a result, *M. suis* was found in intracellular vacuoles within the erythrocytes.

A similar endocytosis-like mechanism of erythrocyte invasion has been described for *Plasmodium falciparum* in malaria (14) and for *Bartonella bacilliformis*, which is responsible for human Oroya fever (3). The finding that *M. suis* was located within vacuole-like structures indicates that the bacteria must initiate and mediate the process leading to their uptake by the RBCs. The formation of deep invaginations during entry is therefore aided either by mechanical forces generated by the adhering bacteria or by cellular factors secreted by *M. suis*. In *B. bacilliformis* a small, hydrophobic molecule named deformin was identified, which causes deformation and invagination of RBC membranes, leading to the formation of intraerythrocytic vacuoles formed by a process similar to endocytosis (32).

In a study carried out by Murphy and coworkers, the chemical composition of drug-induced endovesicle membranes of erythrocytes was compared with that of the host-derived parasitophorous vacuolar membrane in malaria-infected RBCs (36). The results clearly showed that in pathogen-induced en-

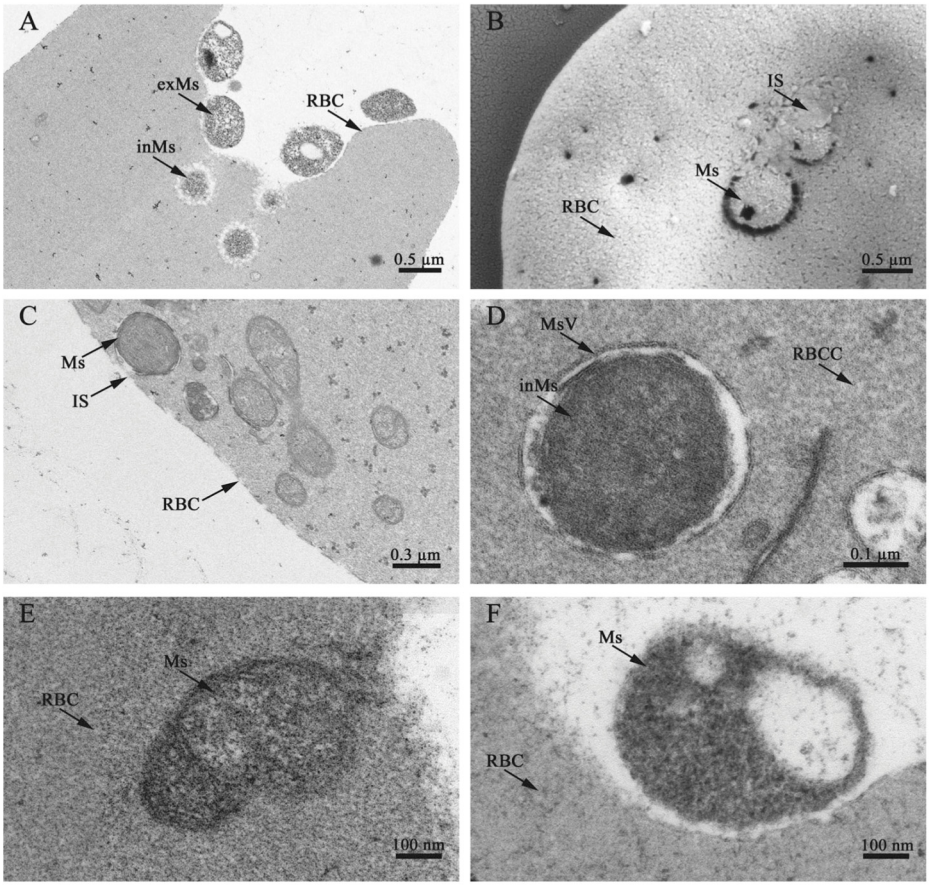

FIG. 3. Invasion of porcine erythrocytes by *M. suis* 08/07 shown by SEM (B) and TEM (A and C to F). During invasion *M. suis* 08/07 is located in deep invaginations of the RBC membrane (A). As invasion progresses, the erythrocyte membrane conforms to the shape of the bacterial cells (A and C), and newly formed membrane material covers the surface of the bacteria (B and C). As a result, invading mycoplasmas are located within an intraerythrocytic vacuole (D). Intracellular forms that are free in the RBC cytoplasm (E) have a shape and size similar to the shape and size of extracellular attached *M. suis* cells (F). exMs, extracellular *M. suis*; inMs, intracellular *M. suis*; IS, invasion scar; Ms, *M. suis*; MsV, *M. suis* vacuole; RBCC, RBC cytoplasm.

dovacuolation specific raft and cytoskeletal proteins, as well as lipids, are actively excluded from the vacuole, e.g., PIP_2, which displays a major phosphoinositide in erythrocyte membranes influencing membrane junctional complex stability. Interestingly, PIP_2 is present in the drug-induced endovesicle whereas it cannot be found in the parasitophorous membrane, suggesting an unknown erythrocyte phospholipid remodeling in the malarial vacuole during invasion of *P. falciparum*. Further studies are necessary to examine whether the *M. suis*-induced endovacuole has a composition similar to that of the parasitophorous vacuolar membrane in malaria.

Sometimes we found that *M. suis* cells were located free in the RBC cytoplasm. These bacterial cells might have corresponded to *M. suis* cells that either used a different mechanism for erythrocyte invasion or escaped from the initial vacuole. Further investigation (e.g., staining of infected erythrocytes with FM4-64 coupled to CLSM) will be done to clearly distinguish *M. suis* located within RBC-derived vacuoles from free forms located in the RBC cytoplasm. FM4-64 is an amphiphilic plasma membrane stain used to investigate endocytosis and vesicle trafficking in living eukaryotic cells.

The central considerations arising from our observations are unquestionable. Does the intraerythrocytic lifestyle of *M. suis* provide any benefit to the organism, and are there any hints that it has an impact on the life cycle of this organism?

Obviously, the intracellular localization of *M. suis* can prevent damage of the bacteria by antibiotics. This conclusion is supported by the fact that it was impossible to cure the high level of bacteremia with tetracycline, the antibiotic which is generally used to treat pigs with acute IAP. Tetracycline is, however, the drug of choice for elimination of obligate intracellular bacteria (22, 29). Thus, it is more probable that *M. suis* developed tetracycline resistance mechanisms. In a study of *M. synoviae*, an increase in resistance to enrofloxacin could be demonstrated after several in vivo treatments of experimentally infected hens (27). However, when we used a microarray-based detection assay used to screen for antibiotic resistance genes in gram-positive

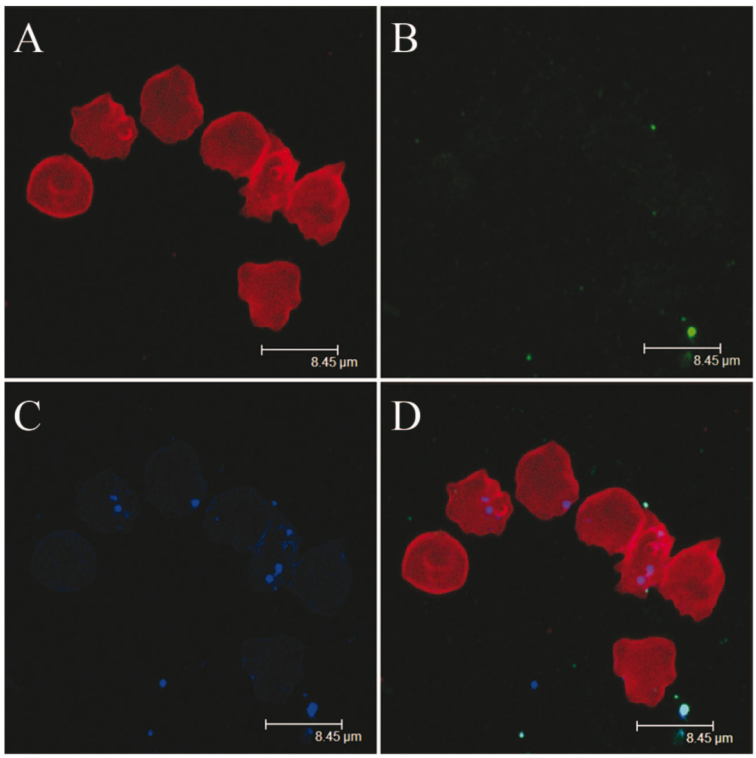

FIG. 4. CSLM of porcine RBCs infected with *M. suis* 08/07 after DIF staining. The same area of a confocal microscopic image was analyzed to visualize extracellular *M. suis* labeled with FITC (green fluorescence) (B) and extra- and intracellular *M. suis* labeled with Alexa Fluor 405 (blue fluorescence) (C). Erythrocytes had a red label due to glycophorin A (A). (D) Superimposition of the green and blue fluorescence images resulted in white fluorescence, indicating extracellular *M. suis* cells, while the blue fluorescence indicates intraerythrocytic mycoplasma cells.

bacteria (39), we did not find any common tetracycline resistance genes (*tetP*, *tetS*, *tetT*, *tetU*, *tetW*, *tetZ*, *tetK*, *tetL*, and *tetM*) in *M. suis*. Therefore, *M. suis* 08/07 might have unknown or uncommon resistance mechanisms.

The presence of *M. suis* within porcine erythrocytes nonetheless has significant clinical implications. It is possible that the internalized bacteria are able to exploit host cell functions and elude host defense mechanisms, such as complement-mediated lysis and circulating phagocytic cells and antibodies (5, 6, 10, 13). Moreover, an intraerythrocytic localization of *M. suis* aggravates the natural turnover of infected RBCs in the spleen (30). The RBCs carrying only cytoplasmic *M. suis* cells do not have modified surfaces and cannot be recognized by spleen macrophages. This conclusion was supported by the findings obtained with experimentally infected pigs that obviously had constant numbers of RBCs that were invaded by *M. suis* in the peripheral blood and the duration of the severe clinical symptoms. Nevertheless, further verification is needed.

The bacterial invasion of erythrocytes is a special feature that has been described previously only for members of the genera *Bartonella* (3, 7, 31, 43) and *Anaplasma* (12) and for *M. gallisepticum* (47). In contrast to the establishment of a persistent stage of *Bartonella*, erythrocyte invasion by *M. suis* 08/07 leads to severe hemolysis and to greater virulence. Furthermore, in contrast to previously described infections with common *M. suis* isolates, a chronic infection is not established upon infection with *M suis* 08/07 due to the fatal course of the disease. To further define whether internalization of *M. suis* occurs in naturally chronically infected pigs and the potential impact of this phenomenon in these animals, TEM studies, as well as CSLM, will have to be performed with samples collected from such pigs. Detection of intracellular *M. suis* bacteria in asymptomatic persistently infected pigs would be a milestone in research on HM, as it would help explain the long-term survival of the organisms and the associated persistence.

We found many erythrocytic precursor cells in the circulating blood using TEM. It is well known from former studies that RBC precursors can be found in the circulation of patients with chronic and acute anemia (48) and in animals infected with HM (11). However, the presence of *M. suis*-infected reticulocytes and normoblasts in the bloodstream is a novel finding for the pathogenesis of HM (data not shown). Further investigations of the bone marrow of infected pigs should reveal whether *M. suis* 08/07 can propagate within the blood-building tissue.

In conclusion, this is the first report to show that a member of the HM group is able to invade the erythrocytes of its host. Our studies clearly showed that the intracellular life cycle of *M.*

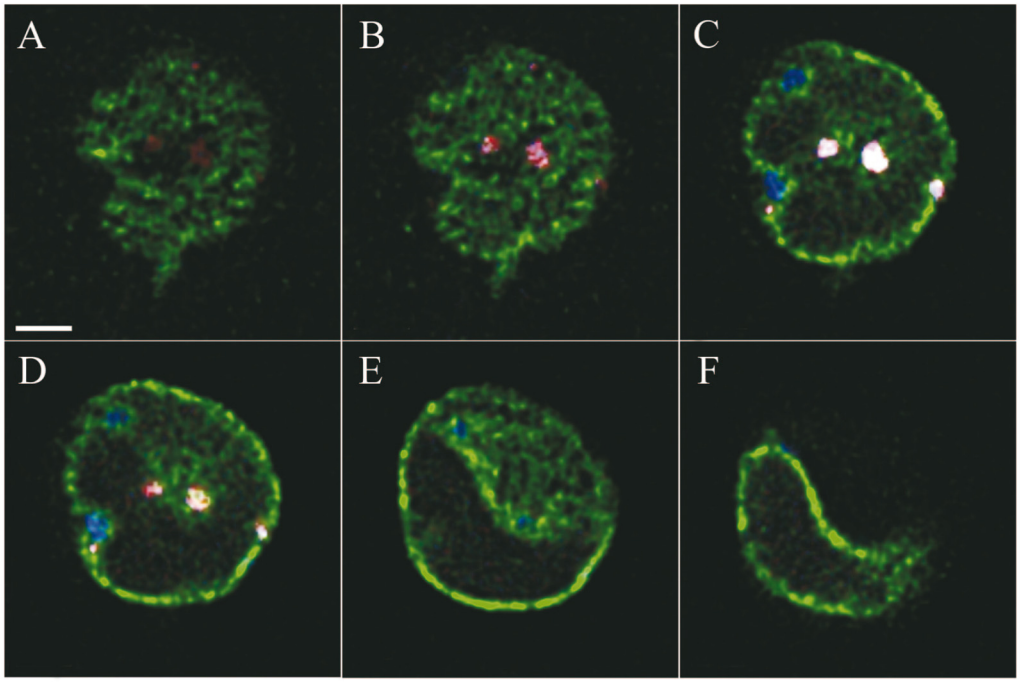

FIG. 5. RBC from an experimental pig infected with *M. suis* 08/07 after DIF staining: six focal scans from a stack from the top (A) to the bottom (F). Erythrocytes have a green label due to glycophorin A. As determined with a colocalization tool (Imaris), extracellular *M. suis* cells stained with TRITC and Alexa Fluor 405 appear to be white, while intracellular *M. suis* cells are blue (Alexa Fluor 405).

suis dramatically increased the virulence of the organism. Further studies are required to understand the cellular interactions and factors that contribute to host cell invasion by *M. suis* 08/07 and to investigate the ability of common *M. suis* isolates to invade erythrocytes.

ACKNOWLEDGMENTS

We thank Gery Barmettler for assistance with electron microscopic preparation of our blood samples.

This work was supported in part by the Forschungskredit of the University of Zurich.

REFERENCES

1. **Archer, G. L., P. H. Coleman, R. M. Cole, R. J. Duma, and C. L. Johnston, Jr.** 1980. Hemotropic bacteria. N. Engl. J. Med. **302:**1151–1152.
2. **Baseman, J. B., M. Lange, N. L. Criscimagna, J. A. Giron, and C. A. Thomas.** 1995. Interplay between mycoplasmas and host target cells. Microb. Pathog. **19:**105–116.
3. **Benson, L. A., S. Kar, G. McLaughlin, and G. M. Ihler.** 1986. Entry of *Bartonella bacilliformis* into erythrocytes. Infect. Immun. **54:**347–353.
4. **Bohlander, S. K., R. Espinosa III, M. M. Le Beau, J. D. Rowley, and M. O. Diaz.** 1992. A method for the rapid sequence-independent amplification of microdissected chromosomal material. Genomics **13:**1322–1324.
5. **Cooper, N. R.** 1988. Complement and infectious agents. Rev. Infect. Dis. **10**(Suppl. 2)**:**S447–S449.
6. **Dallo, S. F., and J. B. Baseman.** 2000. Intracellular DNA replication and long-term survival of pathogenic mycoplasmas. Microb. Pathog. **29:**301–309.
7. **Dehio, C.** 2004. Molecular and cellular basis of bartonella pathogenesis. Annu. Rev. Microbiol. **58:**365–390.
8. **Duarte, M. I., M. S. Oliveira, M. A. Shikanai-Yasuda, O. N. Mariano, C. F. Takakura, C. Pagliari, and C. E. Corbett.** 1992. Haemobartonella-like microorganism infection in AIDS patients: ultrastructural pathology. J. Infect. Dis. **165:**976–977.
9. **Elsinghorst, E. A.** 1994. Measurement of invasion by gentamicin resistance. Methods Enzymol. **236:**405–420.
10. **Finlay, B. B., and P. Cossart.** 1997. Exploitation of mammalian host cell functions by bacterial pathogens. Science **276:**718–725.
11. **Fitzpatrick, J. L., R. C. J. Barron, L. Andrew, and H. Thompson.** 1998. *Eperythrozoon ovis* infection of sheep. Comp. Haematol Int. **8:**230–234.
12. **Foote, L. E., J. C. Geer, and Y. E. Stich.** 1958. Electron microscopy of the Anaplasma body: ultra-thin sections of bovine erythrocytes. Science **128:**147–148.
13. **Gotschlich, E. C.** 1983. Thoughts on the evolution of strategies used by bacteria for evasion of host defenses. Rev. Infect. Dis. **5**(Suppl. 4)**:**S778–S783.
14. **Haldar, K., and N. Mohandas.** 2007. Erythrocyte remodeling by malaria parasites. Curr. Opin. Hematol. **14:**203–209.
15. **Haldar, K., B. U. Samuel, N. Mohandas, T. Harrison, and N. L. Hiller.** 2001. Transport mechanisms in Plasmodium-infected erythrocytes: lipid rafts and a tubovesicular network. Int. J. Parasitol. **31:**1393–1401.
16. **Heinritzi, K.** 1984. A contribution on splenectomy in swine. Tierarztl. Prax. **12:**451–454.
17. **Heinritzi, K. H.** 1990. Untersuchungen zur Pathogenese und Diagnostik der Infektion mit *Eperythrozoon suis*. Professorial dissertation. Ludwig Maximilians University of Munich, Munich, Germany.
18. **Hoelzle, L. E.** 2008. Haemotrophic mycoplasmas: recent advances in *Mycoplasma suis*. Vet. Microbiol. **130:**215–226.
19. **Hoelzle, L. E.** 2007. Significance of haemotrophic mycoplasmas in veterinary medicine with particular regard to the *Mycoplasma suis* infection in swine. Berl. Muench. Tieraerztl. Wochenschr. **120:**34–41.
20. **Hoelzle, L. E., M. Helbling, K. Hoelzle, M. Ritzmann, K. Heinritzi, and M. M. Wittenbrink.** 2007. First LightCycler real-time PCR assay for the quantitative detection of *Mycoplasma suis* in clinical samples. J. Microbiol. Methods **70:**346–354.
21. **Hoelzle, L. E., K. Hoelzle, A. Harder, M. Ritzmann, H. Aupperle, H. A. Schoon, K. Heinritzi, and M. M. Wittenbrink.** 2007. First identification and functional characterization of an immunogenic protein in unculturable haemotrophic mycoplasmas (*Mycoplasma suis* HspA1). FEMS Immunol. Med. Microbiol. **49:**215–223.
22. **Hoerauf, A., K. Nissen-Pahle, C. Schmetz, K. Henkle-Duhrsen, M. L. Blaxter, D. W. Buttner, M. Y. Gallin, K. M. Al-Qaoud, R. Lucius, and B. Fleischer.** 1999. Tetracycline therapy targets intracellular bacteria in the filarial nematode *Litomosoides sigmodontis* and results in filarial infertility. J. Clin. Investig. **103:**11–18.
23. **Kihlstrom, E.** 1977. Infection of HeLa cells with *Salmonella typhimurium* 395 MS and MR10 bacteria. Infect. Immun. **17:**290–295.
24. **Kixmoeller, M., M. Ritzmann, and K. H. Heinritzi.** 2006. Reference ranges

for laboratory parameters in pigs of different breeds. Prakt. Tierärztl. **87:** 204–213.
25. **Kraft, W., U. M. Dürr, M. Fürll, H. Bostedt, and K. Heinritzi.** 2005. Hämatologie, vol. 6. Schattauer-Verlag, Stuttgart, Germany.
26. **Lane, D. J.** 1991. 16S/23S rRNA sequencing, p. 115–147. *In* E. Stackebrandt and M. Goodfellow (ed.), Nucleic acid techniques in bacterial systematics. John Wiley & Sons, Chichester, United Kingdom.
27. **Le Carrou, J., A. K. Reinhardt, I. Kempf, and A. V. Gautier-Bouchardon.** 2006. Persistence of *Mycoplasma synoviae* in hens after two enrofloxacin treatments and detection of mutations in the parC gene. Vet. Res. **37:**145–154.
28. **Lo, S. C., M. M. Hayes, H. Kotani, P. F. Pierce, D. J. Wear, P. B. Newton III, J. G. Tully, and J. W. Shih.** 1993. Adhesion onto and invasion into mammalian cells by *Mycoplasma penetrans*: a newly isolated mycoplasma from patients with AIDS. Mod. Pathol. **6:**276–280.
29. **McOrist, S.** 2000. Obligate intracellular bacteria and antibiotic resistance. Trends Microbiol. **8:**483–486.
30. **Mebius, R. E., and G. Kraal.** 2005. Structure and function of the spleen. Nat. Rev. **5:**606–616.
31. **Mehock, J. R., C. E. Greene, F. C. Gherardini, T. W. Hahn, and D. C. Krause.** 1998. *Bartonella henselae* invasion of feline erythrocytes in vitro. Infect. Immun. **66:**3462–3466.
32. **Mernaugh, G., and G. M. Ihler.** 1992. Deformation factor: an extracellular protein synthesized by *Bartonella bacilliformis* that deforms erythrocyte membranes. Infect. Immun. **60:**937–943.
33. **Mernaugh, G. R., S. F. Dallo, S. C. Holt, and J. B. Baseman.** 1993. Properties of adhering and nonadhering populations of *Mycoplasma genitalium*. Clin. Infect. Dis. **17**(Suppl. 1)**:**S69–S78.
34. **Messick, J. B.** 2004. Hemotrophic mycoplasmas (hemoplasmas): a review and new insights into pathogenic potential. Vet. Clin. Pathol. **33:**2–13.
35. **Much, P., F. Winner, L. Stipkovits, R. Rosengarten, and C. Citti.** 2002. *Mycoplasma gallisepticum*: influence of cell invasiveness on the outcome of experimental infection in chickens. FEMS Immunol. Med. Microbiol. **34:** 181–186.
36. **Murphy, S. C., S. Fernandez-Pol, P. H. Chung, S. N. Prasanna Murthy, S. B. Milne, M. Salomao, H. A. Brown, J. W. Lomasney, N. Mohandas, and K. Haldar.** 2007. Cytoplasmic remodeling of erythrocyte raft lipids during infection by the human malaria parasite *Plasmodium falciparum*. Blood **110:** 2132–2139.
37. **Neimark, H., K. E. Johansson, Y. Rikihisa, and J. G. Tully.** 2001. Proposal to transfer some members of the genera *Haemobartonella* and *Eperythrozoon* to the genus *Mycoplasma* with descriptions of '*Candidatus* Mycoplasma haemofelis,' '*Candidatus* Mycoplasma haemomuris,' '*Candidatus* Mycoplasma haemosuis' and '*Candidatus* Mycoplasma wenyonii.' Int. J. Syst. Evol. Microbiol. **51:**891–899.
38. **Neimark, H., K. E. Johansson, Y. Rikihisa, and J. G. Tully.** 2002. Revision of haemotrophic *Mycoplasma* species names. Int. J. Syst. Evol. Microbiol. **52:**683.
39. **Perreten, V., L. Vorlet-Fawer, P. Slickers, R. Ehricht, P. Kuhnert, and J. Frey.** 2005. Microarray-based detection of 90 antibiotic resistance genes of gram-positive bacteria. J. Clin. Microbiol. **43:**2291–2302.
40. **Pospischil, A., and R. Hoffmann.** 1982. *Eperythrozoon suis* in naturally infected pigs: a light and electron microscopic study. Vet. Pathol. **19:**651–657.
41. **Reynolds, E. S.** 1963. The use of lead citrate at high pH as an electron-opaque stain in electron microscopy. J. Cell Biol. **17:**208–212.
42. **Ristic, M., and J. P. Kreier.** 1979. Hemotropic bacteria. N. Engl. J. Med. **301:**937–939.
43. **Seubert, A., R. Schulein, and C. Dehio.** 2002. Bacterial persistence within erythrocytes: a unique pathogenic strategy of *Bartonella* spp. Int. J. Med. Microbiol. **291:**555–560.
44. **Stipkovits, L., and I. Kempf.** 1996. Mycoplasmoses in poultry. Rev. Sci. Tech. Off. Int. Epizoot. **15:**1495–1525.
45. **Tasker, S., C. R. Helps, M. J. Day, D. A. Harbour, S. E. Shaw, S. Harrus, G. Baneth, R. G. Lobetti, R. Malik, J. P. Beaufils, C. R. Belford, and T. J. Gruffydd-Jones.** 2003. Phylogenetic analysis of hemoplasma species: an international study. J. Clin. Microbiol. **41:**3877–3880.
46. **Taylor-Robinson, D., H. A. Davies, P. Sarathchandra, and P. M. Furr.** 1991. Intracellular location of mycoplasmas in cultured cells demonstrated by immunocytochemistry and electron microscopy. Int. J. Exp. Pathol. **72:**705–714.
47. **Vogl, G., A. Plaickner, S. Szathmary, L. Stipkovits, R. Rosengarten, and M. P. Szostak.** 2008. *Mycoplasma gallisepticum* invades chicken erythrocytes during infection. Infect. Immun. **76:**71–77.
48. **Weick, J. K., A. B. Hagedorn, and J. W. Linman.** 1974. Leukoerythroblastosis. Diagnostic and prognostic significance. Mayo Clin. Proc. **49:**110–113.
49. **Winner, F., R. Rosengarten, and C. Citti.** 2000. In vitro cell invasion of *Mycoplasma gallisepticum*. Infect. Immun. **68:**4238–4244.
50. **Yang, D., X. Tai, Y. Qiu, and S. Yun.** 2000. Prevalence of *Eperythrozoon* spp. infection and congenital eperythrozoonosis in humans in Inner Mongolia, China. Epidemiol. Infect. **125:**421–426.

Editor: J. F. Urban, Jr.

Acknowledgements

My Ph.D. thesis was supported by many people. First of all, I would like to thank PD Dr. L. E. Hölzle for the supervision of my work. Several interesting topics in this thesis originated from his great ideas. In times of crisis he always had solutions for my problems.

I would like to acknowledge Prof. Dr. M. M. Wittenbrink, the head of the Institute for Veterinary Bacteriology, for giving me the opportunity to perform my Ph.D. studies at his institute. He contributed to this work by fruitful comments and annotations.

Thanks to Prof. Dr. L. Eberl for acting as responsible faculty member and as head of my promotion committee and Prof. J. Pernthaler for attending the committee.

I would like to kindly thank Prof. Dr. Renate Rosengarten for evaluating my Ph.D. thesis.

A part of my Ph.D. study time was financially supported by the „Forschungskredit“ of the University of Zurich.

The members of the Center for Microscopy and Image Analysis are acknowledged for the kind co-operation and support. Particularly I like to thank Dr. Urs Ziegler and Dr. Andres Käch for the fruitful inputs and image interpretation as well as Gery Barmettler and Klaus Marquardt for the teaching of electron microscopic techniques.

Prof. Dr. H.-A. Schoon is acknowledged for the preparation and staining of histochemical sections of parenchymas.

I would like to acknowledge Manuela Kramer for doing quantitative PCRs, Dr. Kathrin Felder for the FACS analysis as well as the great time in the office, Dr. Katharina Hölzle for the methodological expertise in the lab and Albina Sokoli for the great practical support during the last month of my Ph.D. Special thanks go to the complete staff of the institute for the regular cake supply and the creation of a good and friendly atmosphere.

A big hug goes to Paula, Kristina, Fabienne, Cilly, Sarah, Dom, Sev, Anne and Sylvi who where there for me whenever I needed a friend.

Above all I thank my family and Christian for motivating and supporting me during the last years. Without them this never had been possible.

Curriculum vitae

Personal data

Name:	Groebel
First Name:	Katrin
Date of birth:	3rd June, 1981
Place of birth:	Leinefelde, Germany
Nationality:	German
Private Address:	Obstgartenstrasse 20, Regensdorf, CH-8105

Education

05/2006 – current	**University of Zurich, Switzerland; Institute for Veterinary Bacteriology** Doctoral Studies in Microbiology; Title: "New Insights into the Pathogenesis of *Mycoplasma suis*"; Member of the Microbiology and Immunology (MIM) Ph. D. program
12/2005	**Georg-August University of Göttingen, Germany** Diploma in Biology (M.Sc.)
01/2005 - 09/2005	**University of Oulu, Finland, Department of Bioprocess Engineering** Diploma Thesis, Title: "Sandwich hybridization assay for detection of *Legionella pneumophila* based on the macrophage infectivity potentiator (*mip*) mRNA"
09/2001 - 08/2002	**University of Oulu, Finland** Erasmus Exchange Student, Concentration: *Bioprocess Engineering, Biochemistry*
09/ 1999 - 11/ 2005	**Georg-August University of Göttingen, Germany** Studies in Biology; Concentration: *Microbiology, Immunology and Genetics*
06/1999	**Friedrich Schiller Grammar School in Bleicherode, Germany** German University Entrance Qualification

Working Experiences and Extra-Curricular Activities

2008	Member of the organisation committee of the MIM retreat
01/ 2004 - 09/ 2004	Research assistant at the group of Prof. Dr. Gerhard Gottschalk, Genomics Laboratory, Institute for Microbiology and Genetics, Georg-August University of Göttingen, Germany
05/ 2003 - 01/ 2004	Research assistant at the group of PD. Dr. Stephan Sigrist, European Neuroscience Institute, Göttingen, Germany
01/ 2002 – 09/ 2002	Researcher at the group of Prof. Dr. Rikkert Wierenga, Department of Biochemistry, University of Oulu, Finland Topic: "Kealases – New Engineered Enzymes for the Stereoselective Synthesis of Chiral Alpha-Hydroxyaldehydes"
09/ 2001 - 12/ 2001	Research assistant at the group of Prof. Dr. Peter Neubauer, Department of Process and Environmental Engineering, Bioprocess Engineering Laboratory, University of Oulu, Finland

Grants and Fellowships

2006 - 2008	Support by the "Forschungskredit" of the University of Zurich
2008	IOM Travel Grant
2005	Leonardo Da Vinci Fellowship
2001	Erasmus Exchange Student Grant (University of Göttingen)

List of publications

Dieckmann SM, Winkler M, Groebel K, Dieckmann MP, Hofmann-Lehmann R, Hoelzle K, Wittenbrink MM, Hoelzle LE. " Haemotrophic Mycoplasma Infection in Horses. " Veterinary Microbiology 2010. Accepted

Felder KM, Hoelzle K, Kilchling T, Schiele D, Heinritzi K, Groebel K, Hoelzle LE. " Programmed cell death of red blood cells influences development of anaemia in pigs infected with *Mycoplasma suis.* " In preparation

Groebel K, Hoelzle K, Wittenbrink MM, Ziegler U, Hoelzle LE. " *Mycoplasma suis* invades porcine erythrocytes. " Infection and Immunity 2008, 77(2): 576-584

Carranza P, Hartmann I, Lehner A, Stephan R, Gehrig P, Grossmann J, Groebel K, Hoelzle LE, Eberl L, Riedel K. " A gel-free quantitative proteomics approach to investigate temperature 1 adaptation of the food-borne pathogen *Cronobacter turicensis* 3032. " Proteomics. Submitted

Willi B, Museux K, Schraner EM, Wild P, Groebel K, Ziegler U, Wolf G, Kessler Y, Tasker S, Lutz H, Hofmann-Lehmann R. " Electron microscopy and phylogeny of 'Candidatus Mycoplasma turicensis'. " In preparation

Casteleijn MG, Alahuhta M, Groebel K, El-Sayed I, Augustyns K, Lambeir AM, Neubauer P, Wierenga RK. " Functional role of the conserved active site proline of triosephosphate isomerase. " Biochemistry. 2006 Dec 26;45(51):15483-94

Contribution to conferences

2008, 17th congress of the International Organisation of Mycoplasmology (IOM) in Tianjin, China. **Talk** entitled "*Mycoplasma suis* invades porcine erythrocytes".

2008, biannual meeting of the division *"Bacteriology and Mycology"* of the German Veterinary Association (DVG), Braunschweig, Germany. **Talk** entitled "*Mycoplasma suis* invades porcine erythrocytes".

2008, 67th annual congress of the Swiss Society for Microbiology (SGM), Interlaken, Switzerland. **Poster** entitled "*Mycoplasma suis* invades porcine erythrocytes".

2007, 6th Symposium of german speaking mycoplasmologists, Fürth, Germany. **Talk** entitled: "Proteinsekretions- und Transportmechanismen in *Mycoplasma suis*"

2007, 66th annual congress of the Swiss Society for Microbiology (SGM), Interlaken, Switzerland. **Poster** entitled "First identification and functional characterization of an immunogenic protein in unculturable haemotrophic Mycoplasmas (*Mycoplasma suis* HspA1)"